The ascent of AKAPs: from architectural elements to isotype selective PKA scaffolds

Jerome Falcone

A thesis

submitted in partial fulfillment of the

requirements for the degree of

Doctor of Philosophy

University of Washington

2025

Reading Committee:

John D. W. Scott, Chair

Yasemin Sancak

Ning Zheng

Program Authorized to Offer Degree:

Pharmacology

University of Washington

Abstract

The ascent of AKAPs: from architectural elements to isotype selective PKA scaffolds

Chair of the supervisory committee:

John D. W. Scott

Department of Pharmacology

The spatiotemporal organization of proteins within cells is essential for complex life. The scaffolding of protein kinase A (PKA) by A-kinase anchoring proteins (AKAPs) allows for the management of a multitude of simultaneous signal cascades within animal cells. AKAPs contain an 18-amino-acid-long amphipathic helix that anchors the docking and dimerization (d/d) domain of PKA regulatory subunits. There are four isoforms of the PKA regulatory subunit, RIα, RIβ, RIIα, and RIIβ, which fall into the two categories of type I and type II PKA (the α and β forms of each regulatory subunit share similar topology). There are >60 known AKAPs, and each one prefers to bind either type I or type II PKA. As PKA originated in the metazoan clade, the presence of 'AKAP' proteins in organisms that lack PKA suggests a PKA-independent function. These ancestral anchoring proteins localize to cilia and flagella across all eukaryotic kingdoms and bind docking and dimerization domain proteins that contain a d/d domain nearly identical to that of PKA, fused to other protein domains.

In this work, we christen these PKA-independent scaffolds as **d**ocking and **d**imerization domain **i**nteracting **p**roteins (DDIPs) and study the co-evolution of d/d proteins, PKA, AKAPs, and DDIPs. Phylogenetic analyses show that PKA and the d/d proteins exhibit telltale signs of divergent evolution. Driven by gene duplication and fusion events, both the structural folds and the primary sequences of these proteins have been highly conserved for over two billion years.

The evolutionary path of AKAPs and DDIPs is strikingly different. Phylogenetic analyses reveal patterns of convergent evolution for these anchors. By tracing the evolution of anchoring domains on extant proteins, we reveal a paradigm of accretion of neutral mutations which eventually form a functional anchoring helix. Once this occurs, the mutation rate slows as this protein region becomes subject to selective pressures.

Finally, I examine the features of AKAP helices which drive preference for either type I or type II PKA. Guided by bioinformatic analysis, we identified an F/Y, A motif at the N-terminus of all type I-selective AKAPs. We hypothesized that this "aromatic, alanine" motif controls AKAP preference. Using a total internal reflection fluorescence (TIRF)–fluorescence recovery after photobleaching (FRAP) assay, we measured the degree of R subunit binding of the characteristic type I and type II AKAPs, smAKAP and AKAP79. We then applied the "aromatic, alanine" motif to the helix of AKAP79, creating mutants with an "FA" on the N-terminus, an "AF" on the C-terminus, and a version with both terminal mutations known as "FAAF". Immunoprecipitation experiments with these mutants revealed that only the FAAF mutant gains the ability to pull down RI. Molecular dynamics simulations on AKAP79 and AKAP79$^{\mathbf{FAAF}}$ reveal a rearrangement of contact points between the helix and the d/d domain which facilitate this preference switch. FRAP experiments confirm that AKAP79$^{\mathbf{FAAF}}$ does switch its preference to RI *in situ*. The significance of this mutation on signaling was confirmed by a rescue of aberrant corticosterone release in an RI-biased Cushing's syndrome model. Finally, we performed a reciprocal experiment in which the 'aromatic, alanine' motif on smAKAP was replaced with two leucines to resemble AKAP79. This mutation was sufficient to impair RI binding by smAKAP in an immunoprecipitation, but did not confer RII binding measured by immunoprecipitation or RII overlay. Together these results clarify the evolutionary paths of these anchoring proteins and their d/d partners, and serve as a call to arms to identify and characterize new DDIPs. The

analysis of AKAP preference will assist in the characterization of new AKAPs and reveals a new facet of what makes this binding interface such a powerful cellular tool.

Table of Contents

List of figures……..……..….viii

Chapter 1 – Background and introduction ……..……..1

1.1 Principles of evolution ……1

1.2 Cyclic AMP signaling and information management ……3

1.3 Protein kinase A (PKA) structure and function ……4

1.4 A-kinase anchoring proteins (AKAPs) ……...5

1.5 Ciliary and flagellar d/d proteins and DDIPs ……...7

Figures ……9

Chapter 2 – Divergent evolution of docking and dimerization domains …….……...14

2.1 Introduction……14

2.2 Methods……..……15

2.3 Three classes of docking and dimerization domain protein ……..……15

2.4 Conservation of docking and dimerization domains ……...16

2.5 Phylogenetic relationships of docking and dimerization domain proteins……18

2.6 Discussion……..18

Figures ……..……21

Chapter 3 – Convergent evolution of AKAPs and DDIPs……..……...26

3.1 Introduction……..……26

3.2 Methods……..27

3.3 AKAP evolution – the metazoan “explosion”……..28

3.4 AKAP79 domain evolution……30

3.5 DDIPs as a category of anchoring protein……31

3.6 Analysis of AKAP gain of function……..……32

3.7 Discussion……..….35

Figures ……..38
Chapter 4 – AKAP helix binding determinants……..50
4.1 Introduction……50
4.2 Methods……..52
4.3 Analysis of type I and type II AKAP helices……...57
4.4 AKAP Preference swap……..……..…59
4.5 Discussion……..62
Figures……..65
Chapter 5 – Final Conclusions……..……75
5.1 Divergent evolution of docking and dimerization domains……..……75
5.2 Convergent evolution of AKAPs and DDIPs……..……..76
5.3 AKAP helix binding determinants……..……77
References……79
Curriculum Vitae……....94

List of Figures

Figure 1.1: Cyclic AMP pathway……9

Figure 1.2: The information bottleneck of cAMP signaling……9

Figure 1.3: Cilia and flagella are home to DDIPs and d/d domain protein pair……..10

Figure 1.4: AKAPs are a subset of DDIPs……11

Figure 1.5: Differences between DDIP and AKAP anchoring……12

Figure 2.1: Docking and dimerization domain protomers share similar architecture……21

Figure 2.2: Conservation of d/d domains across the three domain classes……21

Figure 2.3: Analysis of conserved residues of the DPY-30 docking and dimerization domain……..22

Figure 2.4: Conservation of the PKA RIα docking and dimerization domain……..23

Figure 2.5: Conservation of the PKA RIIα docking and dimerization domain……24

Figure 2.6: Phylogenetic tree of known d/d containing proteins……..25

Figure 3.1: Metazoan cladogram of AKAP origins……..38

Figure 3.2: AKAP79/150 domain analysis……..……39

Figure 3.3: AlphaFold 3 models of representative AKAP150 peptide repeats……..40

Figure 3.4: AKAP79/AKAP150 PKA binding analysis……41

Figure 3.5: DDIP and d/d domain protein pairs were present at the last eukaryotic common ancestor (LECA)……..42

Figure 3.6: Timeline of AKAP gain of function events for OPA1, the ERM proteins, and the AKAP8 family……43

Figure 3.7: OPA1 became an AKAP at the Metazoan clade……..…..……...44

Figure 3.8: ERM proteins and Merlin asynchronous AKAP development……...46

Figure 3.9: The AKAP8 family reveals a single insertion resulting in AKAP development……48

Figure 4.1: Type I and II AKAPs…… ……...…….65

Figure 4.2: Sequence alignments of individual type I AKAPs used to generate the consensus logo……..…66

Figure 4.3: FRAP analysis of smAKAP and AKAP79…….……...….68

Figure 4.4: AKAP79 PKA preference switch…….……70

Figure 4.5: Removal of YA motif on smAKAP abolishes type I PKA binding……...72

Figure 4.6: Rescue of Cushing's syndrome by AKAP79^{FAAF}……..……..73

Acknowledgements

I would like to thank Dr. John Scott for his stewardship of my graduate school tenure and participation in my growth as a scientist. I would also like to thank the many past and present Scott lab members who I have learned from, laughed with, and commiserated with. I would like to especially thank Katherine Forbush, Mingu Kang, Brianna Odle, Kristin Cleveland, and Mitch Omar for guidance and assistance in some of the work contained herein. Many thanks to my supervisory committee, Drs. John Scott, Yasemin Sancak, Smita Yadav, Jesse Zalatan, and Ning Zheng for their sustained guidance and support. I would like to thank my parents, Deane and Celeste Falcone, for instilling a sense of curiosity and of awe at the beauty of the world in all its frames of reference. Lastly, I would like to thank my good friends, Matt Jardine, Colin Montiel-Anatra, Corina Miner, and Ari Fogel for their friendship and camaraderie over the years.

Chapter 1 – Background and introduction

1.1 Principles of evolution

A handful of years ago, in 1859, Charles Darwin released a book about finches (Darwin, 1859). In this landmark work, *On the Origin of Species by Means of Natural Selection*, he introduced the concept of natural selection. This is the process by which traits that enhance an organism's fitness become more common in successive generations, while traits that harm fitness gradually disappear as carrier organisms fail to reproduce. Darwin's idea marked the beginning of the field of evolutionary biology. Over the past 165 years, the field has refined this concept and developed detailed models explaining how life has diversified from simple origins to the remarkable complexity we observe today.

Two main competing hypotheses attempt to explain the origin of life: the "RNA world" hypothesis and the "protein first" hypothesis (Gilbert, 1986; Kocher & Dill, 2024). Both are compelling, as nucleotides and amino acids can form abiotically through reactions of common interstellar chemicals such as cyanide and ammonium (Levy et al., 2000). These molecules have also been detected in asteroid samples (Glavin et al., 2025). Both hypotheses propose that life began with self-replicating biopolymers capable of simultaneously storing information and performing catalytic functions. Over time, these primitive systems are thought to have developed cellular properties, such as lipid-based compartmentalization, metabolic pathways, and the core components of the central dogma of biology: DNA, RNA, proteins, and the polymerases and ribosomes necessary for biopolymer synthesis (Kocher & Dill, 2023).

The "RNA world" hypothesis is supported by evidence that RNA can both store genetic information and perform catalytic roles. It also requires only four types of ribonucleotides (compared to the 20 amino acids required for proteins) and is consistent with the prevalence of RNA-based viruses (Lincoln & Joyce, 2009). However, this hypothesis faces challenges. Catalytic RNA typically requires a relatively large size to function, known ribozymes have limited catalytic capabilities, and RNA polymers are inherently unstable (Bernhardt, 2012).

The "protein first" hypothesis, on the other hand, simplifies the origin of proteins to chains of polar and hydrophobic amino acids. These “HP” chains could fold into globular structures, with exposed hydrophobic

patches acting as catalytic "landing pads" (Guseva et al., 2017). Over time these autocatalytic sets of proteins, driven by the formation of amino acids can form longer and more complex peptides, resulting in more efficient catalysis and a diverse set of functional proteins (Kocher & Dill, 2023).

Whichever abiotic process occurred, it eventually resulted in a last common universal ancestor (LUCA), which has properties that can be inferred through phylogenetics. By comparing proteins in extant organisms, a protein or function which is conserved across the domains of life can be inferred to have been inherited from this ancestor. This organism was an anerobic, thermophilic organism which relied on H_2 to fix CO_2 (Weiss et al., 2016). From this LUCA, emerged the three domains of life: Archaea, Bacteria, and Eukarya (Woese et al., 1990). This dissertation will focus on the molecular evolution of Eukaryotic proteins.

As the field of molecular biology developed, scientists have ascertained molecular drivers of protein evolution. In 1968, Motoo Kimura proposed the theory of “neutral evolution” (Kimura, 1968). By examining amino acid substitutions in hemoglobin in mammals, he derived a substitution rate of one amino acid change in10^7 years for one of the 140 amino acid chains of the protein. While a seemingly low rate, when applied to the whole genome it results in a population level substitution rate of a nucleic acid substitution every 1.8 years. To reconcile this high rate of change with the need for proteins to maintain their function, Kimura theorized that the majority of mutations which become “fixed,” or prevalent within the population, are so-called neutral mutations, which neither provide a fitness advantage nor disadvantage (Kimura, 1983). Some consequences of the neutral mutation rate are that the accumulation of neutral mutations largely overshadows the fixation of advantageous mutations and that while the mutation rate for a protein may be consistent, the mutation rate for important regions of a protein will be lower, and less important regions will have a higher mutation rate (Kimura & Ohta, 1974).

A second concept of molecular evolution is the driver effect of gene duplication. Gene duplication, or the production of an extra copy of a gene, can occur at the level of the single gene, the chromosome, or the entire genome (Ohno, 1970). Once this occurs the extra copy of a gene can escape selection pressure, as its functions are being performed by its twin. This copy, free from selection pressure can accumulate mutations which impair the gene product’s original function but allow for the development of new functions (Bergthorsson et al., 2007). A striking example of this is how plants have leveraged whole-genome

duplications to produce a dizzying array of secondary metabolites through specialized metabolic enzymes (Gaynor et al., 2020). In eukaryotes gene duplication is responsible for the great diversity in protein families such as GPCRs and kinases (Howard et al., 2014; Hu et al., 2017).

There is a disparity between the rates of change between primary and tertiary sequences, where the folded structure of a protein changes more slowly than its amino acid sequence (Theobald & Wuttke, 2005). Using mathematical terminology, the set of protein folds maps redundantly to the set of protein sequences (Bowie et al., 1990). Convergent evolution is enabled by this disparity, as dissimilar sequences can develop into similar structures. The ensemble of oxygen-binding globins across mammals, insects, mollusks, and plants share similar tertiary structures which allow for heme binding despite their diverse sequences indicating unique progenitors (Chothia & Lesk, 1986).

1.2 Cyclic AMP signaling and information management

Organisms constantly face the task of information management (Torday & Miller, 2020). Hallmarks of life such as maintenance of homeostasis, organization, metabolism, growth, adaptation, response to stimuli, and reproduction all involve a selective response to external information (Trifonov, 2012). It is of the utmost importance for an organism to segregate the flows of information required for each of these processes to avoid interference. The transduction of extracellular signals through G-protein coupled receptors and cyclic AMP illustrates one way that organisms manage the flow of information.

G-protein coupled receptors (GPCRs) are the most common and diverse group of receptors found on eukaryotic cells, with over 800 unique family members (Bjarnadóttir et al., 2006). These proteins contain an extracellular N-terminal region, seven transmembrane helices, and an intracellular C-terminus (Venkatakrishnan et al., 2013). The N-terminus and extracellular portions of the transmembrane helices contribute to the formation of an extracellular ligand binding pocket, and the intracellular portions of three helices and the C-terminal tail are the binding site and guanine exchange factor for heterotrimeric G-proteins (Venkatakrishnan et al., 2013).

Agonist binding of a GPCR facilitates the exchange of GTP for GDP, activating the G-protein. G-proteins consist of α and βγ subunits and the G_{α} subunit engages second messenger cascades while its

intrinsic GTPase activity hydrolyzes the bound GTP to GDP, inducing the return of the G-protein to the GPCR (Khafizov et al., 2009). $G_{\alpha s}$ subunits activate the enzyme adenylyl cyclase, which catalyzes the formation of cyclic AMP (cAMP) from ATP (Hanoune & Defer, 2001). Cyclic AMP activates protein kinase A (PKA), and permits phosphorylation of local substrates, as well as activating other cAMP effectors such as exchange factors directly activated by cAMP (EPACs), popeye domain containing proteins (POPDC) channels, and cyclic nucleotide gated ion channels (Stierl et al., 2011) (**Figure 1.1**).

The use of the diffusible small molecule, cAMP, as a second messenger leads to an informational bottleneck in cells (**Figure 1.2**). A given cell will have dozens of $G_{\alpha s}$ coupled GPCRs on its surface which all produce cAMP to transduce unique signals (Atwood et al., 2011). Cells have adopted a number of mechanisms to deal with this problem of multiplexing to ensure that the diversity of signals transmitted through cAMP maintain spatiotemporal fidelity. In the context of PKA signaling, the two regulatory subunits of PKA have different affinities and avidities for cAMP with type I PKA responding at lower levels of the cyclic nucleotide than type II PKA (Cummings et al., 1996). Cells utilize hydrolytic enzymes called phosphodiesterases to break one of the phosphate-ribose bonds in cAMP to form the molecule AMP, which is inert at the molecular targets of cAMP (Strada et al., 1974; Uzunov & Weiss, 1972). Cells can also buffer cAMP by maintaining an excess of cyclic AMP binding proteins which are not coupled to any effector (Sherpa et al., 2024). The presence of buffering proteins prevents the activation of nearby cAMP-responsive elements until cAMP concentrations exceed the capacity of the buffering proteins. Type Iα regulatory subunits can form liquid-liquid phase separated condensates as one mechanism for this buffering (Zhang et al., 2020). None of these techniques would work on their own without the ability to localize cAMP signaling elements to precise regions of the cell. This is done by a class of scaffold proteins called A-kinase anchoring proteins (AKAPs) (Bock et al., 2024). These proteins coordinate all the above strategies to solve the problem of a single small molecule acting as a second messenger for many different processes.

1.3 Protein kinase A (PKA) structure and function

Cyclic AMP dependent protein kinase, or protein kinase A (PKA) was first purified from rabbit skeletal muscle in 1968 (Walsh et al., 1968). This enzyme is unique in that it requires the binding of the second messenger, cyclic AMP (cAMP) in order to catalyze ATP dependent protein phosphorylation (Ueland &

Doskeland, 1976). Later studies revealed an unusual tetrameric structure of PKA, consisting of homodimerized regulatory subunits, each bound to a catalytic subunit (Zoller et al., 1979). The two regulatory subunits of PKA hold the catalytic subunits in an inactive state. Binding of two molecules of cAMP per regulatory subunit monomer induces a conformational change, allowing the catalytic subunits to phosphorylate nearby substrates (Smith et al., 2017).

In vertebrates there are four distinct regulatory subunits which are grouped into structurally distinct classes: I and type II PKA (Banky et al., 2003). Each class has two structurally similar isoforms, α and β, in which the ubiquitously expressed α subunits emerged at the beginning of the metazoan clade. In contrast, the β subunits, which exhibit tissue-specific expression, emerged later with the advent of vertebrates (Bregman et al., 1989; Clegg et al., 1988). All regulatory subunits share a similar domain organization, consisting of an N-terminal docking and dimerization (d/d) domain, which facilitates both homodimerization and AKAP binding; an inhibitory domain resembling the substrate motif RRXA (RI) or RRXS (RII), which facilitates catalytic subunit binding; and two cyclic nucleotide-binding domains (Lu et al., 2019; Newlon et al., 1999; Zoller et al., 1979).

The catalytic subunit of PKA phosphorylates serine or threonine residues within the substrate motif R,R,X,S/T (Kemp et al., 1977). In vertebrates, there are three isoforms of the catalytic subunit (α, β, and γ), with the α isoform being ubiquitously expressed and the β isoform exhibiting sporadic tissue expression (Shoji et al., 1981; Uhler et al., 1986). PKA Cγ, an intronless gene found only in primates, contains distinctive Alu recombination sites, indicating that it arose through the retrotransposition of PKA Cα (Reinton et al., 1998).

1.4 A-kinase anchoring proteins (AKAPs)

A-kinase anchoring proteins (AKAPs) scaffold PKA holoenzymes to confer spatiotemporal control over cAMP signaling (Bock et al., 2024). These scaffolding proteins use an eighteen amino acid-long amphipathic helix to bind to the docking and dimerization domain of PKA regulatory subunits (Götz et al., 2016). The hydrophobic face of the AKAP helix contacts hydrophobic residues on PKA regulatory subunits resulting in a typically high-affinity interaction with a dissociation constant in the nanomolar range (Gold et al., 2006). Through this interaction, PKA tetramers can be sequestered to specific organelles along with

specific sets of downstream effectors and sometimes even adenylyl cyclases and phosphodiesterases to grant fine-grained control of cyclic AMP signaling dynamics (Jackson, 2020).

AKAPs differentially anchor type I and type II PKA regulatory subunits due to differences in the structure of their respective d/d domains (Carlson et al., 2006; Di Benedetto et al., 2008; Gold et al., 2006). The first AKAPs discovered were RII binding proteins, as they were detected by an assay called the RII overlay (Bregman et al., 1989; Bregman et al., 1991; Carr, Hausken, et al., 1992; Lohmann et al., 1984). This far-western assay detected AKAPs separated by polyacrylamide gel electrophoresis, and blotted to a nitrocellulose membrane by incubating with labeled RIIα subunits (Lohmann et al., 1984). Overlays with RI have not proved robust, as the first RI-binding AKAP was detected in a yeast two-hybrid complementation screen (Huang et al., 1997a, 1997b). These AKAPs bind RII preferentially but can bind RI at high-physiological levels (Burgers et al., 2012; Herberg et al., 2000). The first selective RI-binding AKAPs were discovered via chemoproteomic mass spectrometry screens which used analogs of cyclic AMP that preferentially bound to RI or RII (Aye et al., 2009; Burgers et al., 2012). Algorithms have been generated to predict AKAP helices, but they are subject to both false positives and false negatives due to the variety of permissible anchoring helix topologies (Burgers et al., 2015).

Structurally, AKAPs are often intrinsically disordered proteins, decorated along their length with functional domains. The tendency towards disorder allows for AKAPs to dynamically shift conformations, facilitating protein-protein interactions between its scaffolded clients (Nygren et al., 2017). In the context of PKA, this expands the distance over which the anchored kinase is able to phosphorylate substrates (Smith et al., 2013). As different AKAPs are of various sizes, they can vary in the volume of the PKA nanodomain that they form.

Not all AKAPs are intrinsically disordered proteins. For example, GPR161, a GPCR, is an AKAP composed of structured domains (Hoppe et al., 2024). This AKAP is localized in primary cilia, where it anchors type I PKA intracellularly to repress Sonic Hedgehog signaling (Mukhopadhyay et al., 2013). This aligns with the trend that AKAPs with low levels of intrinsic disorder often evolve from existing protein families, incorporating PKA anchoring into their pre-existing functions via the development of the

amphipathic helix. OPA1 and the ERM protein family are additional examples of highly ordered AKAPs that originated from existing proteins. These will be discussed in detail in the results section.

There are even non-canonical AKAPs which bind the regulatory subunits of PKA through domains other than amphipathic helices (Della Sala et al., 2024; Khalil et al., 2023; Perino et al., 2011). Talin-1 anchors PKA in focal adhesions in a stretch-dependent manner, where tension extends helical bundles freeing up the amphipathic helix (Kang et al., 2024). Mutagenesis assays have shown that its conserved binding region spans two helical bundles and is longer than the typical 18-amino-acid region, enabling it to transduce force (Kang et al., 2024). Despite these differences Talin-1 contacts the same region of the d/d domain as classical AKAPs. PI3Kγ is even more distinct, with a short helical region that binds the exterior of the d/d domain, representing a unique and targetable binding interaction (Della Sala et al., 2024). In this thesis, we will focus on “canonical” AKAPs which use one or more conserved amphipathic helices to bind the docking and dimerization domains of PKA regulatory subunits.

1.5 Ciliary and flagellar d/d proteins and DDIPs

The use of docking and dimerization (d/d) domains to anchor one protein to the amphipathic helix of another protein did not originate with protein kinase A and AKAPs. Across the eukaryotic tree, organisms employ proteins containing these domains as structural components in motile cilia and flagella (Jivan et al., 2009; Newell et al., 2008). Motile cilia and eukaryotic flagella are homologous, antenna-like organelles with distinct functions (Haimo & Rosenbaum, 1981). Eukaryotic flagella enable locomotion in unicellular organisms, while motile cilia perform specialized roles in multicellular organisms, such as clearing mucus and debris from the lungs in the human airway (Fahy & Dickey, 2010; Johnson & Rosenbaum, 1992). Both of these organelles share the same internal structure of a core axoneme consisting of nine microtubule doublets surrounding two central pair microtubules (**Figure 1.3**) (Zhao et al., 2019). Dynein motors, anchored to the outer microtubules, generate movement by driving the sliding of microtubule doublets through ATP hydrolysis (Porter & Sale, 2000). This motion is coordinated by radial spoke proteins and central pair complex components, which link the inner and outer microtubules to regulate dynein activity and produce synchronized beating (Yang et al., 2006). The radial spoke complexes contain both d/d

domain–containing proteins and their amphipathic helix partners, highlighting the conserved role of these domains in ciliary and flagellar architecture (Gaillard et al., 2006; Jivan et al., 2009; Newell et al., 2008).

Because PKA-anchoring is not the main function of these amphipathic helices (many of which have existed long before the development of PKA regulatory subunits), we have coined the term “Docking and Dimerization domain Interacting Proteins,” or DDIPs to accurately discuss proteins with such domains. As we have defined them, the class of DDIPs encompasses all non-PKA anchoring amphipathic helices, where AKAPs are any protein which uses such a helix to anchor PKA (**Figure 1.4**). There is some crossover between the two naming conventions as there are AKAPs such as AKAP95 and AKAP28 which anchor both PKA and other d/d containing proteins (Bieluszewska et al., 2018; Kultgen et al., 2002). DDIPs which bind the d/d domain of DPY-30 or similar proteins contact with only four faces of the amphipathic helix, compared to RI-like or RII-like proteins which interface with five turns of the helix (**Figure 1.5**) (Tremblay et al., 2014).

Figures for chapter 1

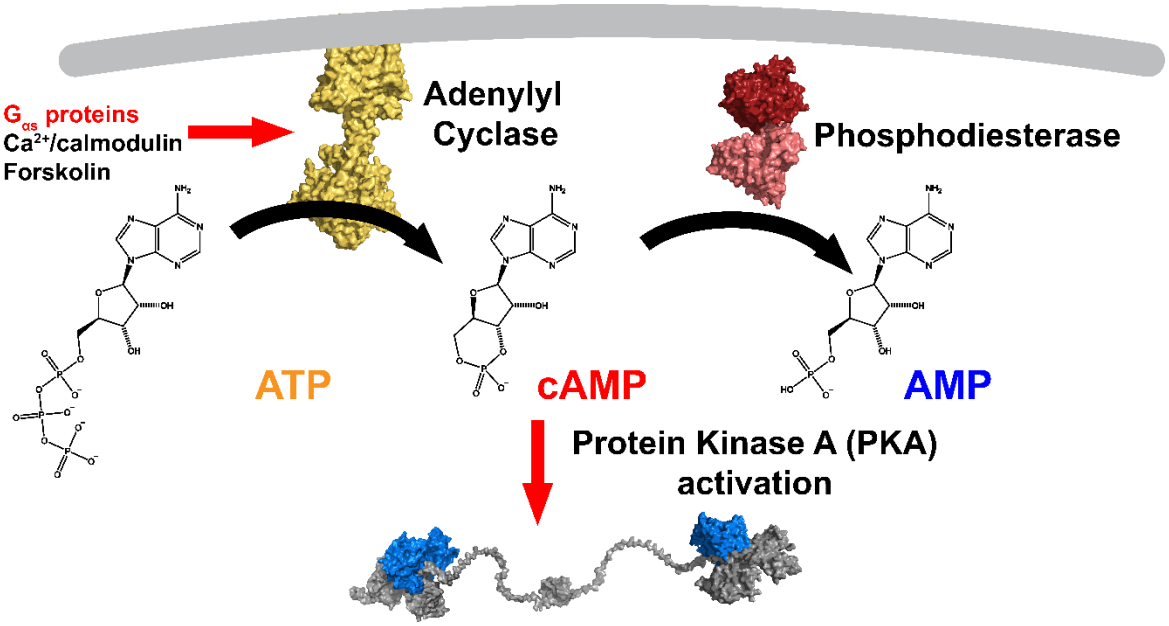

Figure 1.1: Cyclic AMP pathway: Adenylate cyclase is activated by $G_{\alpha s}$ proteins, Ca^{2+} or forskolin. This enzyme catalyzes the formation of cAMP from ATP. The cAMP is now able to bind PKA regulatory subunits, permitting PKA phosphorylation of substrates. This signal is terminated by the action of phosphodiesterase enzymes, which hydrolyze the 3' phosphodiester bond, forming AMP. AMP does not activate PKA.

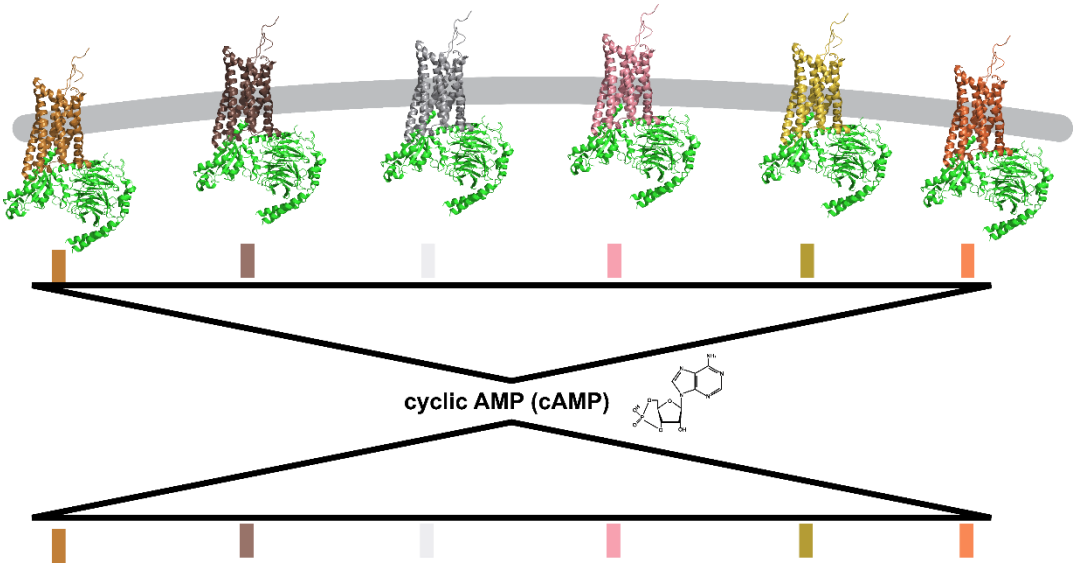

Figure 1.2: The information bottleneck of cAMP signaling: A given cell will have ~30 distinct $G_{\alpha s}$ coupled receptors on its surface. All of these signals will result in the production of cAMP. These receptors vary in their intracellular effects, so spatiotemporal regulation of second messengers is required to maintain the unique identities of each signal cascade to handle this challenge of multiplexing.

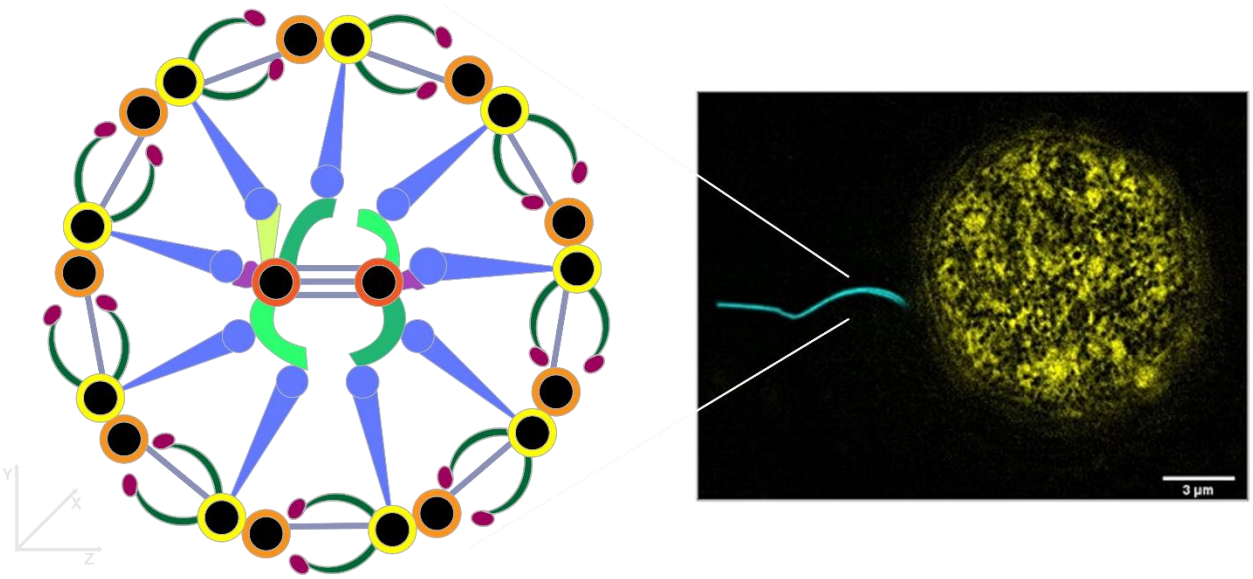

Figure 1.3: Cilia and flagella are home to DDIPs and d/d domain protein pair: The flagellar/ciliary axoneme permits motility of these organelles. Microtubules are arranged in a 9+2 format with 9 outer doublets and 2 central pair microtubules. Outer microtubule doublets are linked to dynein motors which generate force through ATP hydrolysis. DDIPs and d/d domain proteins make up interfaces in the radial spike proteins (blue) and the central pair complex (green) coordinate this force generation to generate whiplike movement (cilia) or regular beating (flagella) providing cellular motility.

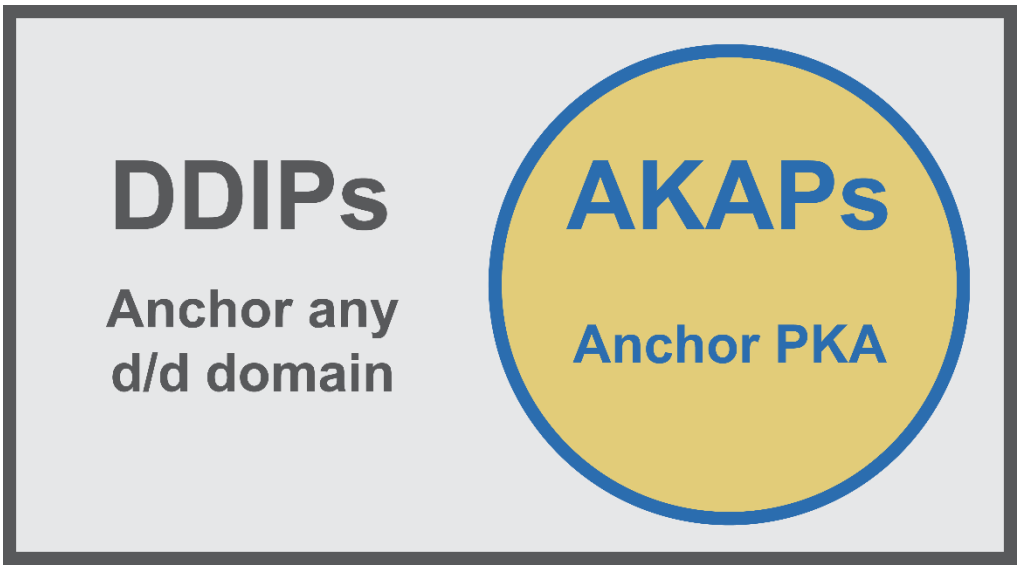

Figure 1.4: AKAPs are a subset of DDIPs: The title of Docking and dimerization domain interaction proteins (DDIPs) was assigned to encompass anchoring proteins which bind to d/d domains via an amphipathic helix, but do not anchor PKA. Lack of PKA binding is either substantiated by the DDIP's presence in a eukaryotic lineage which lacks PKA or through its experimental lack of association with PKA. In this scheme, AKAPs are a subset of DDIPS which bind to PKA. Despite AKAPs being a subset of DDIPs, focused study on these scaffolds has resulted in the identification and characterization of many more AKAPs than DDIPs.

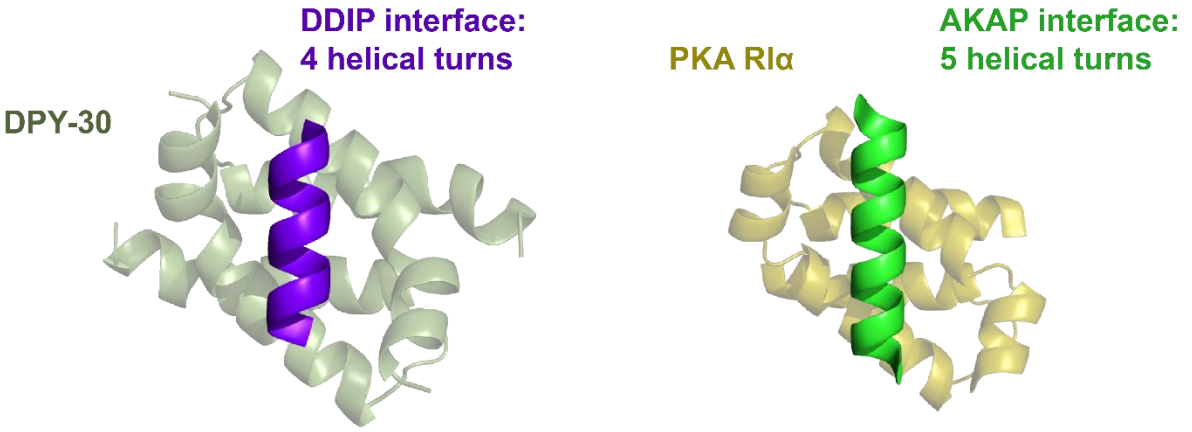

Figure 1.5: Differences between DDIP and AKAP anchoring: DPY-30-like domains are more compact than RID2 or RIID2 domains. DDIPs binding these domains use only 4 helical turns compared to RID2 and RIID2 proteins which are contacted by 5 helical turns.

Chapter 2 – Divergent evolution of docking and dimerization domains

2.1 Introduction

Docking and dimerization (d/d) domains represent an ancestral protein fold which mediates dimerization and provides an interface for binding amphipathic α-helices (Dahlin et al., 2021). These domains were originally characterized in the regulatory subunits of protein kinase A (Scott et al., 1990). Later studies using competitive peptide inhibitors of AKAP binding revealed that the sperm flagellar protein ropporin (ROPN1) has a d/d domain and its interaction with AKAPs is necessary for sperm motility (Carr et al., 2001). This discovery led to interest in other AKAP-binding proteins in flagella, resulting in the classification of SPA17, CABYR, ROPN1, RIIaD1, CATIP, and ROPN1L as RIID2 proteins, as they contain a d/d domain similar to PKA RII (Arafat et al., 2021; Fiedler et al., 2012). Proteins in this family have been observed to heterodimerize, further broadening the combinatorial potential for anchoring clients (Li et al., 2011).

This categorization of RIID2 proteins raised the question of whether there are any d/d domain proteins that resemble type I PKA. Dahlin et al. categorized 10 proteins as members of the RID2 family by primary sequence and tertiary structure similarity (Dahlin et al., 2021). This category includes the proteins FBXL13, enolase (in plants), TPGS1, TEX55, AK5, AK8, VEST1, EFCAB10 and AMY1 (categorized in this work by homology). As with the RIID2 proteins, these are all found in the axoneme of motile cilia and flagella (Bontems et al., 2014; Dougherty et al., 2020; Mitchell et al., 2005; Morohoshi et al., 2020; Ou et al., 2009; Panayiotou et al., 2011; Solaroli et al., 2009).

The third group of d/d domain proteins is the DPY-30-like family. This is the smallest of the three classes of d/d protein, with DPY-30 and AK7 being the sole family members (Dahlin et al., 2021). While DPY-30 is best known for its epigenetic role in the COMPASS complex, it is also found in axonemes (Dong et al., 2005; Gopal et al., 2012). Adenylate kinase 7 is also a component of motile cilia where its loss impairs motility (Milara et al., 2010; Sheridan et al., 2023).

These three classes of d/d protein display telltale signs of divergent evolution. First the d/d domain portions of each protein share a high degree of similarity to the other family members. This

indicates that these proteins evolved in a manner that preserved the primary structure of the domains(Theobald & Wuttke, 2005). Second, examples of each class occurring at the last eukaryotic common ancestor (LECA), which provides a template for the development of latter-occurring family members (van Hooff et al., 2019). Finally the existence of homologous pairs of proteins, such as ROPN1 and ROPN1L or AK5 and AK8 indicates a program of gene duplication and specialization of the copy which is not subject to the selection pressures of the original protein (Fiedler et al., 2012; Panayiotou et al., 2011). Together these d/d domain proteins form a diverse and understudied repertoire of scaffold interactors.

2.2 Methods

Data acquisition and curation

Docking and dimerization protein orthologs were acquired through clustered NCBI BLAST searches on the human isoform of each protein. Non-metazoan orthologs were acquired in tandem with non-clustered BLAST searches excluding the metazoan taxa. The search size limit was set to 1000 sequences to ensure coverage of orthologs. The raw sequences from the blast search were then curated by removing any sequences labeled “hypothetical,” “low quality,” “predicted,” or sequences attributed to different proteins than the target of the search. Finally, the presence of a d/d domain was determined, and proteins lacking the motif were excluded.

Generation of phylogenetic trees

The collections of protein orthologs were aligned in Mega11 using the MUSCLE algorithm or CLUSTALω (the alignment with the fewest gaps was used). Aligned sequences were then fed into the phylogenic tree generating tool IQTREE on the CIPRES gateway for construction of maximum likelihood phylogenetic trees. The program was instructed to test all amino acid substitution models and utilize the best one. 4,000 bootstraps were used to determine the topology of the consensus tree. Trees were visualized using the Interactive Tree of Life (iTOL) server.

Last common ancestor inference

The evolutionary history and identity of the last common ancestor (LCA) of each protein were determined by compiling a list of unique phyla in which extant orthologs are found. This set of orthologous proteins was then used to generate a phylogenetic tree. By tracing backward along the tree, the LCA was identified as the most recent node to which all extant isoforms have in common.

Generation of consensus logos and sequence alignments

Docking and dimerization domains were isolated to make conservation logos of the amino acids contained in each motif using the program Weblogo. Larger letters represent greater degrees of conservation. Example sequences were aligned in Adobe Illustrator to demonstrate regions of low or high conservation. Silhouettes of representative species were used from the public domain collection of the website phylopic.org.

Protein Modeling

Predictive protein models were generated using the Alphafold3 server. Representative models were chosen contingent on convergence of the 5 models provided, as well as agreement with known elements of protein structure (when available). Models were colored and positioned using Pymol 3.1.

2.3 Three classes of docking and dimerization domain protein

The three families of d/d domain were present at the last common eukaryotic ancestor. There were the eponymous DPY-30-like proteins and the RID2 and RIID2 proteins, the latter two being named for folds found in the type I and type II PKA regulatory subunits, respectively (Banky et al., 2000; Dahlin et al., 2021; Gold et al., 2013). This collection of 167 phylogenetically distinct sequences each encode the conserved domain. Although biologically diverse, the anatomy of each protomer is remarkably similar (Dahlin et al., 2021). An N-terminal 8-residue docking determinant (**figure 2.1; blue**) is fused to a 17-residue α-helix (**figure 2.1; α-helix 1, orange**). This is linked via a 4-amino-acid flexible linker (**figure 2.1; purple**) to a 15-residue α-helix (**figure 2.1; α-helix 2, yellow**). DPY-30-like and RID2 domains incorporate an additional helical extension at their N terminus (**figure 2.1; left & mid**). In contrast, the corresponding region in the RIID2 proteins is disordered (Dahlin et al., 2021); **figure 2.1; right**). Conservation logos of the DPY-30 (23 sequences), RID2 (82 sequences) and RIID2 (62 sequences) classes reveal distinguishing features in each

domain family (**figure 2.2**). Each class has a proline at a residue that caps α-helix 1 (**figure 2.2**). This imino-peptide bond introduces rigidity to terminate the first alpha helix and further orients the second helix in a different plane. This ensures a more constrained interface for docking with binding partners. Each d/d domain family contains a signature amino acid at position 4 (**figure 2.2**). DPY-30 and RID2 proteins contain a tyrosine at this position (**figure 2.2A&B**), whereas branched aliphatic chains (leucine, isoleucine or valine) occupy residues 4 and 6 in the RIID2 class (**figure 2.2C**).

Consensus sequence alignments and structural models presented in figures 2.2A-C reveal that each d/d domain is tailored towards its unique function. DPY-30-like and RID2 proteins contain two conserved prolines in the linker (capping both the C-terminus of α-helix 1 and the N-terminus of α-helix 2). They also contain a pair of aromatic and branched aliphatic residues in α-helix 2 (**figure 2.2A&B**). These determinants orient and stabilize the core of the docking and dimerization surfaces respectively. An exclusive property of DPY-30-like proteins is that they have a shorter α-helix 1 than RID2 or RIID2 proteins. This makes the binding surface more compact and reduces the area available for association with amphipathic helices on their binding partners. RIID2 proteins are unique in that the docking region requires two aliphatic residues for AKAP binding. Also, a single proline caps the end of α-helix 1 **(figure 2.2C**). Other characteristic features include a bent helix for DPY-30-like, a helix with a linker for RID2, and an unstructured region for RIID2 proteins (**figure 2.2A-C**). These conserved features induce docking to distinct binding partners. In addition, d/d domains fuse with other modular units to generate a repertoire of scaffolding proteins with various functions (Dahlin et al., 2021). The high degree of conservation between different proteins sharing these three domains indicates divergence from a common ancestor.

2.4 Conservation of docking and dimerization domains

Analysis of the conservation of a given domain and its orthologs reveals a pattern of amino acid conservation that highlights residues necessary for protein function. Examination of d/d domains of DPY-30, PKA RIα, and PKA RIIα reveal similar regions of both conservation and variance, revealing a shared mechanism of the three domain families.

The DPY-30 docking and dimerization interface is conserved in approximately thirty proteins across many phyla (**figure 2.3**). In C. *elegans,* this d/d domain is an essential element of the dosage compensation machinery. In mammalian cells DPY-30 is a core component of the COMPASS histone H3K4 methyltransferase complex that regulates aspects of cell proliferation and differentiation (Dong et al., 2005; Hsu et al., 2019; Tremblay et al., 2014). Sequence alignment of DPY-30 motifs spanning mammals, insects, choanoflagellates, fungi, amoeba, excavates, heterokonts, and plants reveal 40 residue regions of amino acid identity (**figure 2.3; top, yellow**). When this information is transposed onto the three-dimensional structure, poorly conserved residues occur in hinge regions and helical bundles that do not contact anchoring helices ((Hsu et al., 2019); **figure 2.3; bottom**). This is best illustrated when the variant positions (**red**) are portrayed in top, bottom and side views of the DPY-30 d/d domain (**figure 2.3; bottom**). Conversely invariant "functional" amino acids occupy the dimer interface and line the docking pocket (**figure 2.3; bottom**). Despite 2 billion years of evolution, all of the forms of the DPY-30 motif achieve their functional roles through the same manner (Margulis et al., 2006).

The d/d domains of PKA RIα and RIIα share similar patterns of conservation, although as both emerged at the beginning of the metazoan clade, they are more conserved due to less time for neutral mutations to become fixed. Aligned sequences of the RIα d/d domain from representative poriferans, cnidarians, spiralians, ecdysozoans, fish, amphibians, reptiles, birds, and mammals display a high degree of conservation (**figure 2.4; top gold**). Only the end of α-helix 1 (VQLC**XX**R), the penultimate residue in the linker (PE**X**P), the beginning of α-helix 2 (M**X**FLR), and the final residue of α-helix 2 (LEKE**X**) are not conserved (**figure 2.4; top gold**). These regions are akin to the regions of low conservation on DPY-30. The model of RIα variable residues shows that both the binding region of the domain and the aromatic contact points of α-helix 2 are highly preserved (**figure 2.4; bottom**). The areas of low conservation are at regions which have few intra- or inter-molecular contacts (**figure 2.4; bottom red**).

The d/d domain of RIIα shares similar properties, but there is a larger amount of variability (**figure 2.5**). Using orthologs spanning poriferans, cnidarians, spiralians, ecdysozoans, fish, amphibians, reptiles, birds, and mammals, one can observe inserts in the docking determinant region. Present in the poriferan, spiralian, and both ecdysozoan examples this insert varies in both length and composition (**figure 2.5; top**).

This insert, however, does not interfere with the two branched aliphatic amino acids required for binding type II anchoring proteins (**I**X**I**P). While there are regions of low conservation in all of the regions of the domain, the binding region and the interface between the two α-helices are conserved (**figure 2.5 bottom**). This illustrates the regions of these domains which are necessary for anchoring.

2.5 Phylogenetic relationships of docking and dimerization domain proteins

We propose that the DPY-30 and the RID2 and RIID2 classes have evolved divergently, a process by which proteins originating from a common ancestor develop different traits over time. A phylogenetic tree of d/d domain proteins provide further evidence for their divergent evolution (**figure 2.6**). The tree was constructed from sequences from representative species in phylogenetically distinct groups, capturing the breadth of variation across orthologs. The tree was rooted using the DPY-30-like family as an outgroup. The three d/d families distribute separately, with RID2 proteins (**figure 2.6; green**) positioned between the DPY-30-like family (Figure 2.6; purple) and the more distant RIID2 family (**figure 2.6; gray**). A clear pattern of divergence emerges upon examining the relationships between individual proteins (**figure 2.6**). Clusters of d/d orthologs with short branch lengths maintain separation from other proteins (Figure 2.6; colored branches). One exception is the β-forms of PKA regulatory subunits (RIβ and RIIβ) that are nested within the larger groups of the α-forms of the regulatory subunit. Of particular note are the fungal PKA regulatory subunits, Cgs1 and Bcy1 (**figure 2.6; blue lines;** (González Bardeci et al., 2016; Gupta et al., 2011)). These cAMP binding proteins are of the RIID2 class, but both contain d/d domain insertions that affect oligomerization. This favors formation of tetrameric assemblies and precludes binding to anchoring proteins (Bardeci et al., 2021). Both proteins reside in distinct protein clusters but have extremely long branch lengths, inferring considerable evolutionary divergence (**figure 2.6; blue lines**).

2.6 Discussion

The development of three families of docking and dimerization (d/d) domains provides a adaptable toolkit for facilitating protein-protein interactions in cells. While these domains share structural similarities, they have diverged sufficiently to enable selective binding of distinct amphipathic helices. Since proteins containing each of these domains can be traced back to the last eukaryotic common ancestor (LECA), it is not possible—using the methods applied in this thesis—to determine which domain evolved first.

Furthermore, the absence of similar domains in prokaryotes provides no evidence for the identity of a primordial d/d domain, suggesting that this fold is unique to eukaryotes. Ancestral state reconstruction is likely the most effective approach for determining the structure of the original domain (Thornton, 2004).

All of the extant d/d domain proteins fit into these three categories, although RIIaD1, CATIP, and TPGS1 share characteristics of both the RID2 and RIID2 families (Dahlin et al., 2021). The classification of these proteins is based on their docking determinant regions. Given that RIIaD1 dates back to the LECA, it may represent a surviving example of an intermediary domain from which the RID2 and RIID2 families diverged.

Conservation in a protein is an example of survivorship bias. The absence of variation in highly conserved regions does not indicate that mutations do not occur there, but rather that such mutations are deleterious and thus eliminated by natural selection. This phenomenon parallels Abraham Wald's work during World War II on bomber armor placement (Mangel & Samaniego, 1984). Bombers returning from bombing runs were often decorated with bullet holes. Analysts initially suggested reinforcing areas of bombers that frequently sustained bullet holes. However, Wald recognized that these were the planes that had survived their missions, implying that damage in other, unscathed regions was likely fatal. Similarly, the poorly conserved regions of DPY-30, RIα, and RIIα d/d domains resemble the non-critical, damage-tolerant sections of aircraft. Mutations tolerated in d/d domains, therefore, highlight regions that do not participate in protein-protein interactions.

All families of d/d domain proteins are present in motile cilia and flagella, yet the interactions of RID2 and DPY-30-like proteins in these structures remain underexplored. This gap in knowledge reflects a historical bias in AKAP research, as more biochemical tools exist to identify RII-binding proteins, and type II AKAPs are more abundant than those that bind RI (Burgers et al., 2015; Carr & Scott, 1992). Future studies investigating the d/d domain-DDIP interactions of type I binding pairs would help complete our understanding of axonemal interactions. Another challenge in classifying ciliary d/d proteins is nomenclature. *Chlamydomonas reinhardtii*, a widely used model organism for studying ciliary organization, follows a proteomic naming convention distinct from that of its animal orthologs. The

importance of proteomic studies that provide a “Rosetta stone” linking *Chlamydomonas* and animal orthologs cannot be overstated (Zhao et al., 2019).

The high degree of primary sequence conservation of the d/d domain proteins is a hallmark of divergent evolution (Theobald & Wuttke, 2005). This evolutionary trajectory begins with domain duplication, facilitated by gene duplication, exon shuffling, gene fusion, or gene fission (Dohmen et al., 2020; Moore et al., 2008). Domain fusion tends to occur at either the C- or N-terminus of a protein, a pattern reflected in the positioning of d/d domains (Weiner et al., 2006). The most common mutations within a domain are microtranslations—point mutations that do not disrupt secondary structure (Jayaraman et al., 2022). These account for the sequence variability within d/d families. Because modular domain swapping preserves the original gene, there is reduced negative selection pressure on the neofunctionalization of the newly formed protein, allowing it to acquire novel functions (Rastogi & Liberles, 2005). The arrangement of the phylogenetic tree of the d/d domain proteins (**figure 2.6**) provides strong evidence for a divergent evolutionary path.

The conservation of intramolecular interactions between α-helix 1 and α-helix 2 serve as strong evidence against convergence. In cases of convergent evolution, the binding faces of the domains would be similar, as they are sculped by their role in intermolecular interactions with AKAPs/DDIPs. This requires specific amino acid contacts, which would be preserved. The intramolecular interactions maintaining the structure of the domain, however, simply need to stabilize each other. This could be achieved through a variety of methods, such as salt bridges, covalent disulfide bonds, hydrogen bonds, and simple hydrophobic interactions. The high conservation of aromatic pi-bond interactions provides a potent argument for a shared protein ancestor of these domains.

Figures for chapter 2

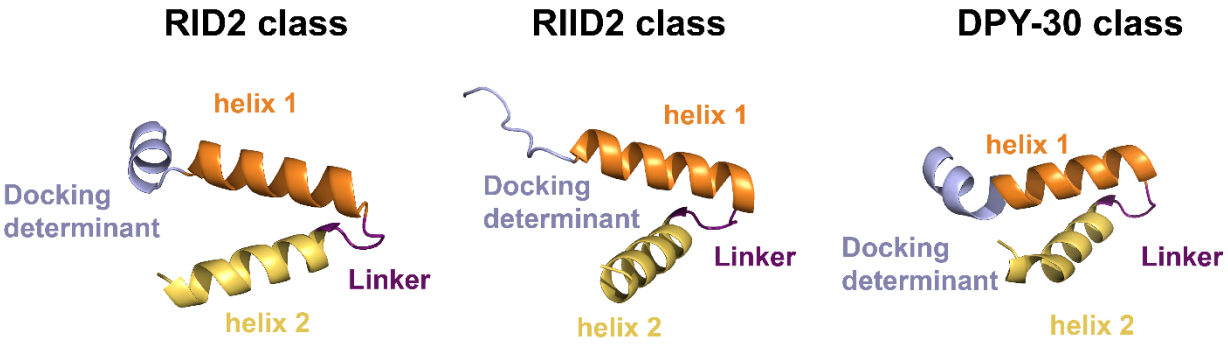

Figure 2.1: Docking and dimerization domain protomers share similar architecture. Models of the three d/d domain class protomers highlighting the docking determinant region (blue), α-helix 1 (orange), hinge region (purple), and α-helix 2 (yellow).

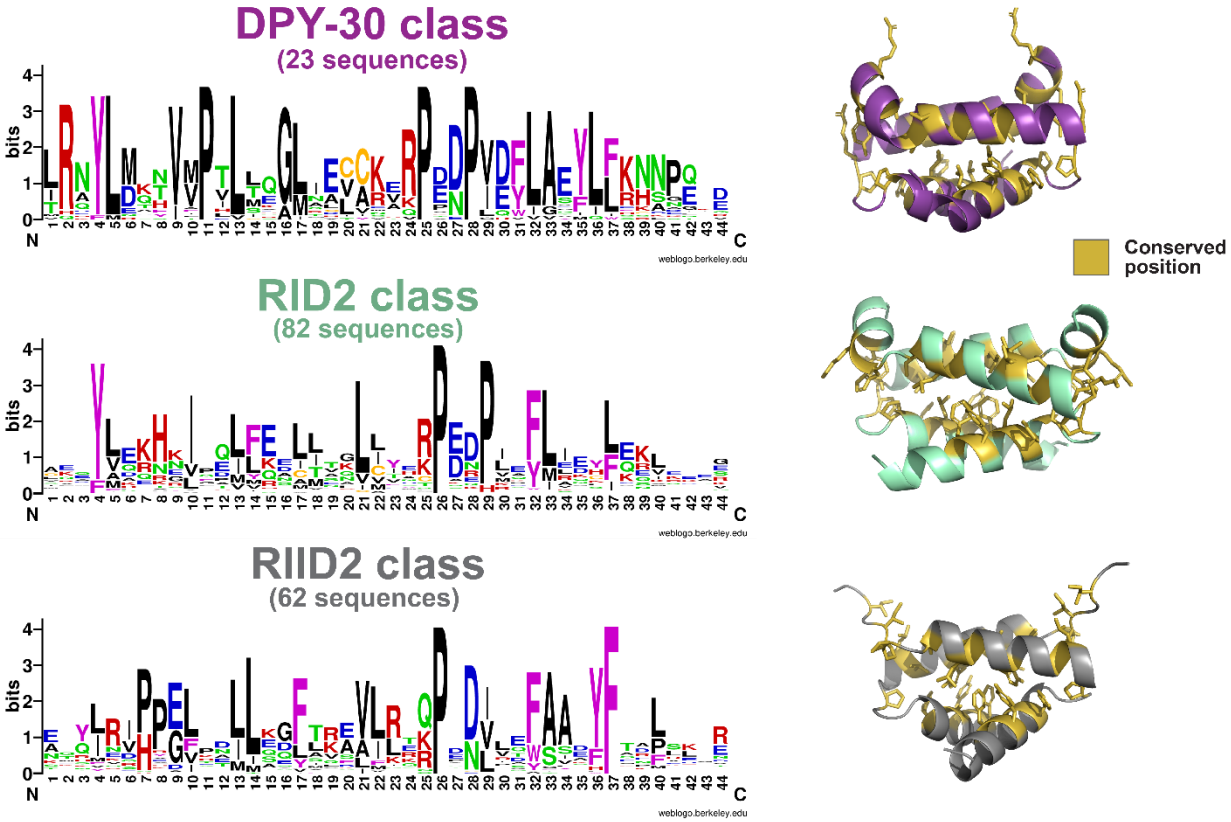

Figure 2.2: Conservation of d/d domains across the three domain classes. A). Conservation logo of DPY-30-like proteins (2 proteins and 23 evolutionarily distinct orthologs) (left). DPY-30 d/d domain with conserved residue side chains colored gold (right). **B).** Conservation logo of RID2 proteins (10 proteins and

82 evolutionarily distinct orthologs) (left). RIα d/d domain with conserved residue side chains colored gold (right). **C).** Conservation logo of RID2 proteins (9 proteins and 62 evolutionarily distinct orthologs) (left). RIIα d/d domain with conserved residue side chains colored in gold (right).

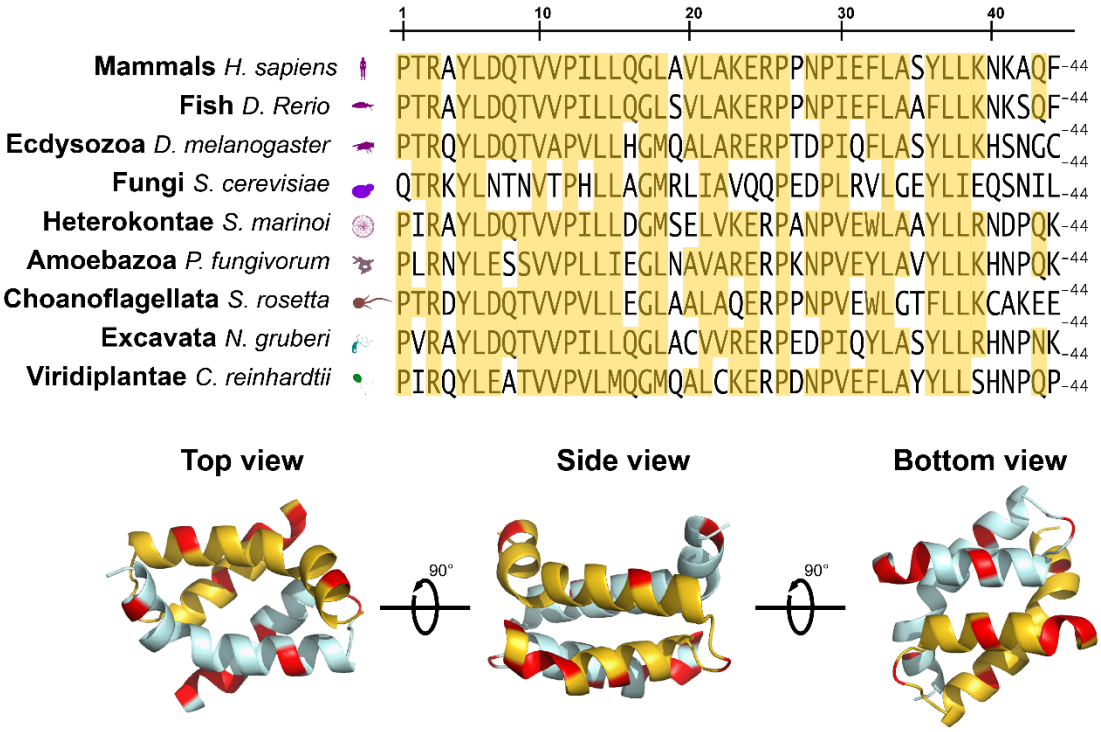

Figure 2.3: Analysis of conserved residues of the DPY-30 docking and dimerization domain (Top) Aligned sequences of DPY-30 d/d domains in mammals, fish, ecdysozoans, fungi, choanoflagellates, heterokonts, amoebozoans, excavates, and plants. Conserved residues are highlighted in yellow. (**Bottom)** Three models of the DPY-30 d/d domain with poorly conserved residues highlighted in red.

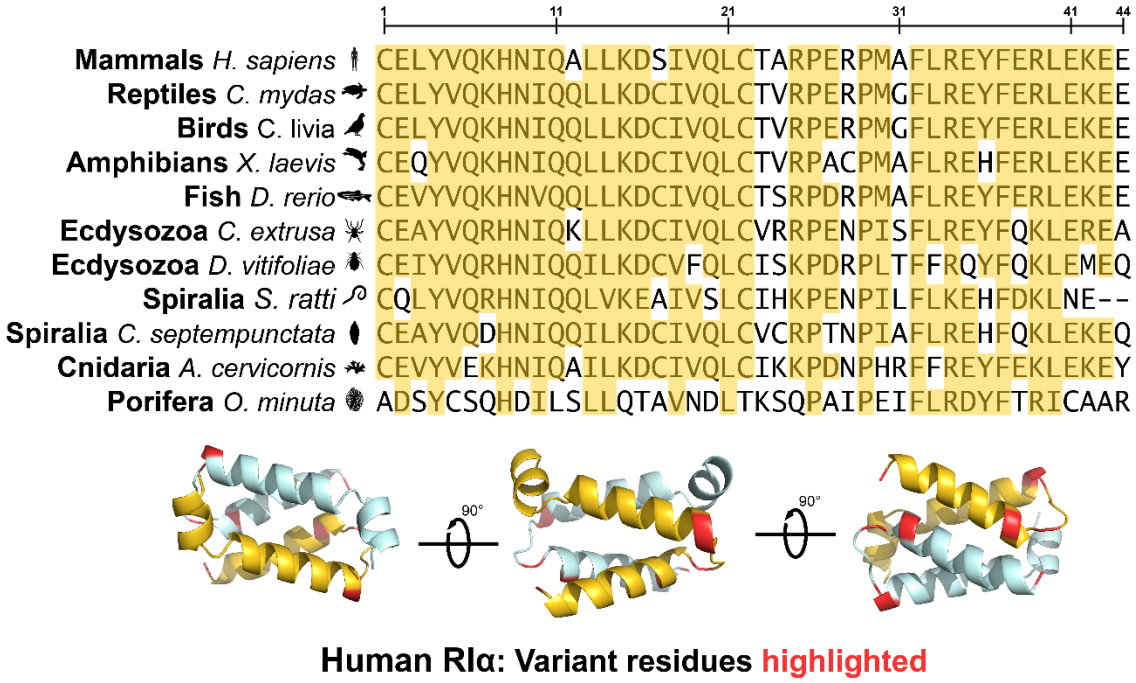

Figure 2.4: Conservation of the PKA RIα docking and dimerization domain. (Top) Aligned sequences of PKA RIα d/d domains in mammals, reptiles, birds, fish, ecdysozoans, spiralians, cnidarians, and poriferans. Conserved residues are highlighted in yellow. (**Bottom)** Three models of the PKA RIα d/d domain with poorly conserved residues highlighted in red.

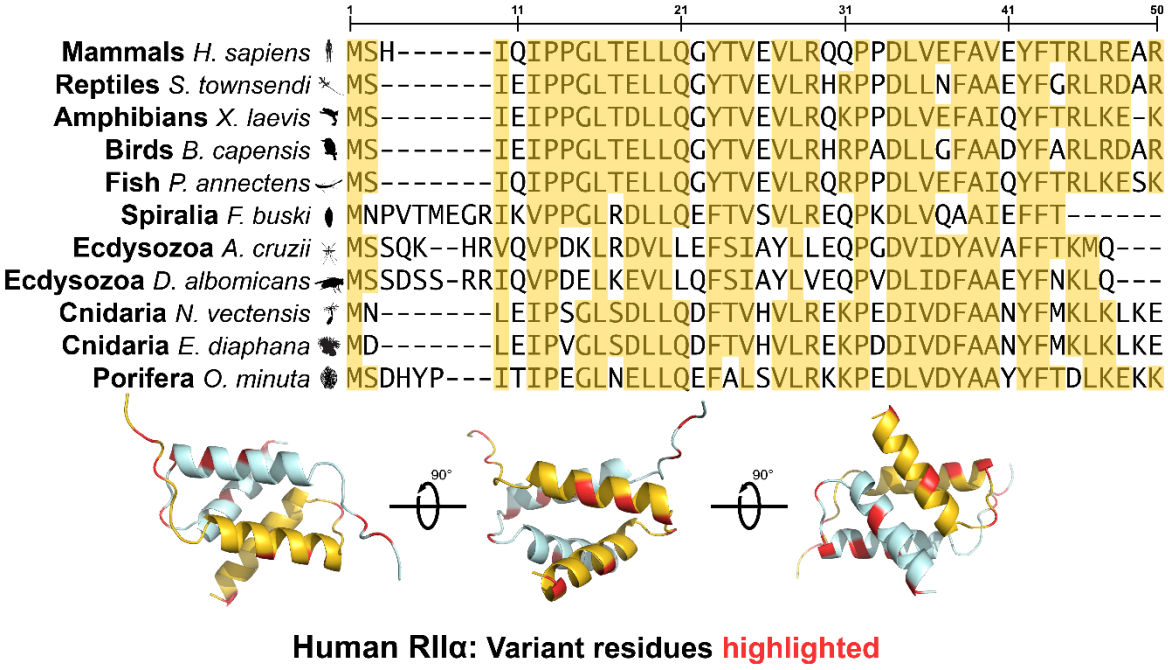

Figure 2.5: Conservation of the PKA RIIα docking and dimerization domain. (Top) Aligned sequences of PKA RIIα d/d domains in mammals, reptiles, amphibians, birds, fish, spiralians, ecdysozoans, cnidarians, and poriferans. Conserved residues are highlighted in yellow. (**Bottom)** Three models of the RIIα d/d domain with poorly conserved residues highlighted in red.

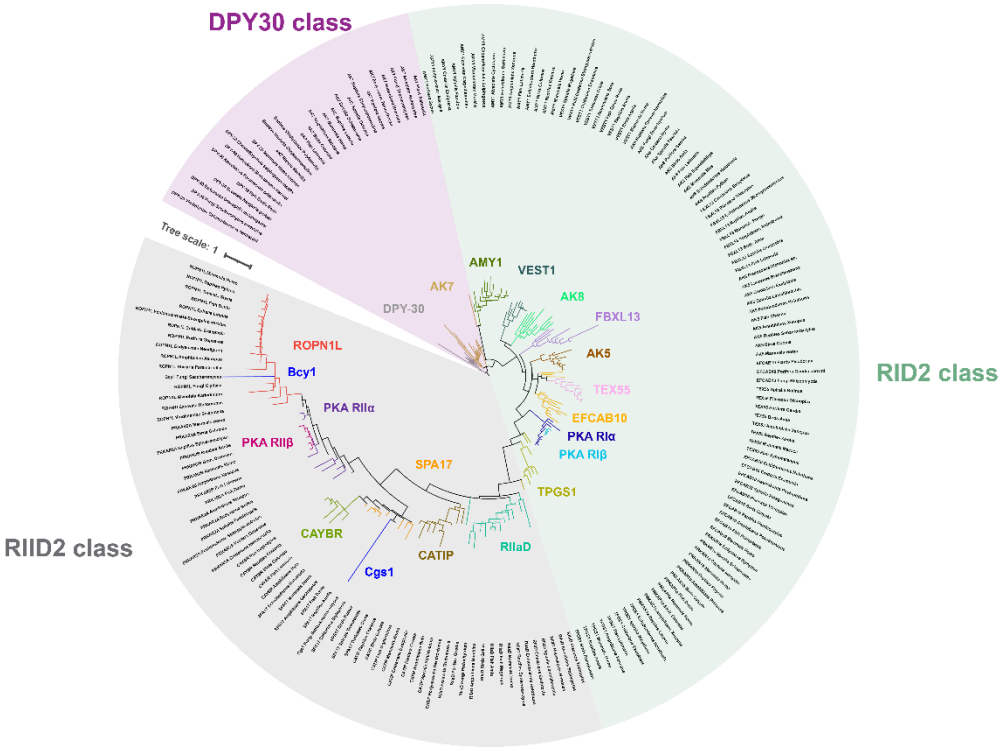

Figure 2.6: Phylogenetic tree of known d/d containing proteins. Each family of d/d protein arranges into distinct groups on this tree (DPY-30-like – purple, RID2 – green RIID2 – grey). Individual protein families cluster together (colored branches and labels) indicating a divergent pattern of development. The DPY-30 family was used as an outgroup.

Chapter 3 – Convergent evolution of AKAPs and DDIPs

3.1 Introduction

“Variations on a theme” are often the realm of composers such as Mozart, Brahms, Haydn and Benjamin Britten. Yet varying the use of a conserved molecular interface across a range of cellular contexts is also a sound biochemical principle. Modular protein-protein interactions are heavily utilized to connect enzyme binding partners and structural proteins that shape the architecture of the cell (Good et al., 2011; Scott & Pawson, 2009). Accordingly, interaction modules are a versatile group of protein domains that participate in the assembly of macromolecular machines, cell signaling networks and the subcellular tethering of enzymes. Prototypic examples include **P**lextrin **h**omology (PH) and **S**rc **h**omology 2 (SH2) domains (Lemmon, 2008; Lemmon et al., 1995; Pawson & Nash, 2003). Both are found in vertebrate, Drosophila, C. *elegans* and yeast proteins. This suggests an ancient origin of fundamental importance to eukaryotic biology. These polypeptide units support protein-lipid and protein-protein interactions to potentiate a variety of cell signaling responses. The PH domain is a highly conserved structure of approximately 120 amino acids that binds phospholipids in biological membranes and proteins, including the b-g subunits of heterotrimeric G proteins (Lemmon et al., 1995). Similarly, SH2 domains are about 100 amino acids that fold to form binding modules that recognize phosphotyrosine on the surface of target proteins (Pawson & Nash, 2000). Mutational and gene fusion events underlie the adaptive changes necessary for organisms to develop more elaborate functions and increasingly sophisticated tissue types. Thus, investigating the expansion of modular domains offers a fascinating glimpse into the complex evolution of protein networks.

According to Darwin’s theory of natural selection, mutations which harm the fitness of an organism are selected against. At a molecular level this leads to functionally important regions of a protein being conserved (Capra & Singh, 2007; Lisanza et al., 2024). Conversely, regions with a high degree of variability are sometimes less critical to the protein’s function. These regions can often sustain alterations in amino acids without adversely impacting the organism’s fitness (Nei & Kumar, 2000). This process is illustrated in the emergence of "docking and dimerization domains" (d/d domains) (Newlon et al., 2001; Newlon et al., 1999; Scott et al., 1990). These modules were originally discovered within the dimeric regulatory (R) subunits of Protein Kinase A (PKA). These structures mediate antiparallel dimerization of each peptide

chain to create a binding site for **A**-**k**inase **a**nchoring **p**roteins (AKAPs; (Banky et al., 2000; Banky et al., 2003; Carr et al., 1991; Gold et al., 2006; Gold et al., 2011)). The bioinformatic and phylogenetic studies presented in this perspective argue that the origins of the protein kinase A interface with AKAPs can be traced to unicellular organisms which existed long before the emergence of either the kinase or anchoring proteins (Langeberg & Scott, 2015; Omar & Scott, 2020).

3.2 Methods

Data acquisition and curation

AKAP protein orthologs were acquired through clustered NCBI BLAST searches on the human isoform of each protein. Non-metazoan orthologs were acquired in tandem with non-clustered BLAST searches excluding the metazoan taxa. The search size limit was set to 1000 sequences to ensure coverage of orthologs. The raw sequences from the blast search were then curated by removing any sequences labeled “hypothetical,” “low quality,” “predicted,” or sequences attributed to different proteins than the target of the search. Finally, the presence of an amphipathic helix was determined, and proteins lacking the motif were excluded.

Last common ancestor inference

The evolutionary history/last common ancestor identity of each protein was determined by compiling a list of unique phyla in which extant orthologs are found.

Generation of phylogenetic trees

The collections of protein orthologs were aligned in Mega11 using the MUSCLE algorithm or CLUSTALω (the alignment with the fewest gaps was used). Aligned sequences were then fed into the phylogenic tree generating tool IQTREE on the CIPRES gateway for construction of maximum likelihood phylogenetic trees. The program was instructed to test all amino acid substitution models and utilize the best one. 4,000 bootstraps were used to determine the topology of the consensus tree. Trees were visualized using the Interactive Tree of Life (iTOL) server.

Generation of consensus logos and sequence alignments

Anchoring helices were isolated to make conservation logos of the amino acids contained in each motif using the program Weblogo. Larger letters represent greater degrees of conservation. Example sequences were aligned in Adobe Illustrator to demonstrate regions of low or high conservation. Silhouettes of representative species were used from the public domain collection of the website phylopic.org.

Protein Modeling

Predictive protein models were generated using the Alphafold3 server. Representative models were chosen contingent on convergence of the 5 models provided, as well as agreement with known elements of protein structure (when available). Models were colored and positioned using Pymol 3.1.

3.3 AKAP evolution – the metazoan "explosion"

Informatic analyses suggest that the evolutionary path of AKAPs occurred after the existence of PKA catalytic and regulatory subunits. While invertebrate animals, including the Tunicates and lancelets, encode a single PKAc subunit gene, the *PRKACA* and *PRKACB* genes rose from a gene duplication event in early vertebrates (Søberg et al., 2017). In contrast the *PRKACG* gene is intronless, only appears in primates, and seems to be retrotransposon derived (Reinton et al., 1998).

Evolution of the regulatory subunits (RIα and RIIα) has followed a more circuitous path. These genes arose from an early event where a primordial four helix like bundle called the docking, and dimerization (d/d) domain. This region became fused to cyclic nucleotide binding domains analogous to the bacterial catabolite transcriptional activator gene (Dahlin et al., 2021; Toda et al., 1987). Structural studies show clear differences between the homodimerizing d/d domains of RIα and RIIα (Fig. 1, insets). In RIα, a stable helical cluster at the N terminus of each RIα protomer forms a proteinase resistant dimer held together by inter-subunit disulfide bonds ((León et al., 1997; Taylor et al., 2012) **figure 3.1** inset 1). In contrast, the more flexible d/d domain of RII adopts a conventional four-helix bundle-like configuration that lacks flanking helices ((Dahlin et al., 2021; Gold et al., 2006), **figure 3.1**, inset 2). Phylogenetic projections presented in Fig. 1 depict the *PRKAR1* and *PRKARII* genes as appearing around the same time as the duplication of Cα and Cβ genes at the metazoan last common ancestor (LCA, **figure 3.1**).

Twenty-three AKAPs were arranged on a cladogram of metazoan classes according to each protein's last common ancestor (**figure 3.1**). Last common ancestors were calculated by detecting the nearest node on the metazoan tree which would explain a protein's distribution in extant species collected by protein BLAST searches (Nei & Kumar, 2000). Three primordial AKAPs emerged at this point: OPA1, dAKAP2, and AKAP28 (**figure 3.1**). These are the only AKAPs present in the sponge class Porifera. OPA1 anchors PKA to the outer mitochondrial membrane, AKAP28 is a stabilizing architectural element of motile cilia whereas the biological role of dAKAP2 is more varied (Kultgen et al., 2002; McCartney et al., 1995; Pidoux et al., 2011; Rogne et al., 2018; Tingley et al., 2007).

The appearance of dAKAP1 and Merlin coincided with the advent of ParaHox genes, which dictate the development of more complex anatomy. Merlin connects PKA to the cytoskeleton whereas dAKAP1 resides at the outer mitochondrial membrane and regulates translation (Gabrovsek et al., 2020; Grönholm et al., 2003). Hence, AKAP targeting of PKA is unique to animals (Peng et al., 2015). Tracing the appearance of AKAPs through the metazoan clade reveals an increase in anchoring proteins as the biological complexity of animal cells expanded.

The principal explosion in AKAP complexity occurs at the base of the vertebrate lineage (**figure 3.1**). Fourteen AKAPs originate here, including dual-helix AKAPs (SKIP and AKAP220). At this point we see the emergence of type I R subunit selective AKAPs (GPR161 and smAKAP). This burst in AKAPs is consistent with their role in spatially targeting PKA holoenzymes upon development of nervous systems and the increased complexity of multicellular organisms (Ilouz et al., 2012; Ilouz et al., 2017). These events are concomitant with the appearance of the RIβ and RIIβ isoforms (**figure 3.1**).

After the onset of vertebrates, fewer AKAPs emerged. The tetrapod linage saw the debut of AKAP4 which synchronizes sperm flagella action and AKAP79/150, a membrane proximal scaffolding protein that coordinates phosphorylation of hippocampal AMPA receptors in long term potentiation (**figure 3.1, red text**). The amniote lineage expanded on the organization of sperm flagella with AKAP3, sharing a preference of anchoring type I PKA with AKAP4. Around this time other specialized RI anchoring proteins appeared including mitochondrial SKIP and the membrane tethered smAKAP (**figure 3.1, red text**). The phylogenetic data in **figure 3.1** indicate that early AKAPs appeared after the formation of the alpha Isoforms

of their R subunit binding partners and the advent of PKAcα and PKAcβ. A major expansion of the AKAP class occurred in vertebrates.

3.4 AKAP79 domain evolution

AKAP150 repeat sequences alter anchored holoenzyme topology. AKAP79 and AKAP150 are products of the *AKAP5* gene (**figure 3.3 A**; (Tunquist et al., 2008)). Early studies recognized a repeat sequence in murine AKAP150 that was not present in human AKAP79 (Bregman et al., 1989; Carr, Stofko-Hahn, et al., 1992; Sarkar et al., 1984). Both anchoring proteins contain an invariant PKA anchoring helix and conserved calcineurin binding domains ((Vincent M. Coghlan et al., 1995; Dell'Acqua et al., 1998) **figure 3.2E**). Three conserved polybasic regions anchor adenylyl cyclases and PKC and assist in plasma membrane tethering via palmitoyl groups (Bauman et al., 2006; Delint-Ramirez et al., 2011; Faux et al., 1999; Fraser et al., 2000; Kang et al., 2008; Keith et al., 2012). AKAP150 family members are classified by an amino acid repeat sequence that is predicted to form a beta solenoid linker (**figures 3.2 A, & 3.3**).

Cladograms of AKAP79 and AKAP150 exhibit distinct patterns of species distribution indicating two separate events leading to their formation (**figure 3.2B & C).** AKAP79 is present in all classes of tetrapod: amphibians, reptiles, birds, and mammals. AKAP150 resides in 27 rodent species and 17 species of passerine birds (**figure 3.2C**). Remarkably, rodent AKAP150 repeat sequences differ in amino acid composition and length from passerine forms (**figure 3.2C & D**). Rodents harbor an octapeptide VGQAEEAT sequence that repeats imperfectly 8-44 times (**median 32; figure 3.3C & D; blue**). Passerine birds encode a DAVSVQ hexapeptide repeat between 40 and 69 times (**median 57; figure 3.3C & D; green**). The median length for rodents is 256 amino acids (**figure 3.3D**; **blue**) as compared to 342 amino acids for birds (**figure 3.3D; green**). These data raise an interesting conundrum. Do AKAP150 repeat sequences alter recruitment of binding partners or allosterically impact scaffolded enzyme activities?

AKAP150 alters the topology of the anchored PKA holoenzyme. Despite their distinct primary structure, the rodent and passerine AKAP150 repeat units fold into a beta solenoid composed of parallel beta sheets as predicted by AlphaFold 3 (Abramson et al., 2024). Rodent repeats have a wider region of beta strand (**figure 3.3)** These substructures confer stability and rigidity by forming a planar network of hydrogen bonded and extended polypeptide strands (Nowick, 2008). Molecular modeling of anchored PKA

holoenzymes infer that structural differences between AKAP79 and AKAP150 manifest changes in the range of motion of their anchored PKA holoenzymes (**figure 3.4A & B**). AKAP79 adopts a tightly packed configuration where all five protein members of the macromolecular complex are compressed (**figure 3.4A**). In contrast the beta solenoid repeat of AKAP150 separates the flanking R-C dimers to induce a more extended configuration of the anchored PKA holoenzyme (**figure 3.4B**).

To test this postulate human AKAP79 and rat AKAP150 binding to R subunits was measured by FRAP (**figure3.4 C-F**). The RII half-times for AKAP79 is 14.42±2.1 s but it decreases to 12.26±0.9 s in the presence of AKAP150 (**figure 3.4C-E; silver**). As expected AKAP79 and AKAP150 recovery rates for RII were comparable at 0.049±0.007 s^{-1} and 0.057±0.004 s^{-1} respectively (**figure 3.4 C, D, & F; silver**).

Measuring rates of photorecovery serve as indices for altered membrane mobility and steric hindrance. AKAP79's recovery rate of 0.079±0.003 s^{-1} for RIα is lower than AKAP150's rate of 0.11±0.01 s^{-1} (**figure 3.4C, D & F; silver & gold**). This indicates that AKAP150 binds RI more poorly than AKAP79. This is perhaps more evident when we compare rate constants showing that RI (gold) is more readily released from AKAP150 than from the more compact AKAP79 ortholog (**figure 3.4E & F; gold**). This is the first evidence that the extended beta solenoid linkers in AKAP150 subtly impact PKA anchoring.

3.5 DDIPs as a category of anchoring protein

All three of the d/d domain classes interact with helical regions that in some respects resemble PKA anchoring proteins. This previously unidentified group of interactors do not bind protein kinases. Therefore, we have named this burgeoning family **D**/**D** domain **i**nteracting **p**roteins (DDIPs). This new scaffolding protein class exhibits a broad range of biological roles that include constraining the architecture of motile cilia and flagella, assembly of the nuclear histone methylation machinery, and the formation of macromolecular complexes that participate in cell metabolism.

Structural modeling predicts that DDIPs associate with their binding partners in a manner that is distinct from AKAPs. For example, DPY-30 family members only require four turns of an amphipathic helix for high affinity interaction with their binding partners (Tremblay et al., 2014). In contrast, five helical turns are necessary for R subunits of PKA binding to AKAPs (Alto et al., 2003; Brondani et al., 2013; Carr & Scott,

1992; Carr et al., 1991; Gold et al., 2006) Figure 3A, green). An evolutionary tree of the DDIP class reveals that most of its members are more ancient than PKA anchoring proteins (**figure 3.5**). Also, DDIPs are predominantly found in cilia and flagella, where they play a structural role in the axoneme (Rao et al., 2024). For example, CFAP65 first appeared in diaphoretickes (a parent clade of plants, diatoms and flagellates) as a structural component of the ciliary axoneme ((Rao et al., 2024); **figure 3.5**). Interestingly, certain proteins originally designated as PKA anchoring proteins such as AKAP28 could be reclassified as DDIPs, as they bind RIID2 proteins (Kultgen et al., 2002). In keeping with this notion, both CFAP65 and AKAP28 participate in protein-protein interactions that provide rigidity to support dynein motor function in cilia and flagella. These DDIP scaffolding proteins also integrate other signaling elements, such as calcium-responsive components, E3 ligases, and adenylate kinases (Zhao et al., 2019). Interestingly, certain DDIPs are present at the last eukaryotic common ancestor (LECA; **figure 3.5**). ASH2L and BAP18 bind DPY-30, promoting histone methylation and the reading of methylated histones, respectively (Lee et al., 2021). Thus, a key finding is that the conserved DDIP interface maintains the integrity of macromolecular machines that coordinate a broader range of biological processes than A-kinase anchoring proteins.

3.6 Analysis of AKAP gain of function

The sporadic evolution of the PKA binding helix on A-kinase anchoring proteins contrasts with the gradual specialization of R subunits from DDIPs. AKAP helices accumulate neutral mutations that ultimately lead to the creation of a PKA binding helix (Alto et al., 2003; Gold et al., 2013). This program of molecular metamorphosis has occurred through a variety of mechanisms. We provide three examples of anchoring proteins that have developed from extant orthologs that do not anchor PKA. (**figure 3.6**). The evolutionary path of each protein differs in the time from their origin to the appearance of a functional AKAP form (**figure 3.6; circle and bold line**). First, we introduce how the mitochondrial GTPase OPA1 became a PKA anchoring protein at the onset of the Metazoan clade ((Pidoux et al., 2011); **figure 3.7**). Second, we follow the path of the ERM proteins (ezrin, radixin, and moesin) that bring PKA into cortical actin networks that connect to cell membranes ((Dransfield et al., 1997; Funayama et al., 1991; Grönholm et al., 2003;

Semenova et al., 2009); **figure 3.8**). Third, we highlight the AKAP8 family of RNA-binding proteins that exemplify a more recent gain of PKA anchoring function in the form of AKAP95 ((Hausken et al., 1996); **figure 3.9**). A common feature of each exemplar family is that a gradual accumulation of neutral mutations occurred until a PKA anchoring helix emerged.

OPA1

Optic atrophy type 1 (OPA1) is a dynamin related GTPase that regulates mitochondrial morphology, cristae structure, and oxidative phosphorylation (Lee et al., 2023). Mutations in OPA1 underlie optic atrophy, a condition where the optic nerve is damaged and causes blindness (Lenaers et al., 2012; Misaka et al., 2002; Yen et al., 2010). OPA1 originated within the opisthokont lineage, as indicated by its presence in both fungal and metazoan forms. It is one of the earliest metazoan AKAPs, coordinating PKA signaling in lipolysis at the outer mitochondrial membrane (Pidoux et al., 2011). OPA1 dimerizes or oligomerizes into a ring-shaped 34-mer that is composed of antiparallel dimeric units ((Nyenhuis et al., 2023; Von Der Malsburg et al., 2023), **figure 3.7A**). The amphipathic PKA binding helix (yellow) resides on the exposed outer face of each OPA1 dimer in the ring assembly (**figure 3.7A**; **inset**).

Analyzing the OPA1 amphipathic helix from fungal to metazoan phyla reveal an invariant region that begins with a conserved pair of basic residues (lysine, lysine/arginine (**figure 3.7B**). While most AKAPs have hydrophobic residues in this position, OPA1 retains high affinity for both RI (12.5±2.8 nM) and RII (14.0 ±1.4 nM; (Pidoux et al., 2011)). Only fungal OPA1 lacks this region and does not anchor PKA (**figure 3.7B & C**). A phylogenetic tree of OPA1 orthologs further highlights the evolutionary distance between the fungal and metazoan forms (**figure 3.7C**). The fungal OPA1 helix diverges with aspartic acid at position 6 (**Figures 5B & D**). We and others have shown that the substitution of a negatively charged glutamic acid at this position in the amphipathic helix is sufficient to prevent PKA binding in other AKAPs ((Burgers et al., 2016); **figure 3.7E**). These latter studies exemplify the impact of inserting a single charged residue in the AKAP helix as a negative determinant for PKA anchoring.

ERM proteins and Merlin

The ERM proteins ezrin, radixin, and moesin, and their close relative merlin, link the plasma membrane to the actin cytoskeleton to control cell shape (Michie et al., 2019). Unlike the previous example, only about half of vertebrate ERM proteins have gained AKAP function. This is best demonstrated in a phylogenetic tree of this family (**figure 3.8A**). All merlin orthologs cluster together and anchor PKA, while metazoan ERM proteins form separate groups (**figure 3.8A**). Invertebrate ERM proteins cluster by phylum, with cnidarian, ecdysozoan, and spiralian forms showing closer relationships. Structurally each ERM family member shares a similar domain organization consisting of a globular FERM domain fused to an extended helical stalk ((Tsukita & Yonemura, 1999); **figure 3.8B**) .

The AKAP helix emerged within the coiled-coil stalk of ERM proteins (**figure 3.8B; yellow**). By aligning the AKAP helix sequences of radixin across metazoan phyla, we observe a gradual accumulation of neutral mutations leading up to the vertebrate AKAP form (**figure 3.8C; red**). As with OPA1, once the helix acquires PKA-anchoring capability, it becomes highly conserved (**figure 3.8C; blue**). To illustrate this point, each sequence is paired with its percent identity to the *Homo sapiens* FERM domain, highlighting that even distantly related orthologs, such as those from poriferans, maintain a much higher degree of conservation (**figure 3.8D**). Lastly, a helical wheel comparison of the human radixin anchoring helix with a poriferan ortholog from *Oopsacas minuta* reveals a key structural distinction. The human helix features an extended hydrophobic face that enables PKA binding (**figure 3.8D; top**), whereas the poriferan version has fewer hydrophobic residues, thereby rendering it insufficient for PKA anchoring. Hence, the transition of ERM proteins toward becoming A kinase anchoring proteins is partial whereas merlin has always had the capacity to anchor PKA.

The AKAP95/AKAP8 family

The AKAP95/AKAP8 family highlights a different pathway for PKA anchoring evolution. This anchoring protein gained an amphipathic helix via insertion. AKAP95, the first member of the family to be identified, was discovered in a protein interaction screen using radiolabeled RIIα (V.M. Coghlan et al., 1995; Coghlan et al., 1994; Eide et al., 1998). Subsequently, other AKAP8 family members were identified including ZNF326, AKAP8L/ha95, and AKAP95. All of these proteins are involved in RNA splicing (Clister et al., 2019; Close et al., 2012; Coghlan et al., 1994; Collas et al., 1999; Eide et al., 1998; Hu et al., 2016;

Kvissel et al., 2007; Yang et al., 2001). These proteins share common domains, including a YG domain which drives RNA binding and phase condensation, a nuclear membrane targeting sequence (AKAP8 and AKAP8L only), a nuclear localization sequence and two zinc fingers (Li et al., 2020) (**figure 3.9A**). Only mammalian AKAP95 orthologs possess an amphipathic helix (**figure 3.9B**). Alignment of AKAP95 orthologs suggests that the helix was inserted, as flanking regions are conserved in non-PKA anchoring orthologs (**figure 3.9C**). Moreover, the acquisition of a PKA anchoring helix in AKAP95 is a relatively recent evolutionary event as this anchoring protein is only found in mammals (**figure 3.9**). Interestingly, the PKA anchoring role of AKAP8/AKAP95 remains somewhat controversial. This anchoring protein resides in the nucleus and hence is partitioned from PKA that is exclusively cytoplasmic during most of the cell cycle (Langeberg & Scott, 2015). Hence, the PKA anchoring function of AKAP95 may only occur during mitosis at nuclear envelope breakdown (Coghlan et al., 1994; Eide et al., 1998; Hetzer, 2010; Zhang et al., 1996). Intriguingly, the PKA-binding domain of AKAP95 is essential for direct interaction with DPY-30 (Bieluszewska et al., 2018). This anchoring protein may function as both an AKAP and a DDIP.

3.6 Discussion

AKAPs predominantly evolved in metazoans in response to the appearance of anchorable PKA regulatory subunits. This reflects the development of earlier DDIPs which conformed to existing d/d domains (figure 3.1). Without AKAPs and DDIPs, a docking and dimerization domain still serves a functional purpose, in that it permits dimerization. In the absence of d/d domains, however the AKAP/DDIP helices serve no role beyond providing the structure of an α-helix. While the d/d domain proteins display hallmarks of divergent evolution, their partner anchoring proteins portend convergence. This requires the antecedent existence of d/d domains to serve as a die which evolutionary pressures formed the anchors against.

The DDIPs ASH2L and BAP18 illustrate this phenomenon, where proteins develop anchoring capabilities in response to an unmet need. They are involved in writing and detection of histone methylation at H3K4 (Ma et al., 2022; Vermeulen et al., 2010). Both complex with DPY-30, their predecessor which occurred at the LECA (**figure 3.5**). ASH2L emerged later at the opisthokont lineage, and enhances the histone methylation capabilities of the COMPASS complex (Lee et al., 2021). BAP18 changes the COMPASS complex to act as an H3K4 methylation reader (Sun et al., 2020). This DDIP originated in the

metazoan lineage, following both ASH2L and DPY-30 (**figure 3.5**). These proteins follow a logical order, where DPY-30 originated first, as it is sufficient to allow the COMPASS complex to mono and di-methylate H3K4 (Tremblay et al., 2014). Next, ASH2L refined this ability, stabilizing the COMPASS complex to efficiently tri-methlyate H3K4 (Lee et al., 2021). Finally, BAP18 emerges to read the trimethylated histones (Sun et al., 2020). The emergence of each of these proteins both refines the process of epigenetic signaling and creates a new niche which is filled by the emergence of a later protein.

The functionalization of the AKAP5 gene products illustrates convergent evolution of separate domains in an AKAP. While the amphipathic helix is highly conserved across all orthologs of AKAP79/150 it has gained other domains over its existence to fine-tune its function. The calcineurin-anchoring VIVIT motif emerged during the tetrapod clade as there are amphibians with and without the motif (**figure 3.2E**). Reptiles and birds ubiquitously have the VIVIT motif, while mammals have a similar motif, the PIXIT motif (**figure 3.2E**). These motifs are highly conserved indicating that fixation of each refinement readily occurred.

The fixation of the AKAP150 repeat regions in rodents and passerine birds exists as a riddle. The similarity of the topology of each repeat suggests, nay, screams out the process of convergent evolution (**figure 3.3**). But the repeats' function remains nebulous. The repeats do not modulate kinase anchoring (**figure 3.4),** so their function is likely to be more subtle, such as regulating crosstalk between enzymes anchored by the AKAP. Crystallization of rodent and passerine forms of the domain to validate the structural models, as well as functional experiments are needed to elucidate the specifics about this beguiling fold.

The temporal requirements of AKAP convergent evolution are perhaps best illustrated in the evolutionary tree presented in figure 3.1. Three anchoring proteins (OPA1, dAKAP2 and AKAP28) were present coincidentally with RIα and RIIα at the last common ancestor before the "vertebrate AKAP explosion" (**figure 3.1**). Of note is that merlin emerged around the appearance of the ParaHox genes which pattern the anterior–posterior development in most animals (Rawat et al., 2012). This process requires close coordination with the actin cytoskeleton, and is very much in keeping with merlin's role in maintaining the structural integrity of cells (Morrow & Shevde, 2012). Also, merlin is an essential gene whereas its relatives ezrin, radixin, and moesin are non-essential genes (Morrow & Shevde, 2012). Loss of one ERM protein can be successfully complemented by increased expression of another member of the family

(Viswanatha et al., 2013). Most AKAPs can only be traced to vertebrates, where an expansion of 16 anchoring proteins were utilized to coordinate spatial integration of cAMP signaling events ((Omar & Scott, 2020); **figure 3.1; blue-tinted box**). This time frame was where certain ERM proteins began to take on PKA anchoring function.

Another emerging feature is that certain scaffolding proteins may fall under both the DDIP and AKAP designations. The *Chlamydomonas reinhardtii* axonemal radial spike protein, RSPH3, was christened AKAP240 after the discovery of two amphipathic helices, one which prefers DPY-30 and one which prefers RIID2 proteins (Rao et al., 2024). It was designated as an AKAP despite the fact that plants lack PKA (Peng et al., 2015). We hope that the designation of DDIP both provides correct attribution to the function of these ancient scaffolds and incites research to identify more of these proteins, as there as a great disparity between the 23 known d/d domain proteins and the 5 non-AKAP DDIPs (**figure 3.5**).

For a metazoan example of a covert DDIP, AKAP28 is a structural element in motile cilia that not only binds R subunits but interacts with other RIID2 proteins such as SPA17A and RopN1L (Dahlin et al., 2021; Omar & Scott, 2020). Likewise, AKAP95 retains the ability to bind RII and DPY-30 depending upon which subcellular compartment this anchoring protein occupies (Bieluszewska et al., 2018; Kultgen et al., 2002). These anchoring proteins are components of motile cilia, sperm flagellum, and radial spoke proteins that control axoneme motility in *Chlamydomonas reinhardtii* (Gaillard et al., 2001; Macleod et al., 1994; Mei et al., 1997; Rao et al., 2024). Most of these AKAPs were discovered by interaction cloning strategies that used the RII-overlay, a far-Western blot procedure as the screen. Consequently, these d/d domain interacting proteins may have been inadvertently misassigned as PKA anchoring proteins (Carr & Scott, 1992; Lohmann et al., 1984). Needless to say, it is likely that new variations of DDIP interfaces that fine tune cellular behavior will make their début soon.

Figures for chapter 3

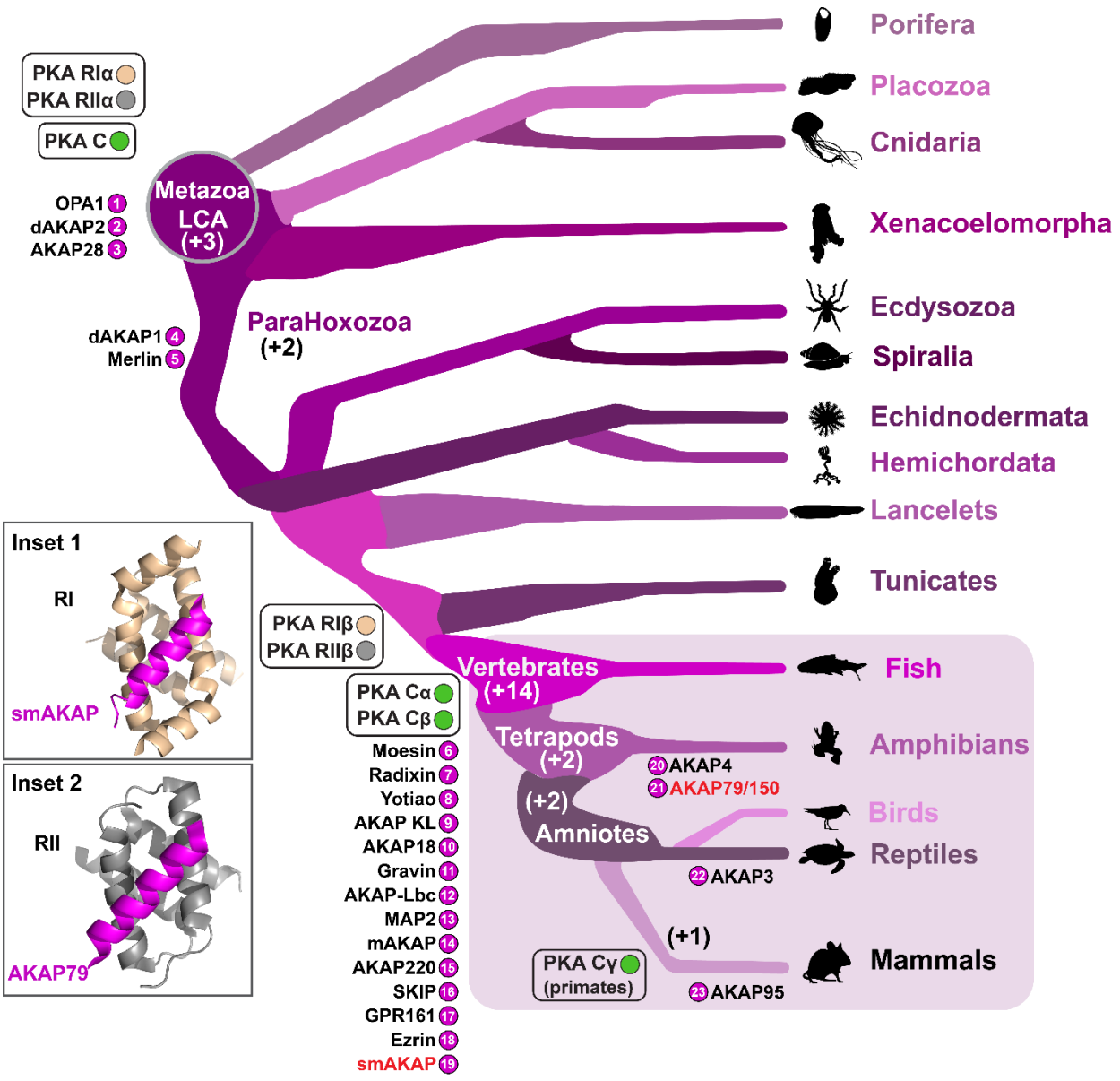

Figure 3.1: Metazoan cladogram of AKAP origins. Three AKAPs (OPA1, dAKAP2, and AKAP28) were present in the last common metazoan ancestor. Two additional AKAPs (dAKAP1 and Merlin) arose in the parahoxozoa clade. The vertebrate clade experienced an expansion in AKAP diversity, with the majority of AKAPs originating in this lineage.

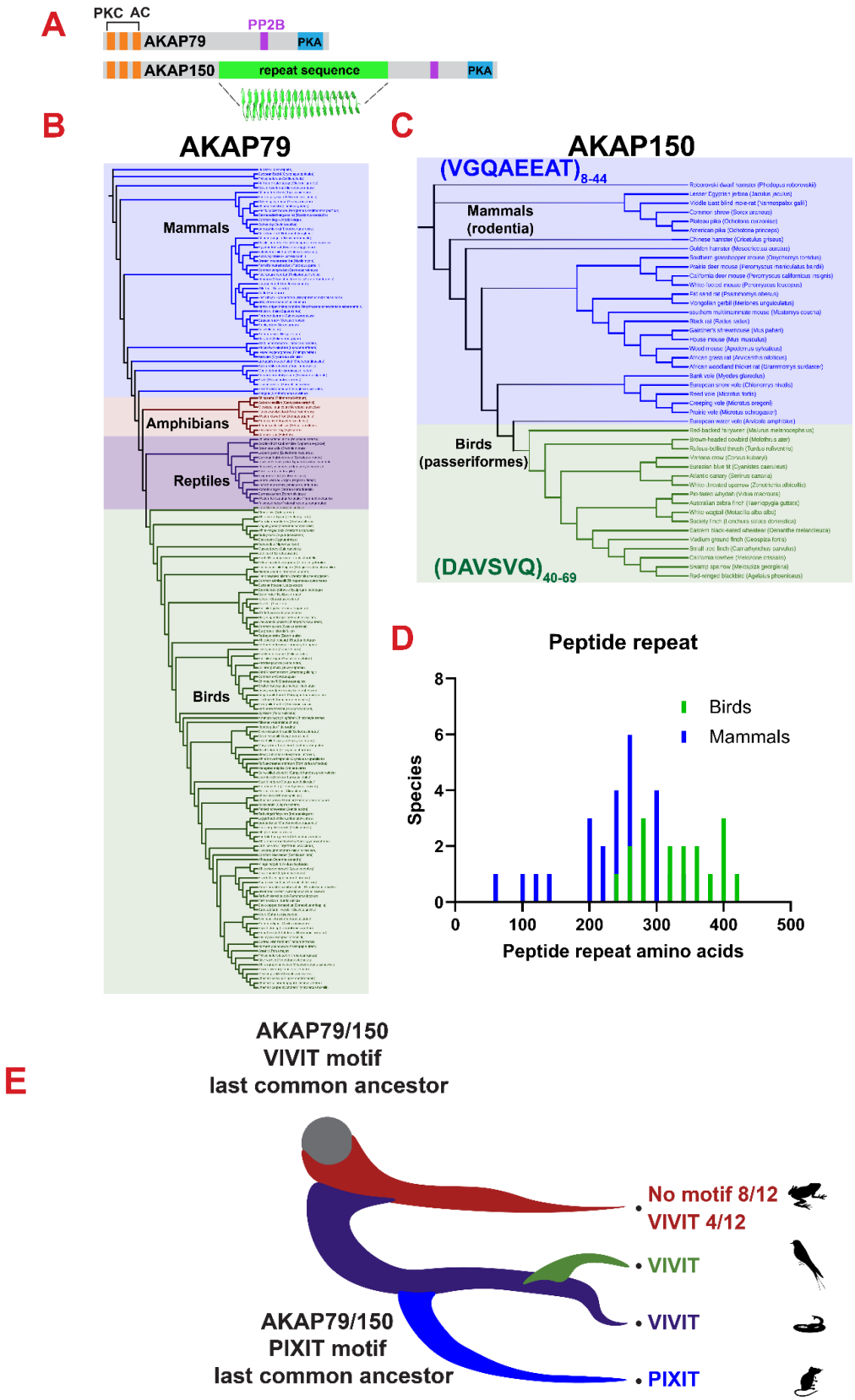
A
PKC AC
PP2B
AKAP79
PKA
AKAP150
repeat sequence
PKA
B
AKAP79
Mammals
Amphibians
Reptiles
Birds
C
AKAP150
(VGQAEEAT)8-44
Mammals
(rodentia)
Birds
(passeriformes)
(DAVSVQ)40-69
D
Peptide repeat
Birds
Mammals
Species
0
2
4
6
8
0
100
200
300
400
500
Peptide repeat amino acids
E
AKAP79/150
VIVIT motif
last common ancestor
No motif 8/12
VIVIT 4/12
VIVIT
VIVIT
PIXIT
AKAP79/150
PIXIT motif
last common ancestor

Fig. 3.2: AKAP79/150 domain analysis. (A) Diagram of domains on AKAP79 and AKAP150. Anchoring domains are conserved, but AKAP150 contains a unique a beta-helical peptide repeat. **(B)** Cladogram of AKAP79-containing species present in all tetrapod classes. **(C)** Cladogram of AKAP150-containing species. AKAP150 restricted to the Passerine bird order and the rodent mammal order, with distinct repeat sequences: VGQAEEAT for rodents and DAVSVQ for birds. Repeat number varies by species. **(D)** Histogram of the repeat lengths (amino acids) for both passerine (green) and rodent (blue) forms, with passerine repeats being longer due to containing more repeating units. **(E)** Cladogram of calcineurin binding motifs in AKAP79/150.

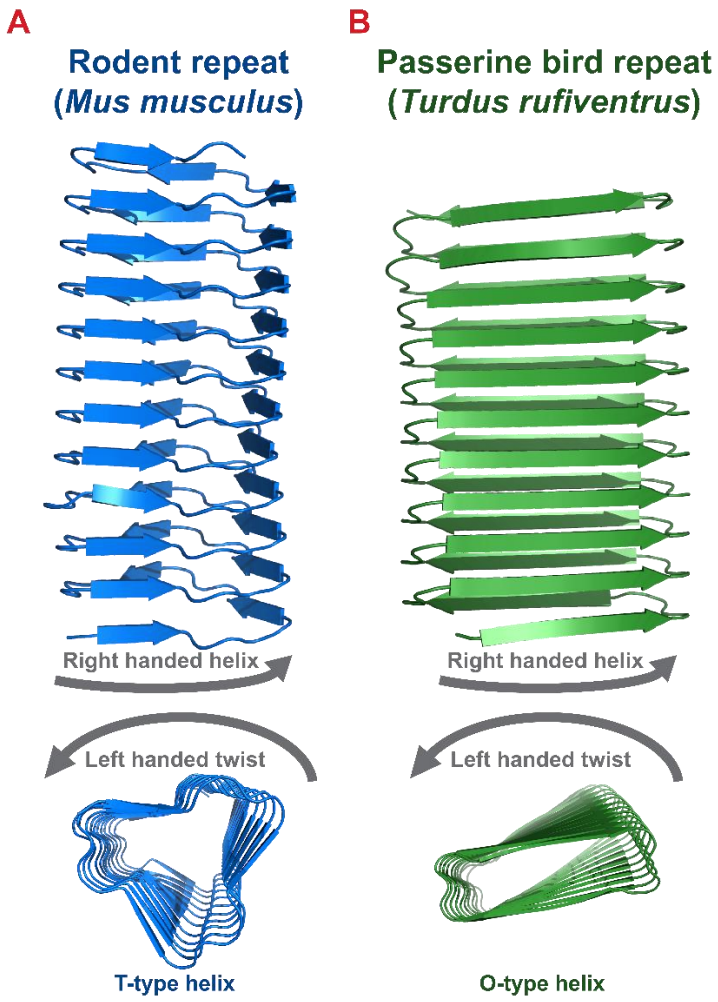

Figure 3.3: AlphaFold 3 models of representative AKAP150 peptide repeats. Both repeats are shown in two orientations to highlight differences in topology. Both are right-handed beta helices with a left-handed twist: (**A**) The rodent repeat from *Mus musculus* forms a triangular T-type helix with beta sheets of 4 amino acids, separated by linkers of 4 amino acids. (**B**) The passerine bird repeat from *Turdus rufiventris* forms an ovoid O-type helix with beta sheets of 9 residues, separated by linkers of 3 residues.

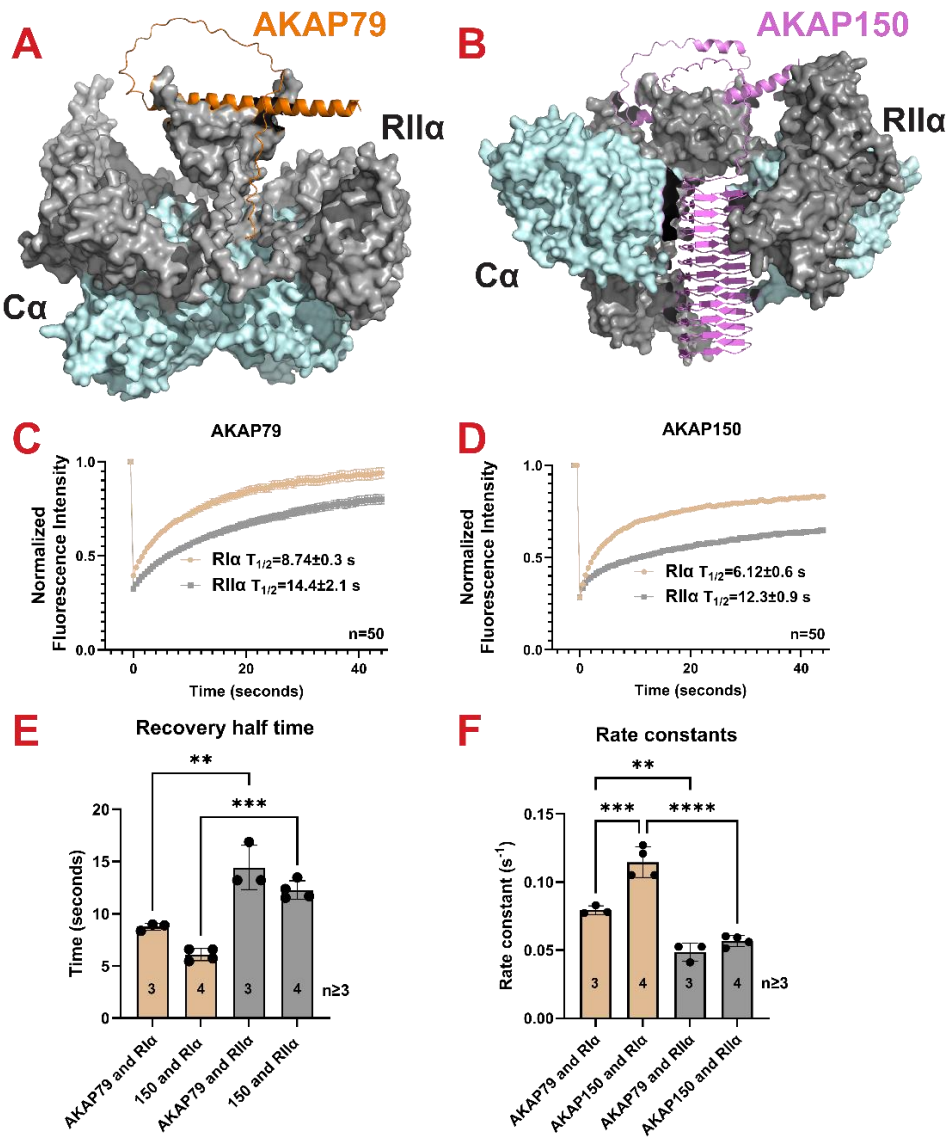

Figure 3.4: AKAP79/AKAP150 PKA binding analysis. (A) Alphafold 3 model of AKAP79 bound to the type II PKA holoenzyme, demonstrating the close positioning of regulatory subunits. **(B)** AKAP150 modeled

with type II PKA holoenzyme. The octapeptide repeat helix wedges between the two regulatory subunits, creating an extended conformation. **(C-D)** Representative FRAP recovery curves of AKAP79 (**C**) and AKAP150 **(D)** bound RIα (gold) and RIIα (silver), displayed as mean±SEM (n=50). Mean±SD recovery half time values included. **(E)** Recovery half times of AKAP79 (left) and AKAP150 (right) bound RIα (gold) and RIIα (silver). **(F)** Recovery rate constants of AKAP79 (left) and AKAP150 (right) bound RIα (gold) and RIIα (silver). Means±SD (n=3) *One-way ANOVA with Tukey's multiple comparisons test:* **P<0.01, ***P<0.00, ****P<0.0001.

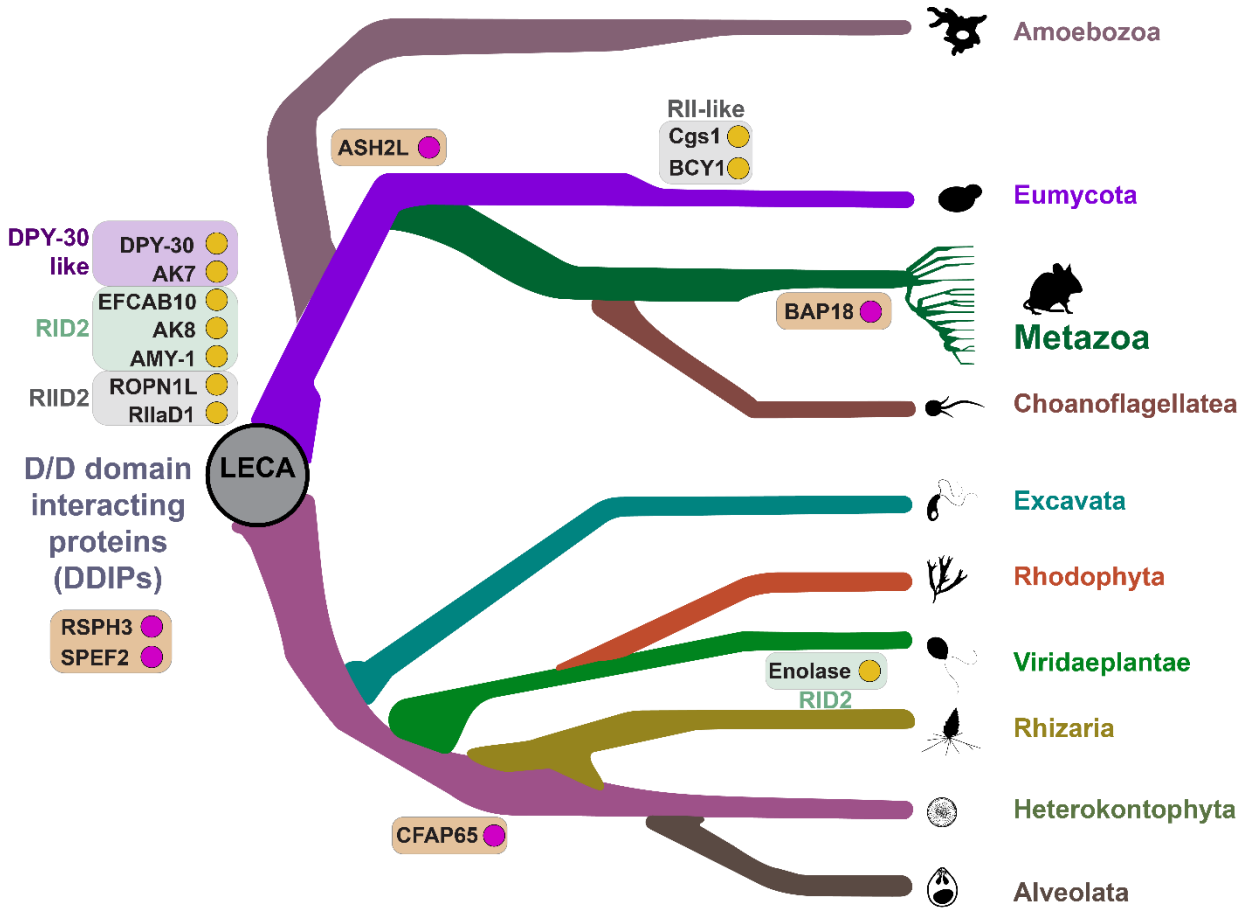

Figure 3.5: DDIP and d/d domain protein pairs were present at the last eukaryotic common ancestor (LECA). A cladogram showing DDIPs (orange boxes) and d/d domain proteins (purple box-DPY-30-like, green box-RID2, and grey box-RIID2 proteins) distributed across the eukaryotic domain.

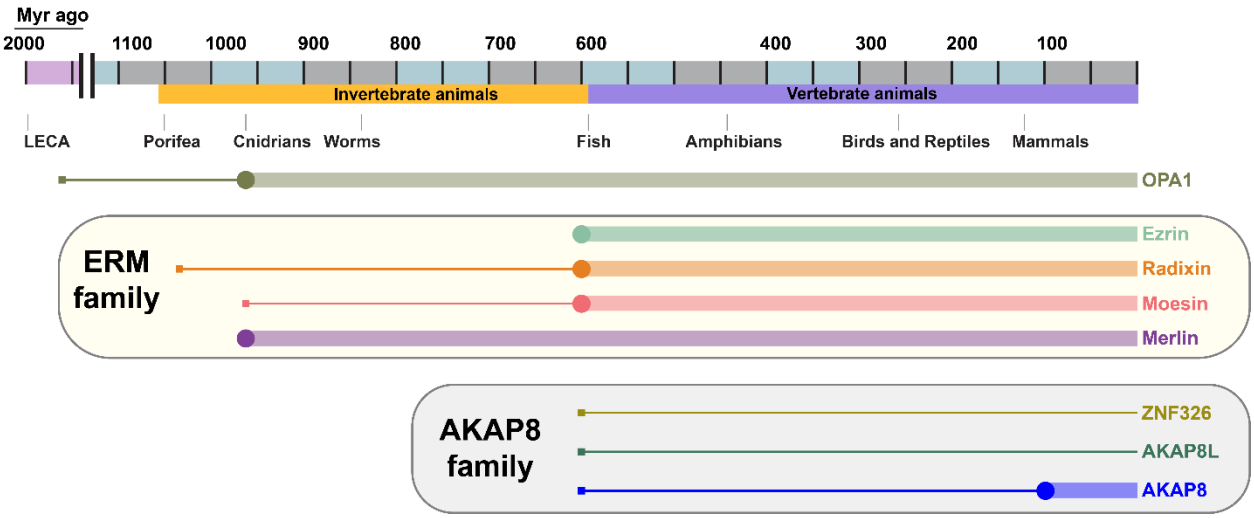

Figure 3.6: Timeline of AKAP gain of function events for OPA1, the ERM proteins, and the AKAP8 family. **i).** OPA1 (tan) originated in the opisthokont lineage and gained PKA anchoring capability in the metazoan lineage. **ii).** The ERM protein family exhibits varied AKAP development. Merlin (purple) was an AKAP from its origin in the parahoxozoa lineage. Radixin (orange) formed at the last metazoan common ancestor and gained anchoring capabilities at the onset of vertebrates. Moesin (pink) originated in the parahoxozoa lineage and became an AKAP at the start of the vertebrate lineage. Ezrin (mint green) became an AKAP at the vertebrate lineage. **iii).** AKAP8 (blue) appeared alongside ZNF326 (olive) and AKAP8L (teal) at the start of the vertebrate lineage. AKAP8 became an AKAP in the mammalian lineage, whereas ZNF326 and AKAP8L have no extant AKAP forms.

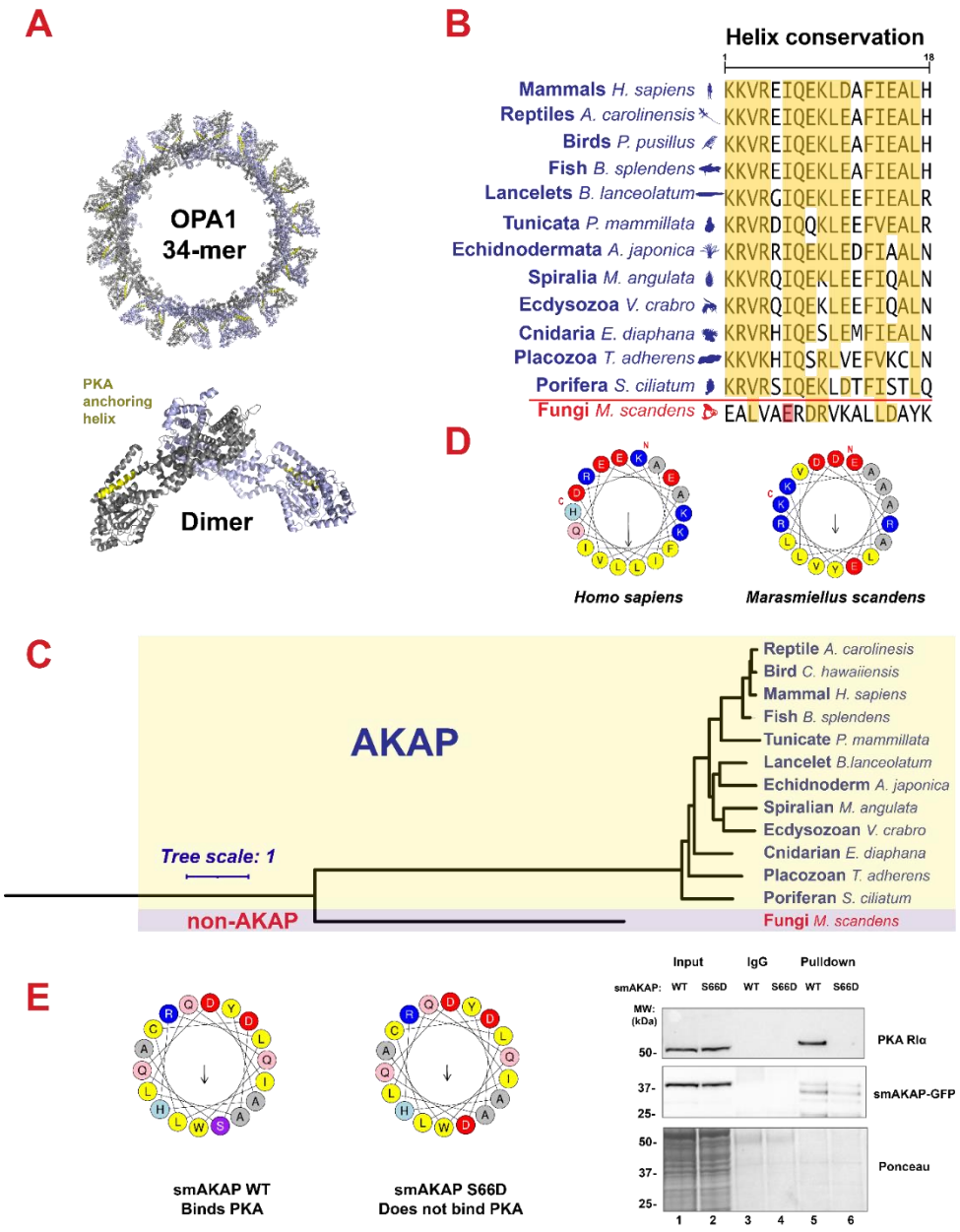

Figure 3.7: OPA1 became an AKAP at the Metazoan clade A). OPA1 sculpts the outer mitochondrial membrane by altering its oligomerization state from dimers to cyclic 34-mers. **B).** Functional AKAP forms of metazoan OPA1 are highly conserved (yellow highlighting), while fungal OPA1 sequences are less conserved and contain a glutamic acid residue on one hydrophobic face (red).**C).** Phylogenetic tree of OPA1 orthologs. AKAP (yellow) metazoan forms cluster together, reflecting the evolutionary relationships of constituent phyla, while non-AKAP (purple) fungal forms serve as the outgroup. **D).** Helical projections of human and fungal OPA1 helices show a glutamic acid disrupting the amphipathic helix in the fungal form.

E). Helix projection (left) and immunoprecipitation (right) of smAKAP wild type and smAKAP S66D, where an analogous mutation introduces a charged residue that disrupts PKA anchoring.

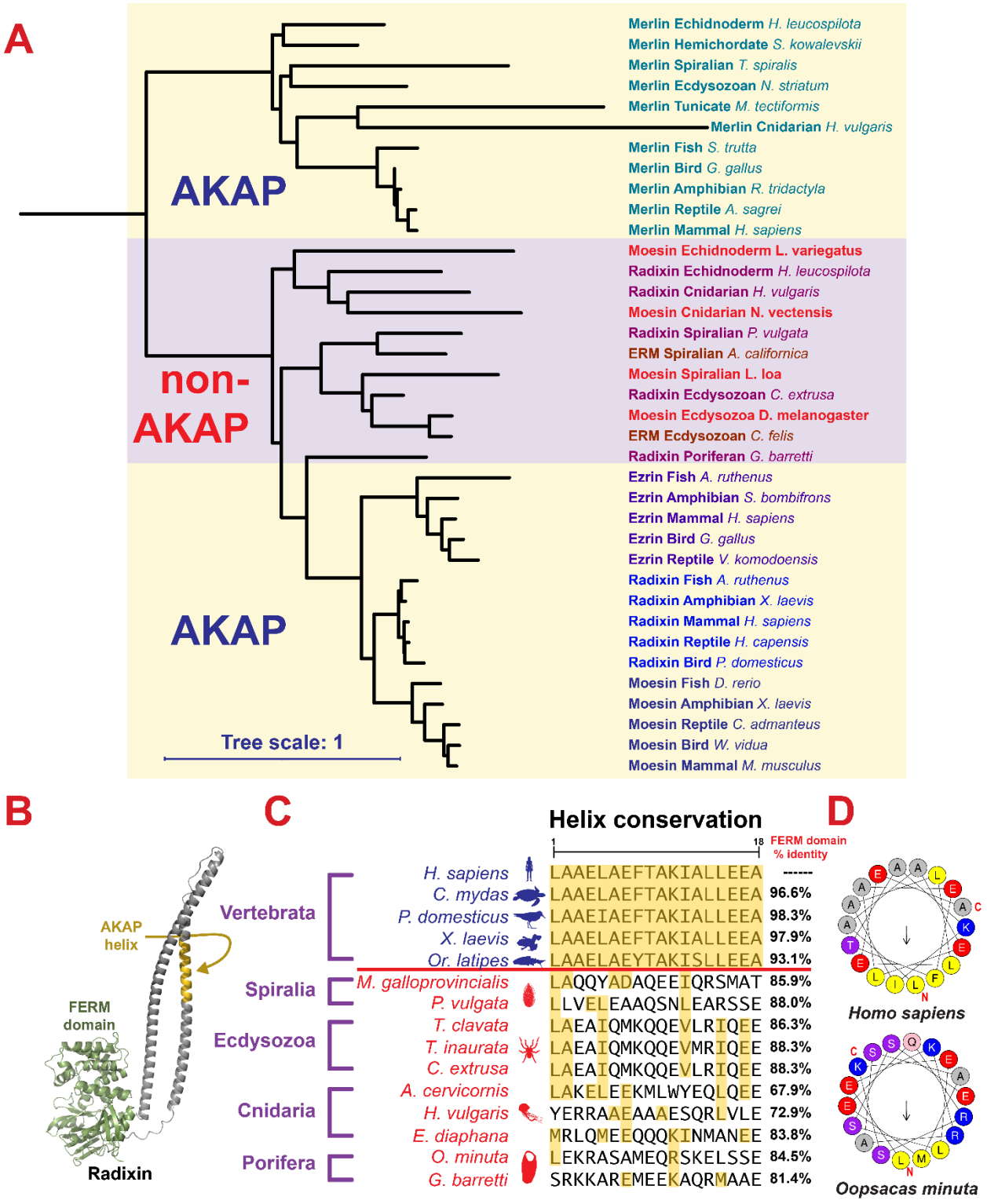

Figure 3.8: ERM proteins and Merlin asynchronous AKAP development A). Phylogenetic tree of the ERM family and Merlin. Merlin orthologs cluster together and are all AKAPs (yellow; top). Vertebrate ERM

proteins cluster by identity and are functional AKAPs (yellow; bottom). Invertebrate ERM proteins lack AKAP functionality (purple; middle) and cluster by phylogeny rather than protein identity. **B).** Structure of human Radixin, highlighting its FERM domain (green) and AKAP helix (yellow). **C).** Alignment of the amphipathic helix region of Radixin orthologs shows an accumulation of neutral mutations in non-AKAP forms, followed by stringent conservation (yellow) once PKA anchoring developed. FERM domain percent identity to human radixin shows that these orthologs are conserved despite variability of the helix. **D).** Helix projections of human (top) and sponge (bottom) demonstrate difference in size of hydrophobic face in AKAP and non-AKAP forms.

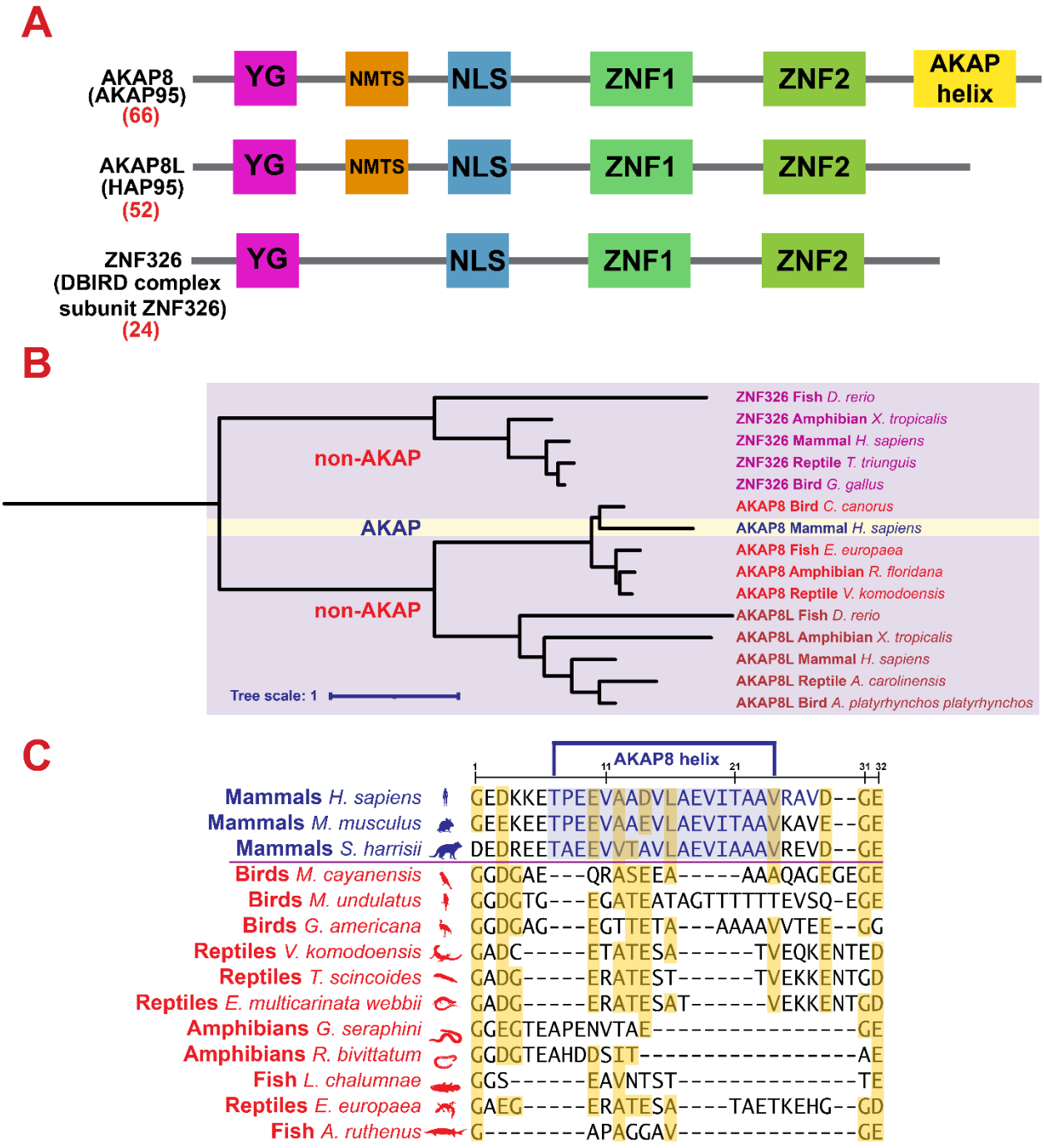

Figure 3.9: The AKAP8 family reveals a single insertion event resulting in AKAP development: A). Schematic of conserved domains in AKAP8 (top), AKAP8L (middle), and ZNF326 (bottom). Only AKAP8 has functional AKAP orthologs. **B).** Phylogenetic tree of the AKAP8 family. The three proteins cluster together, but only mammalian AKAP8 forms can anchor PKA (yellow). **C).** Alignment of AKAP8 orthologs shows that the mammalian helical region (blue) extends into conserved regions in non-mammalian forms

(red). The AKAP8 helix arose from an insertion, requiring gaps in the alignments of non-AKAP forms of AKAP8 between conserved flanking regions (yellow).

Chapter 4 – AKAP helix binding determinants

4.1 Introduction The nucleotide 3',5'-cyclic adenosine monophosphate (cAMP) is a versatile molecule utilized throughout the archaebacteria, eubacteria, plant and animal kingdoms (Blanco et al., 2020; Turnham & Scott, 2016). In animals cAMP is often utilized as a second messenger to relay information to effector proteins embedded in membranes or enzymes located deep inside the cell (Langeberg & Scott, 2015). Binding of cAMP to regulatory subunits of cAMP-dependent protein kinases (PKA) triggers the phosphorylation of substrates to potentiate hormone action (Krebs et al., 1985), exchange proteins directly activated by cAMP (Epac) regulate small GTPases (Bos, 2003), transcription factors such as the cAMP receptor protein (CRP) drive certain gene reprogramming paradigms (Fuchs Erin et al., 2010), and cAMP binding to ion channels directly modulates their conductance (Zheng et al., 2020). Arguably the most common use of cAMP is to activate PKA (Turnham & Scott, 2016). This family of serine/threonine protein kinases exist as tetrameric holoenzymes (Wong & Scott, 2004). A regulatory subunit dimer maintains two bound catalytic subunits (PKAc) in an autoinhibited state (Taylor et al., 2012). Recruitment of cAMP to binding sites on regulatory subunits relieves autoinhibition of the kinase allowing the phosphorylation of target substrates (Smith et al., 2017). Three genes encode the PKAc α, β and γ isoforms whereas four genes encode the type I regulatory (RI α and RI β) and type II regulatory (RII α and RII β) subunits (Skalhegg & Tasken, 2000). These gene products are assembled into type I or type II PKA holoenzymes that exhibit different sensitivities to cAMP and subcellular locations (Omar & Scott, 2020).

Spatiotemporal organization of cAMP signaling offers an efficient mechanism that directs PKA phosphorylation to precise locations within the cell. These signaling events occur within the confines of highly organized signaling nanodomains (Zaccolo & Kovanich, 2024). Recently three independent areas of research have converged to inform a new appreciation of how precise local signaling can be (Bock et al., 2024). First, advanced optical mapping techniques defined local cAMP environments that are formed by buffered diffusion of the second messenger (Anton et al., 2022; Bock et al., 2021). These "Receptor-associated independent cAMP nanodomains" (RAINs) not only sustain local cAMP synthesis but limit where localized signaling is operational. Second, G protein-coupled receptor (GPCR) signal transduction is now recognized to occur at subcellular compartments that are distinct from the plasma membrane (Irannejad et

al., 2015). This generates discrete intracellular sites of cAMP synthesis to further propagate local signaling. Third, structural analyses of intact PKA-AKAP complexes reveal that anchored holoenzymes exist as a montage of flexible tripartite configurations (Smith et al., 2017). For example, type II PKA holoenzyme-AKAP18γ complexes are bestowed with a 200-400 Å range of motion. These refined parameters of cAMP action not only emphasize the value of three dimensional intracellular signaling but stress the important role that AKAPs play in determining where and when PKA acts inside the cell (Bock et al., 2024).

PKA anchoring proceeds through modular protein-protein interactions (Scott & Pawson, 2009). An emblematic feature of AKAPs is a 14-18 amino acid segment that folds to form an amphipathic helix (Carr et al., 1991). This region binds with high affinity to a docking and dimerization domain formed by the first 45-50 residues of the type I or type II regulatory subunits of PKA. Biochemical, structural and cell-based studies show that this high affinity protein-protein interaction is the principal mode of PKA anchoring (Newlon et al., 1999). Moreover, peptide antagonists are effective reagents that are used to disrupt the PKA-AKAP interface. Ht 31, AKAP-*is,* and RIAD peptides have proven to be useful tools to establish the physiological role of type I and type II PKA anchoring in a range of cellular contexts (Alto et al., 2003; Carlson et al., 2006; Carr, Hausken, et al., 1992). Structural elucidation of docking and dimerization domains reveals subtle but significant differences in the organization of the RI/AKAP and RII/AKAP binding interfaces (Gold et al., 2006; León et al., 1997). The first 50 residues of each RI protomer form a tightly packed helical structure that is stabilized by interchain disulfide bonds. This conserved domain creates a binding grove that accepts an amphipathic helix on the AKAP with intermediate binding affinities (Banky et al., 2003). Conversely, the more malleable d/d domain of RII adopts a conventional four-helix bundle-like configuration that bonds AKAPs with low nanomolar binding affinities (Gold et al., 2006). These findings argue that cryptic side chain determinants reside within AKAP helices that favor anchoring of type I or type II PKA.

In this chapter, biophysical, biochemical and functional studies define conserved side chain determinants for type I PKA anchoring that reside at both ends of AKAP anchoring helices. Functional studies show that introduction of these RI anchoring determinants is sufficient to switch the isotype selectivity of a canonical RII binding protein to accommodate an association of type I PKA holoenzymes.

4.2 Methods

FRAP experiments

Wild-type U2OS cells were cultured in DMEM (Gibco) with 10% FBS on 35 mm glass bottom culture dishes (Mattek) at a starting density of 100,000 cells/dish. Cells were co-transfected with an iRFP tagged regulatory subunit (RIα or RIIα) and an mRFP tagged AKAP 48 hours before imaging using TransIT-LT1 (Mirus) in Opti-MEM (Life Technologies) according to manufacturer's instructions. Media was replaced with HBSS media prior to imaging. Imaging was performed on a Deltavision OMX using a 60X TIRF objective lens and immersion oil with a refractive index of 1.522.

FRAP experiments were conducted on the Cy5 channel, with an excitation wavelength of 640 nm, an exposure time of 21ms, and a transmittance (%T) of 80% in TIRF mode. FRAP videos had a frame rate of 500 ms and a duration of 45 seconds. Photobleaching on spot mode occurred 2 after 2 baseline frames and lasted for 1 frame. The photobleach duration was 50 ms at 80% power. 91 frames in total were collected. FRAP videos were not deconvolved or in any other way processed prior to analysis and quantification.

FRAP video analysis

Bleach spots, whole cell area, and background were measured in ImageJ (FIJI) with a 2.022 micron diameter circle on each frame of the video (Schindelin et al., 2012). These were collected into 50 sets of measurements per experiment. These sets were uploaded to the EasyFRAP server, which performed background normalization, background photobleaching correction, and normalization of the curves ("double normalization") (Giakoumakis et al., 2017). The points of each FRAP recovery curve (n=50) were then displayed in GraphPad Prism. Analysis of each curve was performed by deleting the pre-bleach points and performing a one phase association curve-fit equation $Y = Y_0 + (Plateau - Y_0) \cdot (1 - e^{-Kx})$. The rate constants ($s^{-1}$) and recovery half-times were collected in bar graphs to compare differences in AKAP anchoring of regulatory subunits.

Protein Modeling

Predictive protein models were generated using the Alphafold3 server (Google DeepMind). Representative models were chosen based on agreement of the 5 models provided, as well as agreement with known elements of protein structure (when available). Models were colored and positioned using Pymol 3.1 (Schrödinger).

Molecular dynamics

To assess mutations that would confer RI affinity to AKAP79, we performed molecular dynamics simulations using *Amber23* on AKAP-d/d domain complexes (Case et al., 2005). The solution NMR structure of AKAP79 bound to the Rattus norvegicus RIIα d/d domain [PDB: 2H9R] and the co-crystal structure of human smAKAP bound to the Bos taurus RIα d/d domain [PDB:5HVZ] were the starting structures for mutant generation. The crystal structures were first processed using the module *pdb4amber*, which removes water, ions, and hydrogens from the PDB structures, and designates cysteines that form disulfide bridges. Mutagenesis on the AKAP helices was performed using the program *scwrl4*. AKAP79 and RI mutants were created with emphasis on keeping the hydrophobic anchor points aligned with corresponding positions of the smAKAP helix. Both wild-type and mutant structures were then parameterized using the LEAP module of Amber, using the protein force field ff19sb, and the water force field “optimal” three-charge, four-point rigid water model (OPC). Protein negative charges were neutralized with sodium ions, then solvated in a 12.0 angstrom octahedral solvent box, then both sodium and chloride ions were added to achieve a physiological salt concentration of 150 mM.

MD simulations were performed using the Amber module *pmemd*. The proteins were equilibrated by running two minimization runs, first with no bond restraints, and then with restraints on hydrogen bonds. Each minimization starts with the steepest descent method, and for 1000 cycles and then switches to conjugate gradient descent. Step size after both minimizations is 2 femtoseconds. Heating occurred over 50 ps from 0 K to 300 K using Langevin dynamics and H-bond restraints. Pressure was raised to 1 bar over 50 ps using the Berendson barostat while maintaining temperature at 300 K with H-bond restraints. Equilibration occurred over 500 ps with no restraints on H-bonds, at 300K and 1 bar. The output files were processed in *cpptraj* to assess total energy, density, temperature, and backbone RMSD.

Output coordinate files from the equilibration were used to perform production runs on *pmemd*. Four identical unrestrained MD production simulations were performed sequentially for 8 ns with a step size of 2 fs, using the pressure and temperature conditions as the equilibration run with trajectories being sampled every 10 ps. Simulations were combined, and trajectories were processed using *MMPBSA.py* using Poisson Boltzmann models to measure the binding free energy of the complex, and then to break down the energetic contribution of individual amino acids. In Pymol 3.1, the per-residue binding energy of each AKAP helix amino acid was normalized to highlight the influence of each sidechain and mapped onto a gradient of blue to magenta (with blue representing a more negative ΔG and magenta a more positive ΔG) and used to color the individual amino acids of the AKAP helix according to binding free energy (Schrödinger, 2024).

Generation of AKAP79 mutants The AKAP79 FA, AF, FAAF mutants were generated from a human 10xHIS-AKAP79-EGFP N1 construct cloned in with *HindIII* (NEB) and *AgeI* (NEB) followed by site-directed Phusion mutagenesis with the following primers (**FA mutant** forward primer-AATATGAAACATTCGCAATTGAAACAGCCTCTTCTCTAG, reverse primer-GTTCTGAAGTTCTATCCTCAAAACCATTATCATTAG, **AF mutant** forward primer-GTTAATGAAATGGCCTCTGATGATAATAAAATAAAC, reverse primer-CAGCTGTTCAAATGCCAACTGAATAG, and **FAAF mutant** forward primer-CGTTATCCTCGAACTGCTGCATAGACTGAGC, reverse primer-CAGCTGTTCAAATGCCAACTGAATAG). PCR was run for 25 cycles using Phusion Plus Green master mix at a T_M of 60° C (Thermo Fisher) with 1.6 ng of template DNA and 0.4 µL of 10 µM forward and reverse primers each. Methylated parent plasmid DNA was digested with the restriction enzyme *DPNI* (NEB) for 1 hour at 37° C, then linear DNA was phosphorylated with T4 polynucleotide kinase (NEB) for 30 minutes at 37° C and ligated with T4 ligase (NEB) before transformation into GC10 chemically competent cells (Genessee Scientific). mRFP and iRFP fusion plasmids were simultaneously generated through restriction cloning of the AKAPs into the mRFP and iRFP backbones using *AgeI* (NEB) and *HindIII* (NEB).

Cell culture and Generation of lentiviral lines

U2OS cells were maintained in culture using DMEM (Gibco) with 10% FBS (Thermo Fisher) at 37° C and 5% CO_2. For FRAP experiments U2OS cells were transiently co-transfected with fluorescently tagged AKAP and R subunit constructs using TransIT-LT1 (Mirus) in Opti-MEM (Life Technologies) according to manufacturer's instructions.

WT and FAAF AKAP79 N1 constructs were used to generate AKAP79$^{WT/FAAF}$ pSMAL lentiviral plasmids using Gateway cloning (Invitrogen) in STBL3 cells (Thermo Fisher). Viral particles were produced in HEK293T cells via contransfection of the pSMAL constructs, PMD2.G, and psPAX2 (gifts from Didier Trono; Addgene plasmid #12259 [RRID:Addgene_12259] and plasmid #12260 [RRID:Addgene_12260]) with lipofectamine 2000 (Invitrogen). Viral particles were collected and spin concentrated using PEG-IT (System Biosciences). ATC7L PKACW196G pSMALB cells were transduced with 10, 50, 200, and 500 µL concentrated viral particles using 1 µg/µL polybrene (Santa Cruz). Green fluorescence was monitored on a Keyence BZ800 microscope, and the 500 µL virus condition cells were chosen due to robust expression. The cells were then sorted on a BD FACS ARIA III for expression of both BFP (PKAC^{W196G}) and GFP (AKAP79$^{WT/FAAF}$). Cells were treated with 1nM ACTH (Sigma-Aldrich) in DMSO (Thermo Fisher) after sorting to promote even expression of corticosterone biosynthesis proteins. ATC7L cell lines were maintained in culture using DMEM/F12 (Cytiva) with 1X ITS supplement (Sigma Aldrich), 2mM l-glutamine (Cytiva), 5% horse serum (Life Technologies), and 5% fetal bovine serum (Thermo Fisher) and maintained at 37° C and 5% CO_2.

Immunoprecipitations

Cell lysates were prepared from HEK293 cells transfected with 1 µg of AKAP79$^{WT/FA/AF/FAAF}$-EGFP N1 using HSEF lysis buffer containing 0.5% Triton X-100 (Sigma-Aldrich), 150 mM NaCl (Thermo Fisher), 20 mM NaF (Sigma-Aldrich), 2 mM EDTA (Sigma-Aldrich), and 50 mM tris (pH 7.5 at 4°C) (Fisher scientific) along with 1 mM 4-(2-aminoethyl)benzenesulfonyl fluoride (AEBSF) (Sigma-Aldrich), 10 µM leupeptin (Sigma-Aldrich), and 1 mM benzamidine (Sigma-Aldrich). Lysates were incubated for 10 min on ice then spun at 15,000g for 10 min at 4°C. Protein concentration was measured by BCA (Thermo Fisher) and lysates were diluted to 1 mg/ml using lysis buffer. Samples (500 µL) were precleared by rotating with 20 µL of protein G agarose (Thermo Fisher) (50% in lysis buffer) for 1 hour at 4°C. Supernatants were then incubated with 1

µg of goat anti-GFP antibody (Rockland) for 16 hours. 30 µL of protein G agarose (50% in lysis buffer) was then added, and samples were returned to rotation for 1 hour. Beads were washed with HSEF lysis buffer, centrifuged for 1 minute at 6000g and 4° C three times, and the buffer was aspirated with a 27-gauge needle before resuspending in 1× lithium dodecyl sulfate polyacrylamide gel electrophoresis (LDS-PAGE) sample buffer (Thermo Fisher) (3% β-mercaptoethanol (Sigma-Aldrich), final) and heating at 85° C for 10 min. IP lanes were paired with input conditions made from the same lysate, with the volume adjusted to load 30 µg of protein per condition and heated alongside IP samples. Samples were run on Bolt 4-12% Bis-Tris Plus gels (Invitrogen). Proteins were transferred onto nitrocellulose for immunoblotting and probed with α-PKA RIα rabbit (Cell Signaling), α-PKA RIIα mouse (BD), or α-GFP rabbit (Life Technologies) primary antibodies. Detection was achieved with HRP conjugated mouse and rabbit secondary antibodies (GE Life Sciences), followed by treatment with SuperSignal West Dura Extended Duration Substrate (Thermo Fisher) and imaging on an iBright FL1000 gel imaging system (Invitrogen). Densitometry was performed using NIH ImageJ (FIJI) software. Band intensity was normalized to total protein loading via ponceau stain. Figures are representatives of three experimental replicates.

Corticosterone measurements

Cells were washed in phosphate-buffered saline (PBS) (Cytiva) and the media was replaced with DMEM/F12 (no supplements) (Cytiva) 24 hours before harvest. Media samples were snap-frozen prior to analysis. Cells were lysed in HSEF lysis buffer and protein levels were measured via BCA (Thermo Fisher). Media samples were diluted and subjected to measurement using Corticosterone ELISA kits (Cayman). The absorbance of three replicates per sample was measured using a plate reader. Data was fit to a standard curve. Measurements were completed in three separate biological replicates. Measurements were first normalized to protein concentration and then to the control for each replicate.

Statistical analysis

Statistical analyses were performed in GraphPad Prism using either two-tailed Student's t-tests (for comparisons of two groups) or one-way ANOVAs with Tukey's multiple comparison test (for comparisons

of more than two groups). The number of measurements (n) is provided on representative FRAP timecourses and number of independent experiments (n) is provided on graphs of combined data.

Sample size and replicates

The sample size was not experimentally determined. For photobleaching experiments n=50 measurements were conducted across n≥3 independent experiments. For both the immunoprecipitation and corticosterone experiments n=3 separate experiments were conducted.

4.3 Analysis of type I and type II AKAP helices

Deriving consensus RI and RII anchoring motifs. The defining feature of AKAPs is a 14-18 residue region that folds into an amphipathic helix (Carr, Hausken, et al., 1992; Carr et al., 1991; Gold et al., 2006). This structural motif snugly fits into a cleft on the docking and dimerization domains of R subunits (Omar & Scott, 2020). We reasoned that computational alignment of AKAP helices might uncover amino acid determinants for R subunit isotype selectivity. Orthologs of 7 AKAPs which anchor type I PKA (1265 sequences, Figs. 2A & S2), and 13 AKAPs which prefer type II PKA (**2255 sequences, figures 4.1 & 4.2**) were aligned with the MUSCLE algorithm (Edgar, 2004). Sequence conservation logos highlight regions of homology (Crooks et al., 2004). Side chain conservation was more pronounced on the hydrophobic faces of each helix (residues 2, 5, 6, 9, 10, 13, 14, and 17). This surface directly interfaces with d/d domains (Götz et al., 2016). There is less conservation on polar face of the amphipathic helixes (Gold et al., 2013). Strikingly, type I AKAPs exhibit high conservation at the amino terminus of the binding helix. A phenyl group (F or Y) at position 1 is strongly favored and an almost invariant alanine occupies position 2 (**figure 4.1A**). This “FA motif” is ubiquitous among type I selective AKAPs across the Metazoan clade (**figure 4.2**). Hydrophobic side chains are also favored at positions 17 and 18, although the stringency of conservation is less (**figure 4.1A**). In contrast there was more degeneracy across the consensus RII binding motif, although the hydrophobic core of the amphipathic helix was conserved (**figure 4.1B**).

Phylogenetic analysis of smAKAP: a representative type I anchoring protein. Biochemical studies indicate that smAKAP is a prototypic type I PKA anchoring protein (Burgers et al., 2016; Burgers et al., 2012; Burgers et al., 2015). A phylogenetic tree was generated from a BLAST search yielding 219 high

quality orthologs of smAKAP (**figure 4.1C**). Sequences were aligned using the MUSCLE algorithm, and phylogenetic representation was generated using IQ-TREE on the CIPRES gateway with 2000 bootstraps (Kozlov et al., 2019; Minh et al., 2020). Mammalian, amphibian, fish, and bird smAKAP orthologs segregate into distinct lineages (**figure 4.1C**). Interestingly reptiles are divided into two groups that reside within the bird cluster (**figure 4.1C**). These are the paired reptilian orders Squamata and Rhynchocephalia (snakes and lizards) and the lone Testudines order (turtles and tortoises).

This information allowed us to derive a cladogram that reveals the smAKAP origin at the base of the vertebrate lineage (**figure 4.1D**). A consensus smAKAP helix motif from 219 sequences indicates the chemical properties of conserved side chains (**figure 4.1E**). Although early positions in the RI binding site are invariant, it is pertinent to note that the nature of individual hydrophobic and hydrophilic side chains vary within the core of the helix (**figure 4.1E**).

Phylogenetic analysis of AKAP79: a representative type II anchoring protein. The AKAP79 family of anchoring proteins are emblematic type II PKA anchoring proteins (Bregman et al., 1989; Carr et al., 1991; Nygren et al., 2017). A phylogenetic tree was generated with 271 high quality AKAP79/150 orthologs (Figs. 2F-H). Interestingly AKAP79 is absent in fish (**figure 4.1G**). Mammals and birds display the highest diversity due to the sporadic insertion of repeat sequences (**figure 4.1F**). A cladogram illustrates the origin of AKAP79/150 at the tetrapod lineage (**figure 4.1G**). The conservation logo for the AKAP79 helix reveals a higher degree of conservation with 11 out of 18 positions being invariant (**figures 4.1 & 4.2**). Data in figure 4.1 indicates that RI and RII recognize different anchoring determinants and AKAP79.

Photobleaching measurements of R subunits: Fluorescence recovery after photobleaching (FRAP) measures the diffusion and interactive properties of proteins in membranes of living cells (Giakoumakis et al., 2017). We performed total internal reflected fluorescence (TIRF) photobleaching experiments to measure exchange of PKA subunits from prototypic RI and RII selective anchoring proteins (**figure 4.3A**). As a prelude to these studies RI-iRFP and RII-iRFP were photobleached in the absence of AKAPs (**figure 4.3B**). These data show that free RI and RII diffuse at similar rates. The time to 50% fluorescence recovery for RIα is 1.54±0.6 (n=3 experiments of 50 cells, **figure 4.3C**) seconds. Similarly, the recovery half-time of

RIIα is 2.66±0.6 seconds (n=3 experiments of 50 cells, **figure 4.3C**). Rate constant for RIα is 0.96±0.04 s^{-1} and for RIIα is 0.95±0.01 s^{-1} respectively (**figure 4.3D**).

smAKAP prefers RI. Next, we compared the diffusion properties in the presence of smAKAP. Representative photobleaching images at 1 second intervals show a faster recovery of RII bleach spots than RI bleach spots (**figure 4.3E**). A recovery curve consisting of combined FRAP time courses (50 cells) reveals the slower recovery of RI in the presence of smAKAP (**figure 4.3F**). Quantifying 3 individual experiments measures a mean RIα recovery half-time of 4.39 ± 1.2 seconds for smAKAP (**figure 4.3I; left, gold**). In contrast the mean recovery halftime for RII is 2.19 ±0.5 seconds (**figure 4.3I; left, silver**). The rate constant for smAKAP for RIα is 0.12±0.05 s^{-1} (**figure 4.3J; left, gold**). The rate constant for RIIα is 0.18±0.06 s^{-1} (**figure 4.3I; left, silver**). Thus, smAKAP displays a preference for interaction with RIα inside cells.

AKAP79 prefers RII. Photobleaching experiments with AKAP79 demonstrate greater retention of type II PKA. This anchoring protein has less membrane mobility, so images were collected at 1, 5, and 7 seconds following photobleaching (**figure 4.3D**). Representative recovery curves for AKAP79 exchange (n=50 cells) reveal a preference for RII (**figure 4.3H**). Quantification of 3 individual experiments calculated an RI recovery half-time of 8.74±0.3 seconds (**figure 4.3I; right, gold).** In contrast the recovery half-time for RII is considerably longer at 14.4±2.1 seconds (**figure 4.3I; right, silver**). Rate constants of 0.079±0.003 s^{-1} and 0.049±0.007 s^{-1} were calculated for RIα and RIIα exchange with AKAP79 respectively (**figure 4.3J; right**). These parameters provide quantitative evidence that AKAP79 exhibits selectivity for type II PKA (Carr, Hausken, et al., 1992; Fraser & Scott, 1999).

4.4 AKAP Preference swap

Introducing RI binding determinants into AKAP79. Informatic analyses in Fig. 2A show that type I AKAP helices contain an FA motif at positions 1 and 2. We tested if this 96% conserved motif augments RI binding. Three helix mutants in AKAP79 were created ***i*)** Introduction of the FA motif at residues 1 and 2; ***ii)*** a palindromic AF motif at positions 17 and 18 and ***iii)*** a quadruple mutant with FA and AF at opposite ends of

the helix. Each AKAP79 form was tagged with green fluorescent protein (GFP). GFP immune complexes were isolated from HEK293T cells. Co-fractionation of R subunits was assessed by immunoblotting (**figure 4.4A**). AKAP79^{FAAF} was the only variant to pull down RI (Fig. 6A, top panel, lane 4). Quantification by densitometry of data from three independent experiments confirmed a 3.55-fold enhancement of RI over controls (**figure 4.4B**). Antibody compatibility issues resulted in detection of IgG heavy chain that migrates just above the RI subunit (**figure 4.4A; top panel**).

Individual side chain substitutions at either end of the AKAP79 helix decreased RII binding (**figure 4.4A; upper-mid panel, lanes 2-4**). Densitometric analyses from three experiments confirmed that the FA and FAAF mutants decrease RII binding by 45% and the AF mutant by 22% as compared to wildtype AKAP79 (**figure 4.4C**). Control blots of cell lysates confirmed equivalent expression of endogenous R subunits, and AKAP79-GFP (**figure 4.4A; input panels**). Ponceau staining served as loading controls (**figure 4.4A; input panels**). These biochemical studies indicate that AKAP79^{FAAF} gains a binding preference toward type I regulatory subunits.

Next, we used molecular dynamics to evaluate the contribution of individual side chains in the AKAP79 and AKAP79^{FAAF} helices (**figures 4.4D & E**). Protein-protein interactions were modeled using the Amber22 molecular dynamics suite to measure the contribution of each amino acid to the total binding energy using simulations by Sander and free energy analysis with MMPBSA (Case et al., 2023; D.A. Case, 2023; Miller et al., 2012). Contributions of individual amino acids to the Gibbs free energy of binding (ΔG) are color coded. (Blue depicts increased binding; magenta denotes reduced binding; **figure 4.4D**). For AKAP79 binding to RIIα, leucine-2, leucine-9, and valine-10 provide the largest contributions (**figure 4.4D; top-right**). Hydrophobic side chains at positions13 and14 bond with the central core of the RII docking domain (**figure 4.4D; top-right**).

AKAP79 interaction with RIα proceeds through a different subset of contacts. Isoleucine-18 interfaces with extra helical segments that flank the RI docking surface (**figure 4.4D; top-left**). Remarkably leucine-9 and alanine-13 are negative RI binding determinants (**figure 4.4D; top images**).

AKAP79^{FAAF} displays a distinctive pattern of binding (**figure 4.4D; bottom images**). The FA dimer and its palindromic AF pair alter the overall conformation of the amphipathic helix (**figure 4.4D; bottom-**

left panel). This promotes slight changes in the orientation of Isoleucine-3, valine-10, isoleucine-14, and phenylalanine-18 (**figure 4.4D; bottom-left panel**). Hence, structural alterations at four turns of the helix favor interaction with the d/d domain of RIα. These topological changes act synergistically to bias the AKAP79^{FAAF} helix toward type I PKA anchoring.

Fluorescence recovery after photobleaching (FRAP) was used to test this postulate (Figs. 6F & 6G). AKAP79^{FAAF} demonstrates an RIα preference, with a recovery half-time of 20.5±2.0 (n=3) seconds (**figures 4.4G; gold & 4.4H; brown**). This value is more than double wildtype AKAP79's half-time of 8.74±0.34 seconds (**figures 4.4F; gold & 4.4H; tan).** Conversely, the AKAP79^{FAAF} mutant is less able to bind RII with a recovery half-time of 11.4±2.0 seconds as compared to 14.4±2.1 seconds for wildtype AKAP79 (**figures 4.4F & G; sliver & 4.4I**). Rate constants compare the recovery independent of the mobile fraction (**figures 4.4J & K**). The mean RIα rate constant for AKAP79^{FAAF} is 0.034±0.003 s^{-1} as compared to 0.079±0.003 s^{-1} for AKAP79 (**figure 4.4J**). Rate constants of 0.062±0.01 s^{-1} and 0.049±0.007 s^{-1} were measured for RII interaction with AKAP79^{FAAF} and the wild-type anchoring protein (**figure 4.4K**). These biophysical results argue that the AKAP79^{FAAF} helix switches PKA regulatory subunit binding preference toward RI.

smAKAP loss of YA motif impairs type I PKA preference. The type I AKAP, smAKAP has an FA/YA motif at the N-terminus of its helix in all examined orthologs (**figure 4.1E and figure 4.5A**). As this motif on its own is not sufficient to convert AKAP79 into a type I selective AKAP (**figure 4.4A-C**), we wanted to examine its role on type I AKAP PKA preference. We chose to replace the smAKAP's helical YA with two leucines as to mimic AKAP79's helix (**figure 4.5B**) creating the mutant smAKAP Y61L, A62L or smAKAP^{LL}. Using RFP-tagged smAKAP, smAKAP^{LL}, and AKAP79 (as a positive control for RII binding) we expressed these constructs in HEK cells and pulled down on the RFP tags. Blotting for RI, RIIα, and RFP we observed that the LL mutation abolishes RI binding in smAKAP without a coincident gain of RII binding (**figure 4.5 C; n=3**). To assess RII binding through an orthogonal method, we ran a western blot and performed an RII overlay by incubating the blots in tagged RIIα which will bind type II AKAPs. The RII overlay demonstrates that the LL mutation does not confer type II binding to smAKAP (**figure 4.5D; n=3**). The RI and RIIα bands of three immunoprecipitation biological replicates were quantified by densitometry demonstrating that

replacement of the YA of smAKAP with LL impairs RI binding without facilitating RII binding (**figure 4.5E-F**). Data are presented as mean±SD (n=3). *Student's t-test:* ***P<0.0005, ****P<0.0001.

Functional analyses of AKAP79^{FAAF} action. Adrenal Cushing's syndrome is a disease of cortisol hypersecretion often caused by somatic mutations in the protein kinase A catalytic subunit (Broder et al., 2015; Walker et al., 2019). Cushing's mutations prevent incorporation of PKAc into AKAP signalling islands (Omar et al., 2022; Omar et al., 2023). To test the consequences of biased RI signaling in a physiological context we monitored the ability AKAP79^{FAAF} to impact stress hormone release from adrenal cells (**figure 4.6A**). PKAc-W196G is a recently identified Cushing's kinase that preferentially associates with RI (Omar et al., 2024). Hence PKAc^{W196G} is favourably recruited to type I AKAP signalling islands (Omar et al., 2024). We reasoned that expression of AKAP79^{FAAF} should sequester type I holoenzymes away from mitochondrial PKA substrates that drive stress hormone biosynthesis (**figure 4.6A**).

ATC7L mouse adrenal cells infected with bicistronic lentiviral vectors expressing PKAc^{W196G} /BFP tonically produce corticosterone (the murine cortisol analog) (Omar et al., 2024). These cell lines were co-infected with lentiviral vectors encoding either AKAP79^{WT} /GFP or AKAP79^{FAAF}/GFP. Populations of double fluorescent cells were sorted via FACs. Corticosterone levels were measured by ELISA assay and normalized to total protein content. These hormone measurements revealed that AKAP79^{FAAF} reduced corticosterone levels by 61.5 ± 0.8 % (n=3) as compared to the wildtype anchoring protein (**figure 4.6B**). Thus, introduction of AKAP79^{FAAF} helix in the context of the full-length anchoring protein is sufficient to promote type I PKA signaling inside cells.

4.5 Discussion

Systematic investigation of the smAKAP and AKAP79 helices was performed on these prototypic type I and type II selective anchoring proteins. Both anchoring proteins are amenable to the use of total internal reflection fluorescence (TIRF) microscopy as an analytical tool to track protein dynamics at the plasma membrane (Fish, 2009). As anticipated, the fluorescence recovery after photobleaching (FRAP)

measurements presented in **figure 4.3 F and H** indicate that smAKAP and AKAP79 exhibit clear preferences for their favored R subunit binding partner.

Bioinformatic and biophysical data presented in **figure 4.1** highlights the conservation of FA or YA dipeptides at positions 1 and 2 in AKAP helices as determinants for RI anchoring. This is perhaps most evident in the alignment of six consensus RI anchoring logos presented in **figure 4.2**. This shows that this dipeptide is almost invariant in orthologs of the RI selective anchoring proteins smAKAP, SKIP and AKAP3 (Bachmann et al., 2016; Means et al., 2011). The aromatic side chains phenylalanine or tyrosine are equally tolerated at position 1 with alanine being almost invariant at the second position. Interestingly, the synthetic RI selective anchoring disruptor peptide RIAD contains a YA motif albeit in the second turn of the amphipathic helix (Carlson et al., 2006; Omar & Scott, 2020; Wang et al., 2015). Structural modeling indicates that the “FA” motif interfaces with short flanking helixes that are unique to the docking and dimerization domain of RI. Tandem type I PKA selective helices have been identified in the mitochondrial anchoring protein SKIP (figure 4.2 (Means et al., 2011)). The FA motif is also conserved in the distal PKA anchoring helix (residues 1633-1646) of AKAP220 (Whiting et al., 2015; Whiting et al., 2016). This region exhibits selectivity for RI whereas the proximal site on AKAP220 (residues 610-623) only anchors type II PKA (Whiting et al., 2015). Thus, AKAP220 and SKIP represent a unique class of anchoring proteins that sequester multiple PKA holoenzymes to amplify cAMP responses at vesicles and mitochondria respectively.

Amalgamated sequence alignments of AKAP helices from recognized RI and RII anchoring proteins presented in figure **4.1 A and B** emphasize different regions of conservation. Although hydrophobic pairs are conserved in both consensus logos, alignments of type I selective AKAPs presented in **figures 4.1 and 4.2** identify another conserved hydrophobic pair at the opposite end of anchoring helix. This is particularly evident in smAKAP where the $W^{A}/_{V}$ pair at positions 17 and 18 of the helix is invariant across 219 orthologs (**figure 4.1E**). Molecular dynamic simulations presented in **figure 4.4 E** suggest that RI binding to FA motifs contact the flanking helices of RI. The similar $W^{A}/_{V}$ pair may contribute similar contacts. These residues help to guide the positioning of side chain determinants dispersed along the hydrophobic face of the AKAP amphipathic helix. Such an induced realignment enhances preferential association of type I AKAPs with the more rigid and disulfide-bonded core of the RIα d/d domain. Replacement of the FA motif in smAKAP with

two leucines is sufficient to impair RI binding without any enhancement to RII binding is presented **figure 4.5C-F**. These experiments highlight that the FA motif is a critical binding determinant of type I AKAPs. They additionally reveal an interplay between the FA motif and the remainder of the helix, as seen by the need for AKAP79 to have a palindromic FAAF motif to bind RI, but loss of the FA motif in smAKAP is sufficient to impair RI interactions.

Another intriguing prospect is that hydrophobic pairs at either end of the AKAP helix may form a palindromic binding surface. These determinants can interface with the symmetric RI d/d domain in either a forward or backward orientation. This concept is supported by recent evidence that the PKA binding helix in MAP2 can complex with the R subunits in either an N to C or C to N orientation (Bartošík et al., 2024). Also, residues proximal to the anchoring helix may further contribute to R subunit interactions. For example, hydrophilic anchor points outside the core AKAP18-RIIα interface contribute to PKA anchoring whereas a nonnatural linear segment of a peptide that disrupts the AKAP function of PI3Kγ is being developed as a therapeutic for cystic fibrosis (Della Sala et al., 2024; Götz et al., 2016). These latter examples suggest possible variation as to how AKAPs utilize their anchoring helices to bind R subunits.

Hypercortisolism is a pathological consequence of somatic mutations in PKAc that drive Adrenal Cushing's syndrome (Broder et al., 2015). We took advantage of PKAc^{W196G}, a Cushing's kinase that only associates with RI to test the functionality of recruitment into type I AKAP signaling islands (Omar et al., 2024). Data presented in **figure 4.6** shows that introduction of FA and AF pairs at opposite ends of the AKAP79 helix not only switches binding preference toward RIα but reduces stress hormone production in adrenal cells expressing PKAc^{W196G}. These cell-based studies illustrate how modification of only a few side chains have profound effects on PKA subtype binding preference in the context of a full-length anchoring protein. This may be particularly important for type I AKAPs as accumulating evidence indicates that RIα is elevated in certain endocrine disorders, heart disease and cancers (Chan et al., 2023; Coles et al., 2020; Liu et al., 2017; Rosenthal et al., 2024). A logical next step is to test if PKA association with type I AKAPs is strengthened under pathological conditions to create venues for aberrant cAMP signaling.

Figures for chapter 4

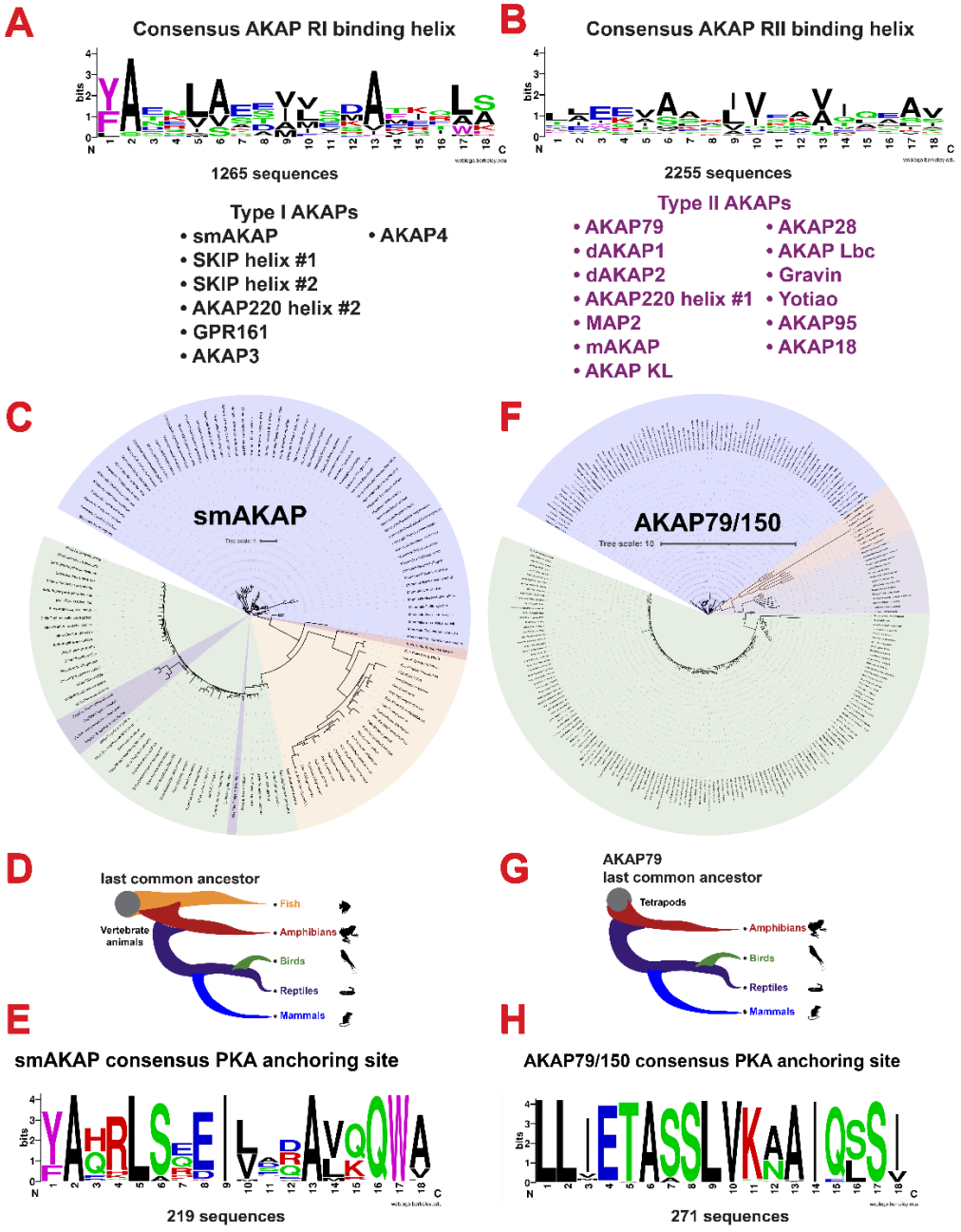

Fig. 4.1: Type I and II AKAPs. **(A)** Consensus logos of 1265 type I AKAP helices, revealing a conserved FA motif (97.7% conservation with F/Y). The AKAPs used are listed below. **(B)** Consensus logos of 2255 type II AKAP helices. **(C)** Phylogenetic tree of smAKAP orthologs **(D)** Cladogram showing the smAKAP distribution among vertebrates. **(E)** Consensus logo of 219 smAKAP ortholog helices. **(F)** Phylogenetic tree

of AKAP79/150 orthologs. **(G)** Cladogram of AKAP79/150 distribution across tetrapods. **(H)** Consensus logo of 271 AKAP79/150 ortholog helices.

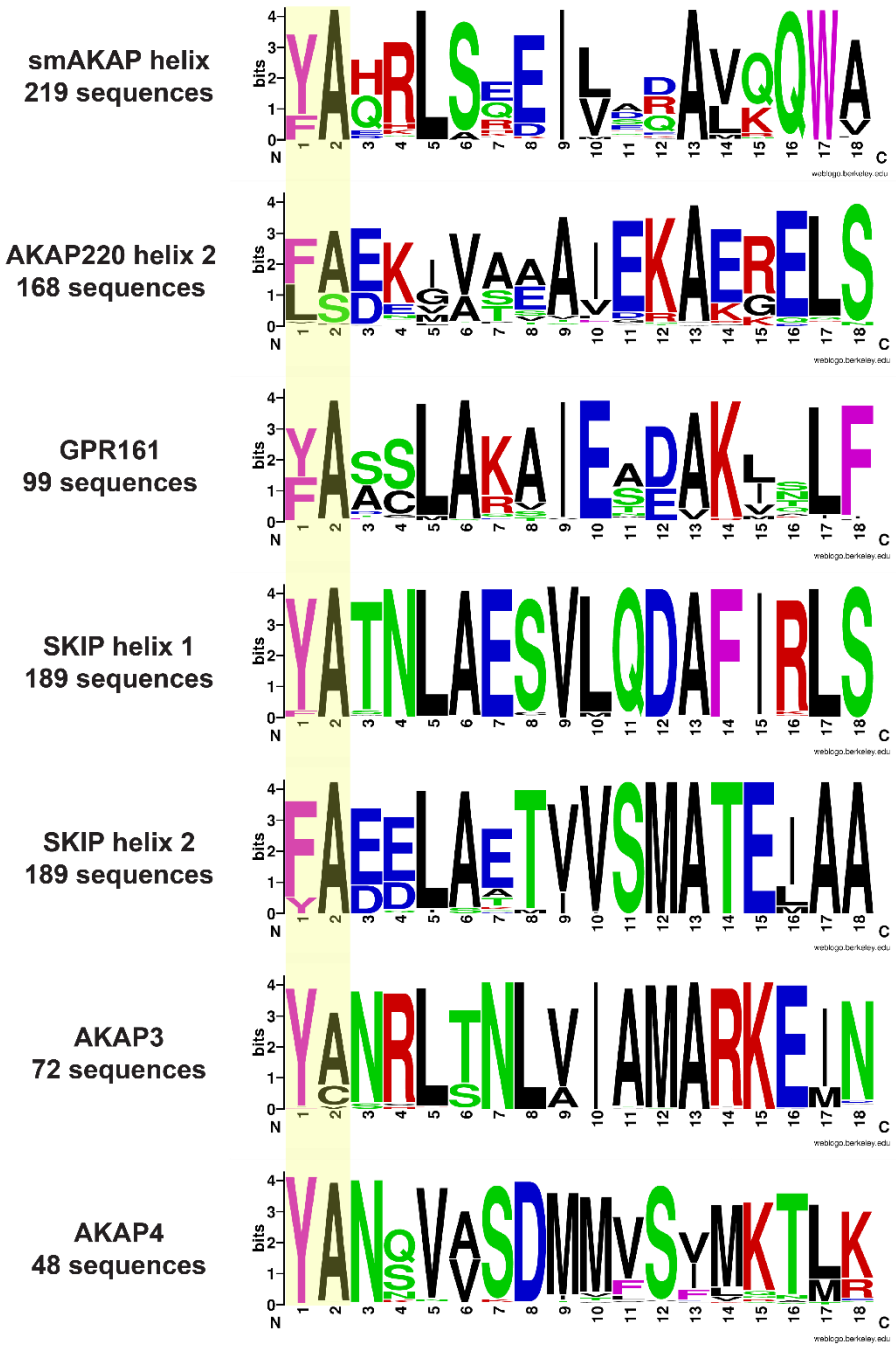

Figure 4.2: Sequence alignments of individual type I AKAPs used to generate the consensus logo. The FA motif is highlighted to display its conservation among individual amphipathic helices. The number of species included in each alignment is noted next to the corresponding logo.

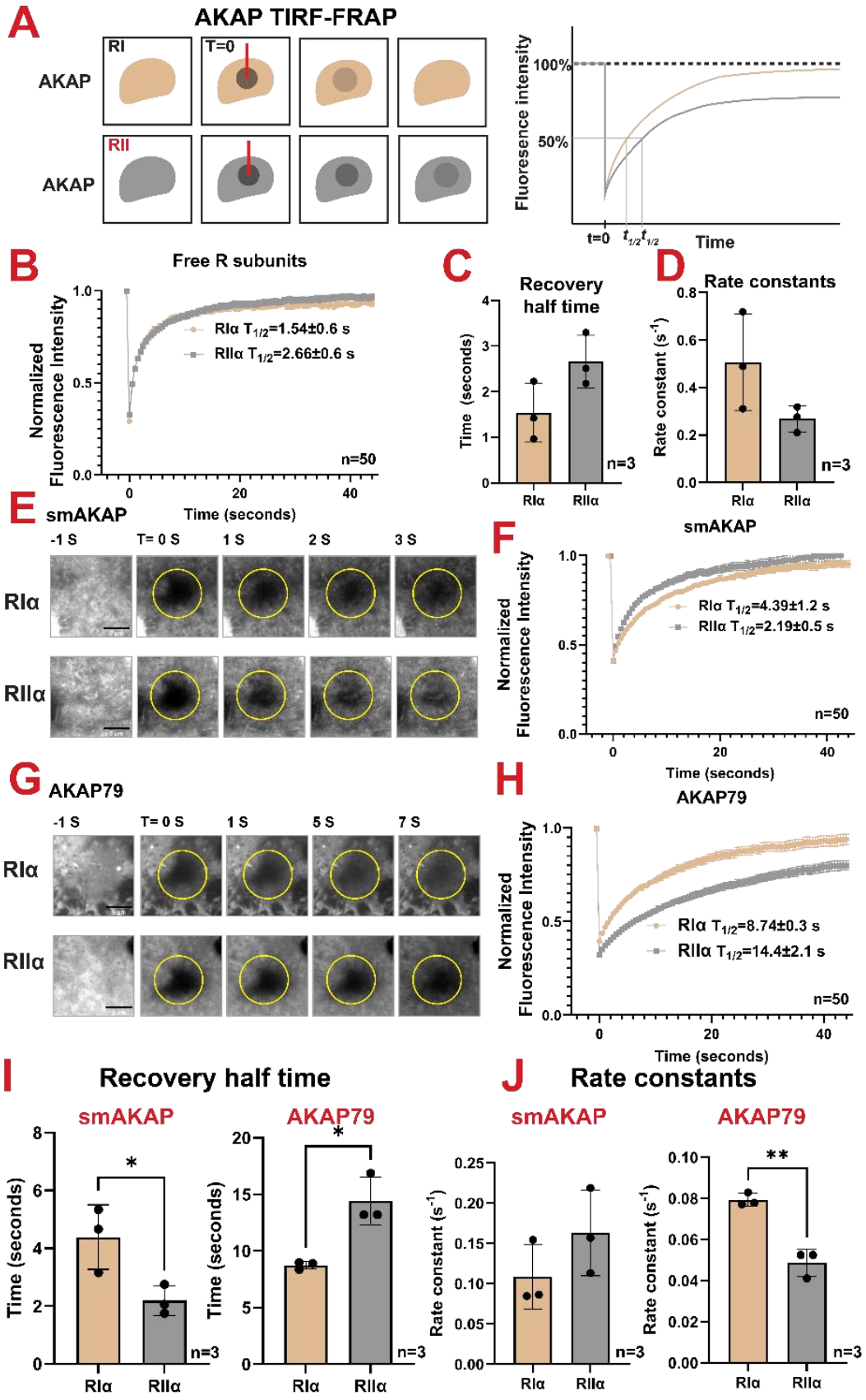
A
AKAP TIRF-FRAP
RI
T=0
AKAP
RII
AKAP
Fluorescence intensity
100%
50%
t=0
$t_{1/2}$
Time
B
Free R subunits
Normalized Fluorescence Intensity
RIα $T_{1/2}$=1.54±0.6 s
RIIα $T_{1/2}$=2.66±0.6 s
n=50
Time (seconds)
C
Recovery half time
Time (seconds)
n=3
RIα
RIIα
D
Rate constants
Rate constant (s^{-1})
n=3
RIα
RIIα
E
smAKAP
-1 S
T= 0 S
1 S
2 S
3 S
RIα
RIIα
F
smAKAP
Normalized Fluorescence Intensity
RIα $T_{1/2}$=4.39±1.2 s
RIIα $T_{1/2}$=2.19±0.5 s
n=50
Time (seconds)
G
AKAP79
-1 S
T= 0 S
1 S
5 S
7 S
RIα
RIIα
H
AKAP79
Normalized Fluorescence Intensity
RIα $T_{1/2}$=8.74±0.3 s
RIIα $T_{1/2}$=14.4±2.1 s
n=50
Time (seconds)
I
Recovery half time
smAKAP
AKAP79
Time (seconds)
*
*
n=3
n=3
RIα
RIIα
RIα
RIIα
J
Rate constants
smAKAP
AKAP79
Rate constant (s^{-1})
**
n=3
n=3
RIα
RIIα
RIα
RIIα

Fig. 4.3: FRAP analysis of smAKAP and AKAP79. (A) Schematic of the TIRF-FRAP paradigm (left) and a representative recovery graph (right). Tighter AKAP binding results in a slower recovery of the photobleached R subunits. **(B)** Representative FRAP recovery curves of free R subunits RIα (gold) and RIIα (silver), displayed as mean±SEM (n=50). Mean±SD recovery half-times included. **(C)** Recovery half times of free RIα (gold) and RIIα (silver). **(D)** Recovery rate constants of free RIα (gold) and RIIα (silver). Means±SD (n=3) *Student's t-test:* *P<0.05, **P<0.005. **(E)** Time course of photobleaching of smAKAP-bound RIα (top) and RIIα (bottom) over 3 seconds. **(F)** Representative FRAP recovery curves of smAKAP bound R subunits RIα (gold) and RIIα (silver) displayed as mean±SEM (n=50). Mean±SD recovery half-times included. **(G)** Time course of photobleaching of AKAP79 bound RIα (top) and RIIα (bottom) over 7 seconds. **(H)** Representative FRAP recovery curves of AKAP79 bound R subunits RIα (gold) and RIIα (silver) displayed as mean±SEM (n=50). Mean±SD recovery half-time values included. **(I)** Recovery half-time of smAKAP (left) and AKAP79 (right) bound RIα (gold) and RIIα (silver). **(J)** Recovery rate constants of smAKAP (left) and AKAP79 (right) bound RIα (gold) and RIIα (silver). Means±SD (n=3). *Student's t-test:* *P<0.05, **P<0.005.

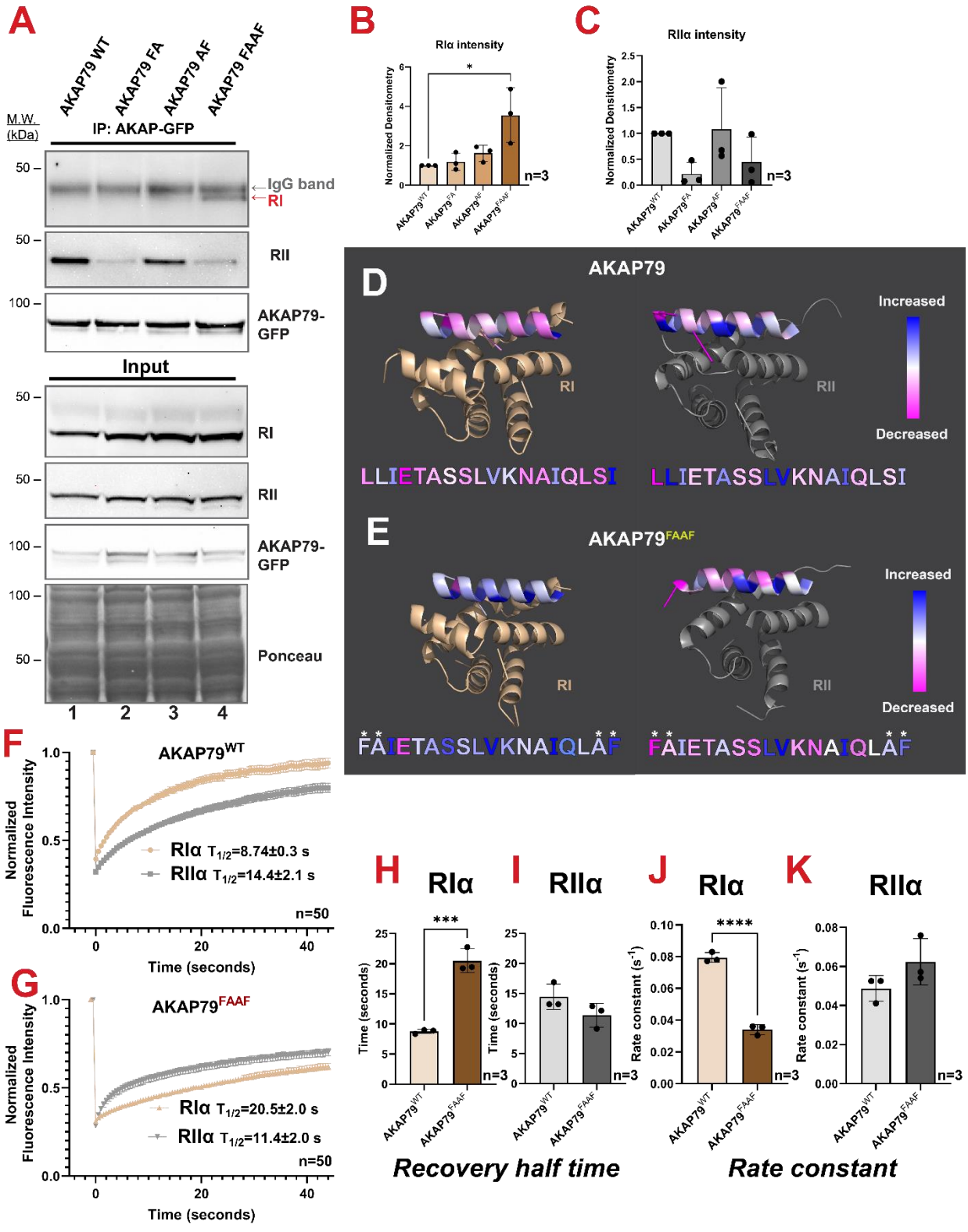

Fig. 4.4: AKAP79 PKA preference switch. (A) Full-length GFP-tagged AKAP79^{WT}, AKAP79^{FA}, AKAP79^{AF}, and AKAP79^{FAAF} mutants were immunoprecipitated from HEK293T cells, and RI and RII coprecipitation was

analyzed via immunoblot. Antibody incompatibility caused the detection of an IgG band above the RI bands (top panel). Only AKAP79^{FAAF} precipitates RI. Both AKAP79^{FA} and AKAP79^{FAAF} show reduced RII binding. **(B)** Quantification of RI pulldown bands, normalized to background. AKAP79^{FAAF} has a band intensity 3.55 times higher than the other mutants. **(C)** Quantification of RII pulldown by AKAP mutants. Data are shown as mean±SD. *One-way ANOVA with Tukey's multiple comparisons test*: *P<0.05. N-terminal helices contribute to reduced RII binding. **(D-E)** ΔG contributions of AKAP helical amino acids from molecular dynamics (MD) experiments. Residues colored on a gradient from blue (more negative ΔG; stronger binding) to magenta (more positive ΔG; weaker binding). AKAP79^{FAAF} shows a switch in preference from RIIα to RIα. **(F-G)** Representative FRAP recovery curves of AKAP79^{WT} **(F)** and AKAP79^{FAAF} **(G)** bound RIα (gold) and RIIα (silver). FRAP curves displayed as mean±SEM (n=50). Mean±SD recovery half-time values included. **(H-I)** Recovery half-times from three replicate FRAP experiments. **(H)** RIα recovery half times from AKAP79^{WT} (tan) and AKAP79^{FAAF} (brown). **(I)** RIIα recovery half times from AKAP79^{WT} (grey) and AKAP79^{FAAF} (slate). **(J-K)** Recovery rate constants from three replicate FRAP experiments. **(J)** RIα rate constants from AKAP79^{WT} (tan) and AKAP79^{FAAF} (brown). **(K)** RIIα rate constants from AKAP79^{WT} (grey) and AKAP79^{FAAF} (slate). Data are presented as mean±SD (n=3). *Student's t-test:* ***P<0.0005, ****P<0.0001.

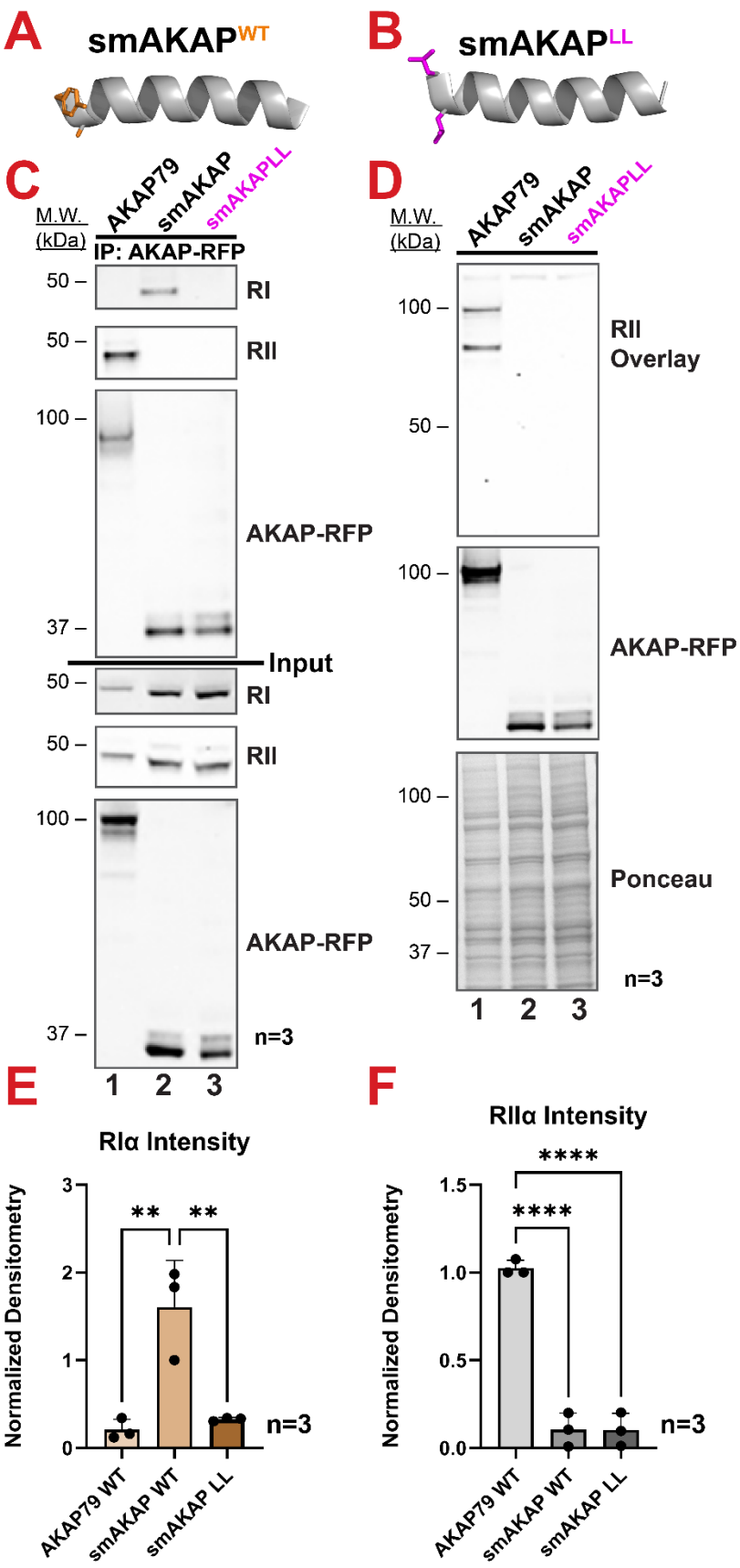
A
smAKAP^WT
B
smAKAP^LL
C
M.W. (kDa)
AKAP79
smAKAP
smAKAPLL
IP: AKAP-RFP
50 –
RI
50 –
RII
100 –
AKAP-RFP
37 –
Input
50 –
RI
50 –
RII
100 –
AKAP-RFP
37 –
n=3
1 2 3
D
M.W. (kDa)
AKAP79
smAKAP
smAKAPLL
100 –
RII Overlay
50 –
100 –
AKAP-RFP
100 –
Ponceau
50 –
37 –
n=3
1 2 3
E
RIα Intensity
Normalized Densitometry
3
2
1
0
**
**
n=3
AKAP79 WT
smAKAP WT
smAKAP LL
F
RIIα Intensity
Normalized Densitometry
1.5
1.0
0.5
0.0
****
****
n=3
AKAP79 WT
smAKAP WT
smAKAP LL

Figure 4.5: Removal of YA motif on smAKAP abolishes type I PKA binding. (A) Wild-type smAKAP helix with N-terminal YA motif sidechains displayed (orange). **(B)** smAKAP^{LL} mutant helix with mutant N-terminal LL motif sidechains displayed (magenta). **(C)** Co-immunoprecipitation of R subunits by AKAP79, smAKAP, and smAKAPLL reveals that the mutant smAKAP loses the ability to pull down RI without gaining the ability to bring down RIIα. **(D)** RII overlay of western blot of AKAP79, smAKAP, and smAKAP^{LL} demonstrates that only AKAP79 is detected by RII overlay. **(E)** Densitometry of the RI band from immunoprecipitation indicates that the LL mutant abolishes the RI interaction of smAKAP. **(F)** Densitometry of the RIIα band from the immunoprecipitation indicates that the LL mutation does not increase RIIα binding. Data in E&F are shown as mean±SD. *One-way ANOVA with Tukey's multiple comparisons test*: **P<0.005 ****P<0.0001

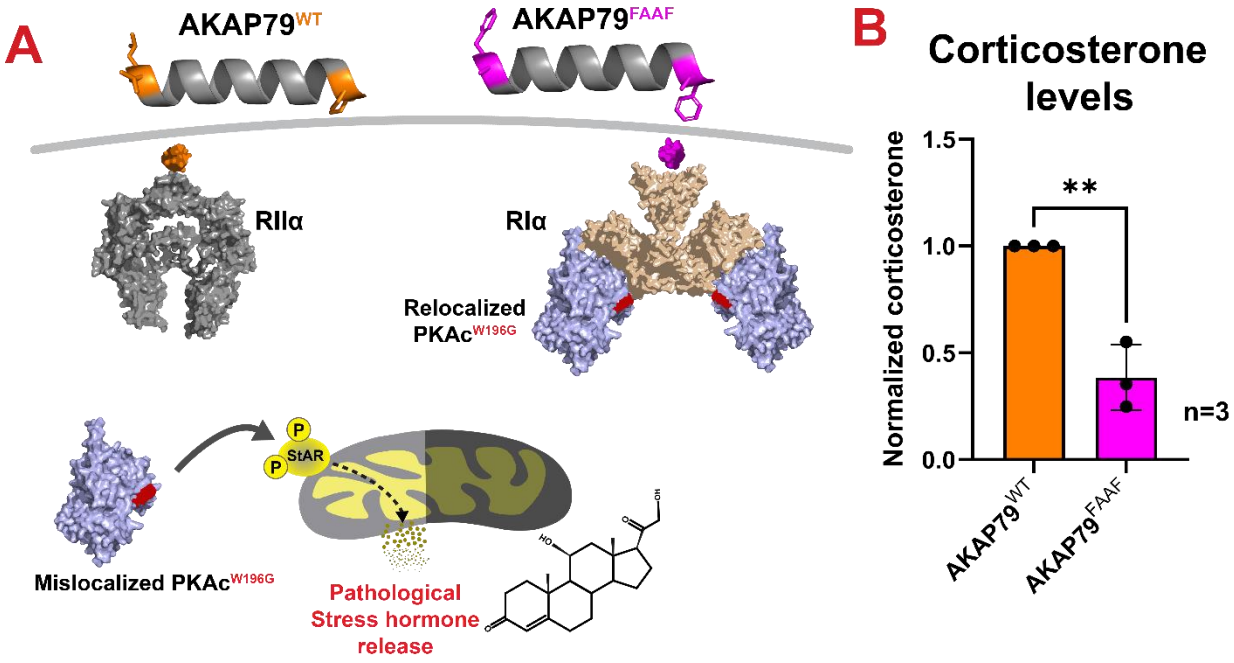

Fig. 4.6: Rescue of Cushing's syndrome by AKAP79^{FAAF}. (A) Model depicting how AKAP79^{FAAF} restores corticosterone release in Cushing's syndrome. PKAcW196G is displaced from type II PKA holoenzymes, such as those bound by AKAP79^{WT} (orange). Mislocalized PKAc drives ectopic phosphorylation of mitochondrial substrates. Membrane relocalization of the type I holoenzyme subunit by AKAP79^{FAAF} (magenta) separates the mutant C subunit from the mitochondria, reducing corticosterone release. **(B)** Normalized corticosterone levels measured from ATC7L PKAcW196G cells stably expressing either

AKAP79WT (orange) or AKAP79FAAF (magenta). Data are presented as mean±SD (n=3). *Student's t-test:* **P<0.005.

Chapter 5 – Final Conclusions

5.1 Divergent evolution of docking and dimerization domains

The examinations of the docking and dimerization domains documented in chapter 2 illustrate a path of divergent evolution for these protein modules. The three domain families, DPY-30-like, RID2, and RIID2 exhibit striking degrees of conservation at both the sequence and structure level. At the tertiary structure level, they differ only in the shape of the N-terminal, docking determinant region with DPY-30-like domains exhibiting a curved helix, RID2 domains presenting a discretely linked helix, and RIID2 domains containing an unstructured region. The remaining structures of these protein modules are analogous between the families. The primary structure of these domains is more variable between the families, but there remain many conserved motifs. The use of prolines in the linker region, aromatic residues on α-helix 2 contributing to the intramolecular interactions of the domains, and the locations of docking determinant residues in each domain are shared between the three families.

The conservation of intramolecular interactions is an especially significant indicator of divergence as the presence but not the nature of these bonds is necessary for the function of the domain. The phylogeny of these domains reflects a paradigm of duplication, fusion, and functionalization to expand the repertoire of scaffolding interactions which agrees with existing models of domain evolution (Gough, 2005; Ponting & Russell, 2002; Weiner et al., 2006).

There remain unanswered questions about the evolutionary journey of d/d domains. As examples in each family existed at the LECA, what was the original template for d/d interaction (and did this originate in eukaryotes, or is it present yet undiscovered in prokaryotes)? There seem to be three main roles for d/d domain proteins: subcellular localization and scaffolding of PKA cascades, organization of flagellar and ciliary elements, and DPY-30's participation in the COMPASS complex; are there any novel roles for this protein interface which have yet to be identified? Lastly is a biochemical question: How much do the unique elements of the various domains alter their affinity for a given anchoring helix? Can the individual members of the three domain families be considered to be interchangeable with regard to AKAP/DDIP binding affinity, or does each domain have a unique ranking of which helix it prefers?

5.2 Convergent evolution of AKAPs and DDIPs

The analyses presented in chapter 3 reveal a path of convergent evolution for AKAP and DDIP proteins. Unlike their partner domains, these motifs are simple amphipathic helices that are a single unit of secondary structure only 18 amino acids long. This feature, plus the permissive attributes of the anchoring helix allow for proteins to gain the ability to scaffold d/d domains through the steady accumulation of neutral mutations.

While there are a few examples of DDIPs which originate at the LECA, the majority of these anchoring proteins have emerged as AKAPs in tandem with the origin of vertebrate animals. This explosion of anchoring proteins greatly expanded the versatility of cAMP signaling, permitting coupling of this second messenger cascade to many other signaling paradigms at precise subcellular locations (Omar & Scott, 2020). These supported the increase in complexity of the vertebrates over the invertebrate animals.

Examining the evolution of these scaffolds reveals a piecewise evolutionary trajectory. AKAP79/150 orthologs all have a functional amphipathic helix, but they have gained other motifs over time. The calcineurin binding PIXIT/VIVIT regions are short linear motifs (SLiMs) which were not present in the most ancestral forms of the protein (Nygren et al., 2017; Wigington et al., 2020). These developed amid the amphibian clade, with frogs and salamanders, but not caecilians containing a VIVIT motif. Reptile and bird orthologs ubiquitously include the VIVIT motif, but all mammalian forms have the PIXIT motif. This tractable formation of a new protein-protein interaction domain demonstrates convergent evolution as the domain has developed apart from the heritage of existing calcineurin binding proteins.

Examinations of AKAP helix development on OPA1, the ERM proteins, and AKAP95 reveal two distinct pathways for acquiring the ability to anchor PKA: the accumulation of neutral point mutations and the introduction of insertion mutations. OPA1, radixin, and moesin have extant non-AKAP orthologs, allowing for the visualization of mutational drift in existing α-helices that ultimately gave rise to a functional anchoring helix. An identifying feature of this evolutionary path is the abrupt cessation of mutational drift once the helix gains the ability to anchor PKA, as it becomes subject to new selection pressures (Ponting & Russell, 2002).

The structure and function of the peptide repeats found in AKAP150 forms are fertile ground for further study. Structural predictions assign a beta solenoid structure to this repeat and indicate that the repeat alters scaffold topology(Kajava & Steven, 2006). The evidence that this structure evolved independently and remains conserved in both rodents and passerine birds suggests that it holds functional significance. Experimental determination of the repeat structure, as well as careful analysis of the crosstalk between anchored enzymes will give clarity to this curiosity.

AKAP95 orthologs reveal the occurrence of an insertion, forming a functional AKAP in mammals exclusively. There is still an observable decrease in mutational drift after this genetic occurrence, but this case differs from the previous examples as the helix was not formed by an accumulation of point mutations.

An imbalance exists in pre-metazoan eukaryotes between d/d domain proteins and DDIPs. This discrepancy is likely due to incomplete identification rather than a true absence of these anchors. AKAPs far outnumber the PKA regulatory subunit isoforms, and the simplicity of amphipathic helices compared to the d/d domain implies that there are many DDIPs yet to be categorized. Characterization of DDIPs will provide a molecular basis for many structural interactions in cilia and flagella.

5.3 AKAP helix binding determinants

AKAPs can be categorized by their preference for binding type I or type II PKA. Analysis of common features of the amphipathic helices reveals the general need for a hydrophobic face to interact with d/d domains, and an N-terminal “aromatic, alanine” motif, a hallmark of type I AKAPs. Experiments in this section illustrate that palindromic installation of this motif is sufficient to confer RI binding to AKAP79.

Through molecular dynamics modeling, FRAP analysis, and an RI-biased Cushing’s syndrome corticosterone rescue experiment, we have shown that AKAP79$^{\mathbf{FAAF}}$ is a type I AKAP. Immunoprecipitation experiments on AKAP79$^{\mathbf{WT}}$, AKAP79$^{\mathbf{FA}}$, AKAP79$^{\mathbf{AF}}$, and AKAP79$^{\mathbf{FAAF}}$ indicate that while only the double mutant is sufficient to bind RI, both N-terminal mutants (FA, and FAAF) decrease RII binding. Replacement of the N-terminal YA with LL on smAKAP’s helix impairs the pulldown of RI compared to

wild-type smAKAP. While this mutation does not enhance RII co-precipitation, more sensitive assays are required to determine the net effects on R subunit preference.

There are other features of AKAP helices which contribute to their binding affinity. Polar residues in AKAP18 and smAKAP are necessary contact points which mediate PKA binding (Götz et al., 2016). The location of these polar substituents on AKAP helices is however less conserved than the “aromatic, alanine” motif on type I AKAPs or the hydrophobic faces of any AKAP. This suggests that AKAP-PKA binding is not “one size fits all,” but instead involves context-specific dependencies between the residues composing the AKAP helices. Testing the generalizability of the “aromatic, alanine” motif on diverse AKAP helices would illuminate the generalizability of this motif as a crucial binding determinant.

References

Abramson, J., Adler, J., Dunger, J., Evans, R., Green, T., Pritzel, A., Ronneberger, O., Willmore, L., Ballard, A. J., Bambrick, J., Bodenstein, S. W., Evans, D. A., Hung, C.-C., O'Neill, M., Reiman, D., Tunyasuvunakool, K., Wu, Z., Žemgulytė, A., Arvaniti, E.,…Jumper, J. M. (2024). Accurate structure prediction of biomolecular interactions with AlphaFold 3. *Nature*, 1-3. https://doi.org/10.1038/s41586-024-07487-w

Alto, N. M., Soderling, S. H., Hoshi, N., Langeberg, L. K., Fayos, R., Jennings, P. A., & Scott, J. D. (2003). Bioinformatic design of A-kinase anchoring protein-in silico: A potent and selective peptide antagonist of type II protein kinase A anchoring. *Proceedings of the National Academy of Sciences of the United States of America*, *100*(8), 4445-4450. https://doi.org/10.1073/pnas.0330734100

Anton, S. E., Kayser, C., Maiellaro, I., Nemec, K., Moller, J., Koschinski, A., Zaccolo, M., Annibale, P., Falcke, M., Lohse, M. J., & Bock, A. (2022). Receptor-associated independent cAMP nanodomains mediate spatiotemporal specificity of GPCR signaling. *Cell*, *185*(7), 1130-1142 e1111. https://doi.org/10.1016/j.cell.2022.02.011

Arafat, M., Harlev, A., Har-Vardi, I., Levitas, E., Priel, T., Gershoni, M., Searby, C., Sheffield, V. C., Lunenfeld, E., & Parvari, R. (2021). Mutation in CATIP (C2orf62) causes oligoteratoasthenozoospermia by affecting actin dynamics. *Journal of Medical Genetics*, *58*(2), 106-115. https://doi.org/10.1136/jmedgenet-2019-106825

Atwood, B. K., Lopez, J., Wager-Miller, J., Mackie, K., & Straiker, A. (2011). Expression of G protein-coupled receptors and related proteins in HEK293, AtT20, BV2, and N18 cell lines as revealed by microarray analysis. *BMC Genomics*, *12*(1), 14. https://doi.org/10.1186/1471-2164-12-14

Aye, T. T., Mohammed, S., van den Toorn, H. W. P., van Veen, T. A. B., van der Heyden, M. A. G., Scholten, A., & Heck, A. J. R. (2009). Selectivity in Enrichment of cAMP-dependent Protein Kinase Regulatory Subunits Type I and Type II and Their Interactors Using Modified cAMP Affinity Resins. *Molecular & Cellular Proteomics : MCP*, *8*(5), 1016-1028. https://doi.org/10.1074/mcp.M800226-MCP200

Bachmann, V. A., Mayrhofer, J. E., Ilouz, R., Tschaikner, P., Raffeiner, P., Röck, R., Courcelles, M., Apelt, F., Lu, T.-W., Baillie, G. S., Thibault, P., Aanstad, P., Stelzl, U., Taylor, S. S., & Stefan, E. (2016). Gpr161 anchoring of PKA consolidates GPCR and cAMP signaling. *Proceedings of the National Academy of Sciences*, *113*(28), 7786-7791. https://doi.org/10.1073/pnas.1608061113

Banky, P., Newlon, M. G., Roy, M., Garrod, S., Taylor, S. S., & Jennings, P. A. (2000). Isoform-specific differences between the type Ialpha and IIalpha cyclic AMP-dependent protein kinase anchoring domains revealed by solution NMR. *J Biol Chem*, *275*(45), 35146-35152. https://doi.org/https://doi.org/https://doi.org/10.1074/jbc.m003961200

Banky, P., Roy, M., Newlon, M. G., Morikis, D., Haste, N. M., Taylor, S. S., & Jennings, P. A. (2003). Related Protein–Protein Interaction Modules Present Drastically Different Surface Topographies Despite A Conserved Helical Platform. *Journal of Molecular Biology*, *330*(5), 1117-1129. https://doi.org/10.1016/S0022-2836(03)00552-7

Bardeci, N. G., Tofolón, E., Trajtenberg, F., Caramelo, J., Larrieux, N., Rossi, S., Buschiazzo, A., & Moreno, S. (2021). The crystal structure of yeast regulatory subunit reveals key evolutionary insights into Protein Kinase A oligomerization. *Journal of Structural Biology*, *213*(2), 107732. https://doi.org/https://doi.org/10.1016/j.jsb.2021.107732

Bartošík, V., Plucarová, J., Laníková, A., Janáčková, Z., Padrta, P., Jansen, S., Vařečka, V., Gruber, T., Feller, S. M., & Žídek, L. (2024). Structural basis of binding the unique N-terminal domain of microtubule-associated protein 2c to proteins regulating kinases of signaling pathways. *Journal of Biological Chemistry*, 107551. https://doi.org/10.1016/j.jbc.2024.107551

Bauman, A. L., Soughayer, J., Nguyen, B. T., Willoughby, D., Carnegie, G. K., Wong, W., Hoshi, N., Langeberg, L. K., Cooper, D. M. F., Dessauer, C. W., & Scott, J. D. (2006). Dynamic Regulation of cAMP Synthesis through Anchored PKA-Adenylyl Cyclase V/VI Complexes. *Molecular Cell*, *23*(6), 925-931. https://doi.org/10.1016/j.molcel.2006.07.025

Bergthorsson, U., Andersson, D. I., & Roth, J. R. (2007). Ohno's dilemma: Evolution of new genes under continuous selection. *Proceedings of the National Academy of Sciences*, *104*(43), 17004-17009. https://doi.org/doi:10.1073/pnas.0707158104

Bernhardt, H. S. (2012). The RNA world hypothesis: the worst theory of the early evolution of life (except for all the others). *Biology Direct*, *7*(1), 23. https://doi.org/10.1186/1745-6150-7-23

Bieluszewska, A., Weglewska, M., Bieluszewski, T., Lesniewicz, K., & Poreba, E. (2018). PKA-binding domain of AKAP8 is essential for direct interaction with DPY30 protein. *The FEBS Journal*, *285*(5), 947-964. https://doi.org/https://doi.org/10.1111/febs.14378

Bjarnadóttir, T. K., Gloriam, D. E., Hellstrand, S. H., Kristiansson, H., Fredriksson, R., & Schiöth, H. B. (2006). Comprehensive repertoire and phylogenetic analysis of the G protein-coupled receptors in human and mouse. *Genomics*, *88*(3), 263-273. https://doi.org/10.1016/j.ygeno.2006.04.001

Blanco, E., Fortunato, S., Viggiano, L., & de Pinto, M. C. (2020). Cyclic AMP: A Polyhedral Signalling Molecule in Plants. *Int J Mol Sci*, *21*(14). https://doi.org/10.3390/ijms21144862

Bock, A., Annibale, P., Konrad, C., Hannawacker, A., Anton, S. E., Maiellaro, I., Zabel, U., Sivaramakrishnan, S., Falcke, M., & Lohse, M. J. (2021). Optical Mapping of cAMP Signaling at the Nanometer Scale. *Cell*, *184*(10), 2793. https://doi.org/10.1016/j.cell.2021.04.043

Bock, A., Irannejad, R., & Scott, J. D. (2024). cAMP signaling: a remarkably regional affair. *Trends in Biochemical Sciences*, *49*(4), 305-317. https://doi.org/10.1016/j.tibs.2024.01.004

Bontems, F., Fish, R. J., Borlat, I., Lembo, F., Chocu, S., Chalmel, F., Borg, J.-P., Pineau, C., Neerman-Arbez, M., Bairoch, A., & Lane, L. (2014). C2orf62 and TTC17 Are Involved in Actin Organization and Ciliogenesis in Zebrafish and Human. *PLOS ONE*, *9*(1), e86476. https://doi.org/10.1371/journal.pone.0086476

Bos, J. L. (2003). Epac: a new cAMP target and new avenues in cAMP research. *Nat. Rev. Mol. Cell Biol.*, *4*(9), 733-738. http://www.ncbi.nlm.nih.gov/entrez/query.fcgi?cmd=Retrieve&db=PubMed&dopt=Citation&list_uids=14506476

Bowie, J. U., Reidhaar-Olson, J. F., Lim, W. A., & Sauer, R. T. (1990). Deciphering the Message in Protein Sequences: Tolerance to Amino Acid Substitutions. *Science*, *247*(4948), 1306-1310. https://doi.org/10.1126/science.2315699

Bregman, D. B., Bhattacharyya, N., & Rubin, C. S. (1989). High affinity binding protein for the regulatory subunit of cAMP-dependent protein kinase II-B: Cloning, characterization, and expression of cDNAs for rat brain P150. *Journal of Biological Chemistry*, *264*(8), 4648-4656. https://doi.org/10.1016/S0021-9258(18)83792-9

Bregman, D. B., Hirsch, A. H., & Rubin, C. S. (1991). Molecular characterization of bovine brain P75, a high affinity binding protein for the regulatory subunit of cAMP-dependent protein kinase II beta. *The Journal of Biological Chemistry*, *266*(11), 7207-7213.

Broder, M. S., Neary, M. P., Chang, E., Cherepanov, D., & Ludlam, W. H. (2015). Incidence of Cushing's syndrome and Cushing's disease in commercially-insured patients <65 years old in the United States. *Pituitary*, *18*(3), 283-289. https://doi.org/10.1007/s11102-014-0569-6

Brondani, D., de Souza, B., B, S. S., Neves, A., & I, C. V. (2013). PEI-coated gold nanoparticles decorated with laccase: a new platform for direct electrochemistry of enzymes and biosensing applications. *Biosens Bioelectron*, *42*, 242-247. https://doi.org/https://doi.org/10.1016/j.bios.2012.10.087

Burgers, P. P., Bruystens, J., Burnley, R. J., Nikolaev, V. O., Keshwani, M., Wu, J., Janssen, B. J., Taylor, S. S., Heck, A. J., & Scholten, A. (2016). Structure of smAKAP and its regulation by PKA-mediated phosphorylation. *FEBS J*, *283*(11), 2132-2148. https://doi.org/https://doi.org/10.1111/febs.13726

Burgers, P. P., Ma, Y., Margarucci, L., Mackey, M., van der Heyden, M. A. G., Ellisman, M., Scholten, A., Taylor, S. S., & Heck, A. J. R. (2012). A Small Novel A-Kinase Anchoring Protein (AKAP) That Localizes Specifically Protein Kinase A-Regulatory Subunit I (PKA-RI) to the Plasma Membrane*. *Journal of Biological Chemistry*, *287*(52), 43789-43797. https://doi.org/10.1074/jbc.M112.395970

Burgers, P. P., van der Heyden, M. A. G., Kok, B., Heck, A. J. R., & Scholten, A. (2015). A Systematic Evaluation of Protein Kinase A–A-Kinase Anchoring Protein Interaction Motifs. *Biochemistry*, *54*(1), 11-21. https://doi.org/10.1021/bi500721a

Capra, J. A., & Singh, M. (2007). Predicting functionally important residues from sequence conservation. *Bioinformatics*, *23*(15), 1875-1882. https://doi.org/https://doi.org/10.1093/bioinformatics/btm270

Carlson, C. R., Lygren, B., Berge, T., Hoshi, N., Wong, W., Taskén, K., & Scott, J. D. (2006). Delineation of Type I Protein Kinase A-selective Signaling Events Using an RI Anchoring Disruptor*. *Journal of Biological Chemistry*, *281*(30), 21535-21545. https://doi.org/10.1074/jbc.M603223200

Carr, D. W., Fujita, A., Stentz, C. L., Liberty, G. A., Olson, G. E., & Narumiya, S. (2001). Identification of Sperm-specific Proteins That Interact with A-kinase Anchoring Proteins in a Manner Similar to the Type II Regulatory Subunit of PKA *. *Journal of Biological Chemistry*, *276*(20), 17332-17338. https://doi.org/10.1074/jbc.M011252200

Carr, D. W., Hausken, Z. E., Fraser, I. D., Stofko-Hahn, R. E., & Scott, J. D. (1992). Association of the type II cAMP-dependent protein kinase with a human thyroid RII-anchoring protein. Cloning and characterization of the RII-binding domain. *Journal of Biological Chemistry*, *267*(19), 13376-13382. https://doi.org/10.1016/S0021-9258(18)42221-1

Carr, D. W., & Scott, J. D. (1992). Blotting and band-shifting: techniques for studying protein-protein interactions. *Trends Biochem. Sci.*, *17*, 246-249. https://doi.org/https://doi.org/10.1016/0968-0004(92)90402-u

Carr, D. W., Stofko-Hahn, R. E., Fraser, I. D., Bishop, S. M., Acott, T. S., Brennan, R. G., & Scott, J. D. (1991). Interaction of the regulatory subunit (RII) of cAMP-dependent protein kinase with RII-anchoring proteins occurs through an amphipathic helix binding motif. *Journal of Biological Chemistry*, *266*(22), 14188-14192. https://doi.org/10.1016/S0021-9258(18)98665-5

Carr, D. W., Stofko-Hahn, R. E., Fraser, I. D., Cone, R. D., & Scott, J. D. (1992). Localization of the cAMP-dependent protein kinase to the postsynaptic densities by A-kinase anchoring proteins. Characterization of AKAP 79. *Journal of Biological Chemistry*, *267*(24), 16816-16823. https://doi.org/10.1016/s0021-9258(18)41856-x

Case, D. A., Aktulga, H. M., Belfon, K., Cerutti, D. S., Cisneros, G. A., Cruzeiro, V. W. D., Forouzesh, N., Giese, T. J., Götz, A. W., Gohlke, H., Izadi, S., Kasavajhala, K., Kaymak, M. C., King, E., Kurtzman, T., Lee, T.-S., Li, P., Liu, J., Luchko, T.,…Merz, K. M. J. (2023). AmberTools. *Journal of Chemical Information and Modeling*, *63*(20), 6183-6191. https://doi.org/10.1021/acs.jcim.3c01153

Case, D. A., Cheatham III, T. E., Darden, T., Gohlke, H., Luo, R., Merz Jr., K. M., Onufriev, A., Simmerling, C., Wang, B., & Woods, R. J. (2005). The Amber biomolecular simulation programs. *Journal of Computational Chemistry*, *26*(16), 1668-1688. https://doi.org/10.1002/jcc.20290

Chan, G. K. L., Maisel, S., Hwang, Y. C., Pascual, B. C., Wolber, R. R. B., Vu, P., Patra, K. C., Bouhaddou, M., Kenerson, H. L., Lim, H. C., Long, D., Yeung, R. S., Sethupathy, P., Swaney, D. L., Krogan, N. J., Turnham, R. E., Riehle, K. J., Scott, J. D., Bardeesy, N., & Gordan, J. D. (2023). Oncogenic PKA signaling increases c-MYC protein expression through multiple targetable mechanisms. *Elife*, *12*. https://doi.org/10.7554/eLife.69521

Chothia, C., & Lesk, A. M. (1986). The relation between the divergence of sequence and structure in proteins. *Embo j*, *5*(4), 823-826. https://doi.org/10.1002/j.1460-2075.1986.tb04288.x

Clegg, C. H., Cadd, G. G., & McKnight, G. S. (1988). Genetic characterization of a brain-specific form of the type I regulatory subunit of cAMP-dependent protein kinase. *Proceedings of the National Academy of Sciences*, *85*(11), 3703-3707. https://doi.org/10.1073/pnas.85.11.3703

Clister, T., Greenwald, E. C., Baillie, G. S., & Zhang, J. (2019). AKAP95 Organizes a Nuclear Microdomain to Control Local cAMP for Regulating Nuclear PKA. *Cell chemical biology*, *26*(6), 885-891.e884. https://doi.org/10.1016/j.chembiol.2019.03.003

Close, P., East, P., Dirac-Svejstrup, A. B., Hartmann, H., Heron, M., Maslen, S., Chariot, A., Söding, J., Skehel, M., & Svejstrup, J. Q. (2012). DBIRD complex integrates alternative mRNA splicing with RNA polymerase II transcript elongation. *Nature*, *484*(7394), 386-389. https://doi.org/https://doi.org/10.1038/nature10925

Coghlan, V. M., Hausken, Z. E., & Scott, J. D. (1995). Subcellular targeting of kinases and phosphatases by association with bifunctional anchoring proteins. *Biochem. Soc. Trans.*, *23*, 591-596. https://doi.org/https://doi.org/10.1042/bst0230592

Coghlan, V. M., Langeberg, L. K., Fernandez, A., Lamb, N. J. C., & Scott, J. D. (1994). Cloning and characterization of AKAP95, a nuclear protein that associates with the regulatory subunit of type II cAMP-dependent protein kinase. *J. Biol. Chem.*, *269*, 7658-7665. https://doi.org/https://doi.org/10.1016/S0021-9258(17)37338-6

Coghlan, V. M., Perrino, B. A., Howard, M., Langeberg, L. K., Hicks, J. B., Gallatin, W. M., & Scott, J. D. (1995). Association of Protein Kinase A and Protein Phosphatase 2B with a Common Anchoring Protein. *Science*, *267*(5194), 108-111. https://doi.org/10.1126/science.7528941

Coles, G. L., Cristea, S., Webber, J. T., Levin, R. S., Moss, S. M., He, A., Sangodkar, J., Hwang, Y. C., Arand, J., Drainas, A. P., Mooney, N. A., Demeter, J., Spradlin, J. N., Mauch, B., Le, V., Shue, Y. T., Ko, J. H., Lee, M. C., Kong, C.,…Sage, J. (2020). Unbiased Proteomic Profiling Uncovers a

Targetable GNAS/PKA/PP2A Axis in Small Cell Lung Cancer Stem Cells. *Cancer Cell*, *38*(1), 129-143 e127. https://doi.org/10.1016/j.ccell.2020.05.003

Collas, P., Le Guellec, K., & Tasken, K. (1999). The A-kinase-anchoring protein AKAP95 is a multivalent protein with a key role in chromatin condensation at mitosis. *J Cell Biol*, *147*(6), 1167-1180. https://doi.org/https://doi.org/10.1083/jcb.147.6.1167

Crooks, G. E., Hon, G., Chandonia, J.-M., & Brenner, S. E. (2004). WebLogo: a sequence logo generator. *Genome Research*, *14*(6), 1188-1190. https://doi.org/10.1101/gr.849004

Cummings, D. E., Brandon, E. P., Planas, J. V., Motamed, K., Idzerda, R. L., & McKnight, G. S. (1996). Genetically lean mice result from targeted disruption of the RIIβ subunit of protein kinase A. *Nature*, *382*(6592), 622-626. https://doi.org/10.1038/382622a0

D.A. Case, H. M. A., K. Belfon, I.Y. Ben-Shalom, J.T. Berryman, S.R. Brozell, D.S. Cerutti, T.E. Cheatham, III, G.A. Cisneros, V.W.D. Cruzeiro, T.A. Darden, N. Forouzesh, G. Giambaşu, T. Giese, M.K. Gilson, H. Gohlke, A.W. Goetz, J. Harris, S. Izadi, S.A. Izmailov, K. Kasavajhala, M.C. Kaymak, E. King, A. Kovalenko, T. Kurtzman, T.S. Lee, P. Li, C. Lin, J. Liu, T. Luchko, R. Luo, M. Machado, V. Man, M. Manathunga, K.M. Merz, Y. Miao, O. Mikhailovskii, G. Monard, H. Nguyen, K.A. O'Hearn, A. Onufriev, F. Pan, S. Pantano, R. Qi, A. Rahnamoun, D.R. Roe, A. Roitberg, C. Sagui, S. Schott-Verdugo, A. Shajan, J. Shen, C.L. Simmerling, N.R. Skrynnikov, J. Smith, J. Swails, R.C. Walker, J. Wang, J. Wang, H. Wei, X. Wu, Y. Wu, Y. Xiong, Y. Xue, D.M. York, S. Zhao, Q. Zhu, and P.A. Kollman. (2023). *Amber23*. In

Dahlin, H. R., Zheng, N., & Scott, J. D. (2021). Beyond PKA: Evolutionary and structural insights that define a docking and dimerization domain superfamily. *The Journal of Biological Chemistry*, *297*(2), 100927. https://doi.org/10.1016/j.jbc.2021.100927

Darwin, C. (1859). *On the origin of species by means of natural selection, or preservation of favoured races in the struggle for life*. London : John Murray, 1859. https://search.library.wisc.edu/catalog/9934839413602122

Delint-Ramirez, I., Willoughby, D., Hammond, G. V. R., Ayling, L. J., & Cooper, D. M. F. (2011). Palmitoylation Targets AKAP79 Protein to Lipid Rafts and Promotes Its Regulation of Calcium-sensitive Adenylyl Cyclase Type 8. *Journal of Biological Chemistry*, *286*(38), 32962-32975. https://doi.org/10.1074/jbc.m111.243899

Dell'Acqua, M. L., Faux, M. C., Thorburn, J., Thorburn, A., & Scott, J. D. (1998). Membrane-targeting sequences on AKAP79 bind phosphatidylinositol-4, 5-bisphosphate. *The EMBO Journal*, *17*(8), 2246-2260. https://doi.org/10.1093/emboj/17.8.2246

Della Sala, A., Tasca, L., Butnarasu, C., Sala, V., Prono, G., Murabito, A., Garbero, O. V., Millo, E., Terranova, L., Blasi, F., Gramegna, A., Aliberti, S., Massarotti, A., Visentin, S., Hirsch, E., & Ghigo, A. (2024). A Non-natural Peptide Targeting the A-kinase Anchoring Function of PI3Kγ for Therapeutic cAMP Modulation in Pulmonary Cells. *Journal of Biological Chemistry*, 107873. https://doi.org/https://doi.org/10.1016/j.jbc.2024.107873

Di Benedetto, G., Zoccarato, A., Lissandron, V., Terrin, A., Li, X., Houslay, M. D., Baillie, G. S., & Zaccolo, M. (2008). Protein Kinase A Type I and Type II Define Distinct Intracellular Signaling Compartments. *Circulation Research*, *103*(8), 836-844. https://doi.org/10.1161/CIRCRESAHA.108.174813

Dohmen, E., Klasberg, S., Bornberg-Bauer, E., Perrey, S., & Kemena, C. (2020). The modular nature of protein evolution: domain rearrangement rates across eukaryotic life. *BMC Evolutionary Biology*, *20*(1). https://doi.org/10.1186/s12862-020-1591-0

Dong, X., Peng, Y., Peng, Y., Xu, F., He, X., Wang, F., Peng, X., Qiang, B., Yuan, J., & Rao, Z. (2005). Characterization and crystallization of human DPY-30-like protein, an essential component of dosage compensation complex. *Biochimica et biophysica acta*, *1753*(2), 257-262. https://doi.org/https://doi.org/10.1016/j.bbapap.2005.08.011

Dougherty, G. W., Mizuno, K., Nöthe-Menchen, T., Ikawa, Y., Boldt, K., Ta-Shma, A., Aprea, I., Minegishi, K., Pang, Y.-P., Pennekamp, P., Loges, N. T., Raidt, J., Hjeij, R., Wallmeier, J., Mussaffi, H., Perles, Z., Elpeleg, O., Rabert, F., Shiratori, H.,…Omran, H. (2020). CFAP45 deficiency causes situs abnormalities and asthenospermia by disrupting an axonemal adenine nucleotide homeostasis module. *Nature Communications*, *11*(1), 5520. https://doi.org/10.1038/s41467-020-19113-0

Dransfield, D. T., Bradford, A. J., Smith, J., Martin, M., Roy, C., Mangeat, P. H., & Goldenring, J. R. (1997). Ezrin is a cyclic AMP-dependent protein kinase anchoring protein. *The EMBO Journal*, *16*(1), 35-43. https://doi.org/10.1093/emboj/16.1.35

Edgar, R. C. (2004). MUSCLE: a multiple sequence alignment method with reduced time and space complexity. *BMC Bioinformatics*, *5*(1), 113. https://doi.org/10.1186/1471-2105-5-113

Eide, T., Coghlan, V., Orstavik, S., Holsve, C., Solberg, R., Skalhegg, B. S., Lamb, N. J., Langeberg, L., Fernandez, A., Scott, J. D., Jahnsen, T., & Tasken, K. (1998). Molecular cloning, chromosomal localization, and cell cycle-dependent subcellular distribution of the A-kinase anchoring protein, AKAP95. *Exp Cell Res*, *238*(2), 305-316. https://doi.org/https://doi.org/10.1006/excr.1997.3855

Fahy, J. V., & Dickey, B. F. (2010). Airway Mucus Function and Dysfunction. *New England Journal of Medicine*, *363*(23), 2233-2247. https://doi.org/10.1056/nejmra0910061

Faux, M. C., Rollins, E. N., Edwards, A. S., Langeberg, L. K., Newton, A. C., & Scott, J. D. (1999). Mechanism of A-kinase-anchoring protein 79 (AKAP79) and protein kinase C interaction. *Biochemical Journal*, *343*(Pt 2), 443-452.

Fiedler, S. E., Sisson, J. H., Wyatt, T. A., Pavlik, J. A., Gambling, T. M., Carson, J. L., & Carr, D. W. (2012). Loss of ASP but not ROPN1 reduces mammalian ciliary motility. *Cytoskeleton*, *69*(1), 22-32. https://doi.org/10.1002/cm.20539

Fish, K. N. (2009). Total internal reflection fluorescence (TIRF) microscopy. *Curr Protoc Cytom*, *Chapter 12*, Unit12.18. https://doi.org/10.1002/0471142956.cy1218s50

Fraser, I. D., & Scott, J. D. (1999). Modulation of ion channels: a "current" view of AKAPs. *Neuron*, *23*(3), 423-426. http://www.ncbi.nlm.nih.gov/cgi-bin/Entrez/referer?http://www.neuron.org/cgi/content/full/23/3/423

Fraser, I. D. C., Cong, M., Kim, J., Rollins, E. N., Daaka, Y., Lefkowitz, R. J., & Scott, J. D. (2000). Assembly of an A kinase-anchoring protein–β2-adrenergic receptor complex facilitates receptor phosphorylation and signaling. *Current Biology*, *10*(7), 409-412. https://doi.org/10.1016/S0960-9822(00)00419-X

Fuchs Erin, L., Brutinel Evan, D., Jones Adriana, K., Fulcher Nanette, B., Urbanowski Mark, L., Yahr Timothy, L., & Wolfgang Matthew, C. (2010). The Pseudomonas aeruginosa Vfr Regulator Controls Global Virulence Factor Expression through Cyclic AMP-Dependent and -Independent Mechanisms. *Journal of Bacteriology*, *192*(14), 3553-3564. https://doi.org/10.1128/jb.00363-10

Funayama, N., Nagafuchi, A., Sato, N., Tsukita, S., & Tsukita, S. (1991). Radixin is a novel member of the band 4.1 family. *The Journal of Cell Biology*, *115*(4), 1039-1048. https://doi.org/https://doi.org/10.1083/jcb.115.4.1039

Gabrovsek, L., Collins, K. B., Aggarwal, S., Saunders, L. M., Lau, H.-T., Suh, D., Sancak, Y., Trapnell, C., Ong, S.-E., Smith, F. D., & Scott, J. D. (2020). A-kinase-anchoring protein 1 (dAKAP1)-based signaling complexes coordinate local protein synthesis at the mitochondrial surface. *Journal of Biological Chemistry*, *295*(31), 10749-10765. https://doi.org/10.1074/jbc.RA120.013454

Gaillard, A. R., Diener, D. R., Rosenbaum, J. L., & Sale, W. S. (2001). Flagellar Radial Spoke Protein 3 Is an a-Kinase Anchoring Protein (Akap). *The Journal of Cell Biology*, *153*(2), 443-448.

Gaillard, A. R., Fox, L. A., Rhea, J. M., Craige, B., & Sale, W. S. (2006). Disruption of the A-Kinase Anchoring Domain in Flagellar Radial Spoke Protein 3 Results in Unregulated Axonemal cAMP-dependent Protein Kinase Activity and Abnormal Flagellar Motility. *Molecular Biology of the Cell*, *17*(6), 2626-2635. https://doi.org/10.1091/mbc.e06-02-0095

Gaynor, M. L., Lim-Hing, S., & Mason, C. M. (2020). Impact of genome duplication on secondary metabolite composition in non-cultivated species: a systematic meta-analysis. *Annals of Botany*, *126*(3), 363-376. https://doi.org/10.1093/aob/mcaa107

Giakoumakis, N. N., Rapsomaniki, M. A., & Lygerou, Z. (2017). Analysis of Protein Kinetics Using Fluorescence Recovery After Photobleaching (FRAP). In Y. Markaki & H. Harz (Eds.), *Light Microscopy: Methods and Protocols* (pp. 243-267). Springer.

Gilbert, W. (1986). Origin of life: The RNA world. *Nature*, *319*(6055), 618-618. https://doi.org/10.1038/319618a0

Glavin, D. P., Dworkin, J. P., Alexander, C. M. O. D., Aponte, J. C., Baczynski, A. A., Barnes, J. J., Bechtel, H. A., Berger, E. L., Burton, A. S., Caselli, P., Chung, A. H., Clemett, S. J., Cody, G. D., Dominguez, G., Elsila, J. E., Farnsworth, K. K., Foustoukos, D. I., Freeman, K. H., Furukawa, Y.,…Lauretta, D. S. (2025). Abundant ammonia and nitrogen-rich soluble organic matter in

samples from asteroid (101955) Bennu. *Nature Astronomy*. https://doi.org/10.1038/s41550-024-02472-9

Gold, M. G., Fowler, D. M., Means, C. K., Pawson, C. T., Stephany, J. J., Langeberg, L. K., Fields, S., & Scott, J. D. (2013). Engineering A-kinase Anchoring Protein (AKAP)-selective Regulatory Subunits of Protein Kinase A (PKA) through Structure-based Phage Selection. *The Journal of Biological Chemistry*, *288*(24), 17111-17121. https://doi.org/10.1074/jbc.M112.447326

Gold, M. G., Lygren, B., Dokurno, P., Hoshi, N., McConnachie, G., Taskén, K., Carlson, C. R., Scott, J. D., & Barford, D. (2006). Molecular basis of AKAP specificity for PKA regulatory subunits. *Molecular Cell*, *24*(3), 383-395. https://doi.org/https://doi.org/10.1016/j.molcel.2006.09.006

Gold, M. G., Stengel, F., Nygren, P. J., Weisbrod, C. R., Bruce, J. E., Robinson, C. V., Barford, D., & Scott, J. D. (2011). Architecture and dynamics of an A-kinase anchoring protein 79 (AKAP79) signaling complex. *Proceedings of the National Academy of Sciences*, *108*(16), 6426-6431. https://doi.org/10.1073/pnas.1014400108

González Bardeci, N., Caramelo, J. J., Blumenthal, D. K., Rinaldi, J., Rossi, S., & Moreno, S. (2016). The PKA regulatory subunit from yeast forms a homotetramer: Low-resolution structure of the N-terminal oligomerization domain. *Journal of Structural Biology*, *193*(2), 141-154. https://doi.org/https://doi.org/10.1016/j.jsb.2015.12.001

Good, M. C., Zalatan, J. G., & Lim, W. A. (2011). Scaffold Proteins: Hubs for Controlling the Flow of Cellular Information. *Science*, *332*(6030), 680-686. https://doi.org/10.1126/science.1198701

Gopal, R., Foster, K. W., & Yang, P. (2012). The DPY-30 Domain and Its Flanking Sequence Mediate the Assembly and Modulation of Flagellar Radial Spoke Complexes. *Molecular and Cellular Biology*, *32*(19), 4012-4024. https://doi.org/10.1128/mcb.06602-11

Götz, F., Roske, Y., Schulz, Maike S., Autenrieth, K., Bertinetti, D., Faelber, K., Zühlke, K., Kreuchwig, A., Kennedy, E. J., Krause, G., Daumke, O., Herberg, Friedrich W., Heinemann, U., & Klussmann, E. (2016). AKAP18:PKA-RIIα structure reveals crucial anchor points for recognition of regulatory subunits of PKA. *Biochemical Journal*, *473*(13), 1881-1894. https://doi.org/10.1042/BCJ20160242

Gough, J. (2005). Convergent evolution of domain architectures (is rare). *Bioinformatics*, *21*(8), 1464-1471. https://doi.org/10.1093/bioinformatics/bti204

Grönholm, M., Vossebein, L., Carlson, C. R., Kuja-Panula, J., Teesalu, T., Alfthan, K., Vaheri, A., Rauvala, H., Herberg, F. W., Taskén, K., & Carpén, O. (2003). Merlin Links to the cAMP Neuronal Signaling Pathway by Anchoring the RIβ Subunit of Protein Kinase A*. *Journal of Biological Chemistry*, *278*(42), 41167-41172. https://doi.org/10.1074/jbc.M306149200

Gupta, D. R., Paul, S. K., Oowatari, Y., Matsuo, Y., & Kawamukai, M. (2011). Multistep regulation of protein kinase A in its localization, phosphorylation and binding with a regulatory subunit in fission yeast. *Current Genetics*, *57*(5), 353-365. https://doi.org/10.1007/s00294-011-0354-2

Guseva, E., Zuckermann, R. N., & Dill, K. A. (2017). Foldamer hypothesis for the growth and sequence differentiation of prebiotic polymers. *Proc Natl Acad Sci U S A*, *114*(36), E7460-e7468. https://doi.org/10.1073/pnas.1620179114

Haimo, L. T., & Rosenbaum, J. L. (1981). Cilia, flagella, and microtubules. *Journal of Cell Biology*, *91*(3), 125s-130s. https://doi.org/10.1083/jcb.91.3.125s

Hanoune, J., & Defer, N. (2001). Regulation and Role of Adenylyl Cyclase Isoforms. *Annual Review of Pharmacology and Toxicology*, *41*(1), 145-174. https://doi.org/10.1146/annurev.pharmtox.41.1.145

Hausken, Z. E., Dell'Acqua, M. L., Coghlan, V. M., & Scott, J. D. (1996). Mutational analysis of the A-kinase anchoring protein (AKAP)-binding site on RII. *J. Biol. Chem.*, *271*, 29016-29022. https://doi.org/https://doi.org/10.1074/jbc.271.46.29016

Herberg, F. W., Maleszka, A., Eide, T., Vossebein, L., & Tasken, K. (2000). Analysis of A-kinase anchoring protein (AKAP) interaction with protein kinase A (PKA) regulatory subunits: PKA isoform specificity in AKAP binding. *Journal of Molecular Biology*, *298*(2), 329-339. https://doi.org/10.1006/jmbi.2000.3662

Hetzer, M. W. (2010). The nuclear envelope. *Cold Spring Harb Perspect Biol*, *2*(3), a000539. https://doi.org/https://doi.org/10.1101/cshperspect.a000539

Hoppe, N., Harrison, S., Hwang, S.-H., Chen, Z., Karelina, M., Deshpande, I., Suomivuori, C.-M., Palicharla, V. R., Berry, S. P., Tschaikner, P., Regele, D., Covey, D. F., Stefan, E., Marks, D. S., Reiter, J. F., Dror, R. O., Evers, A. S., Mukhopadhyay, S., & Manglik, A. (2024). GPR161 structure uncovers the redundant role of sterol-regulated ciliary cAMP signaling in the Hedgehog pathway.

Nature Structural & Molecular Biology, *31*(4), 667-677. https://doi.org/10.1038/s41594-024-01223-8

Howard, C. J., Hanson-Smith, V., Kennedy, K. J., Miller, C. J., Lou, H. J., Johnson, A. D., Turk, B. E., & Holt, L. J. (2014). Ancestral resurrection reveals evolutionary mechanisms of kinase plasticity. *eLife*, *3*. https://doi.org/10.7554/elife.04126

Hsu, P. L., Shi, H., Leonen, C., Kang, J., Chatterjee, C., & Zheng, N. (2019). Structural Basis of H2B Ubiquitination-Dependent H3K4 Methylation by COMPASS. *Mol Cell*, *76*(5), 712-723.e714. https://doi.org/https://doi.org/10.1016/j.molcel.2019.10.013

Hu, G.-M., Mai, T.-L., & Chen, C.-M. (2017). Visualizing the GPCR Network: Classification and Evolution. *Scientific Reports*, *7*(1). https://doi.org/10.1038/s41598-017-15707-9

Hu, J., Khodadadi-Jamayran, A., Mao, M., Shah, K., Yang, Z., Nasim, M. T., Wang, Z., & Jiang, H. (2016). AKAP95 regulates splicing through scaffolding RNAs and RNA processing factors. *Nature Communications*, *7*(1), 13347. https://doi.org/https://doi.org/10.1038/ncomms13347

Huang, L. J.-s., Durick, K., Weiner, J. A., Chun, J., & Taylor, S. S. (1997a). D-AKAP2, a novel protein kinase A anchoring protein with a putative RGS domain. *Proceedings of the National Academy of Sciences of the United States of America*, *94*(21), 11184-11189.

Huang, L. J.-s., Durick, K., Weiner, J. A., Chun, J., & Taylor, S. S. (1997b). Identification of a Novel Protein Kinase A Anchoring Protein That Binds Both Type I and Type II Regulatory Subunits*. *Journal of Biological Chemistry*, *272*(12), 8057-8064. https://doi.org/10.1074/jbc.272.12.8057

Ilouz, R., Bubis, J., Wu, J., Yim, Y. Y., Deal, M. S., Kornev, A. P., Ma, Y., Blumenthal, D. K., & Taylor, S. S. (2012). Localization and quaternary structure of the PKA RIβ holoenzyme. *Proceedings of the National Academy of Sciences*, *109*(31), 12443-12448. https://doi.org/10.1073/pnas.1209538109

Ilouz, R., Lev-Ram, V., Bushong, E. A., Stiles, T. L., Friedmann-Morvinski, D., Douglas, C., Goldberg, J. L., Ellisman, M. H., & Taylor, S. S. (2017). Isoform-specific subcellular localization and function of protein kinase A identified by mosaic imaging of mouse brain. *eLife*, *6*, e17681. https://doi.org/10.7554/eLife.17681

Irannejad, R., Tsvetanova, N. G., Lobingier, B. T., & von Zastrow, M. (2015). Effects of endocytosis on receptor-mediated signaling. *Curr Opin Cell Biol*, *35*, 137-143. https://doi.org/10.1016/j.ceb.2015.05.005

Jackson, P. K. (2020). cAMP Signaling in Nanodomains. *Cell*, *182*(6), 1379-1381. https://doi.org/10.1016/j.cell.2020.08.041

Jayaraman, V., Toledo-Patiño, S., Noda-García, L., & Laurino, P. (2022). Mechanisms of protein evolution. *Protein Science*, *31*(7). https://doi.org/10.1002/pro.4362

Jivan, A., Earnest, S., Juang, Y.-C., & Cobb, M. H. (2009). Radial Spoke Protein 3 Is a Mammalian Protein Kinase A-anchoring Protein That Binds ERK1/2 *. *Journal of Biological Chemistry*, *284*(43), 29437-29445. https://doi.org/10.1074/jbc.M109.048181

Johnson, K. A., & Rosenbaum, J. L. (1992). Polarity of flagellar assembly in Chlamydomonas. *Journal of Cell Biology*, *119*(6), 1605-1611. https://doi.org/10.1083/jcb.119.6.1605

Kajava, A. V., & Steven, A. C. (2006). β-Rolls, β-Helices, and Other β-Solenoid Proteins. In (pp. 55-96). Elsevier. https://doi.org/10.1016/s0065-3233(06)73003-0

Kang, M., Otani, Y., Guo, Y., Yan, J., Goult, B. T., & Howe, A. K. (2024). The focal adhesion protein talin is a mechanically gated A-kinase anchoring protein. *Proceedings of the National Academy of Sciences*, *121*(13). https://doi.org/10.1073/pnas.2314947121

Kang, R., Wan, J., Arstikaitis, P., Takahashi, H., Huang, K., Bailey, A. O., Thompson, J. X., Roth, A. F., Drisdel, R. C., Mastro, R., Green, W. N., Yates Iii, J. R., Davis, N. G., & El-Husseini, A. (2008). Neural palmitoyl-proteomics reveals dynamic synaptic palmitoylation. *Nature*, *456*(7224), 904-909. https://doi.org/10.1038/nature07605

Keith, D. J., Sanderson, J. L., Gibson, E. S., Woolfrey, K. M., Robertson, H. R., Olszewski, K., Kang, R., El-Husseini, A., & Dell'Acqua, M. L. (2012). Palmitoylation of A-Kinase Anchoring Protein 79/150 Regulates Dendritic Endosomal Targeting and Synaptic Plasticity Mechanisms. *The Journal of Neuroscience*, *32*(21), 7119-7136. https://doi.org/10.1523/jneurosci.0784-12.2012

Kemp, B. E., Graves, D. J., Benjamini, E., & Krebs, E. G. (1977). Role of multiple basic residues in determining the substrate specificity of cyclic AMP-dependent protein kinase. *J Biol Chem*, *252*(14), 4888-4894.

Khafizov, K., Lattanzi, G., & Carloni, P. (2009). G protein inactive and active forms investigated by simulation methods. *Proteins: Structure, Function, and Bioinformatics*, *75*(4), 919-930. https://doi.org/10.1002/prot.22303

Khalil, J. S., Saldanha, P. A., Blair, C. M., Ling, J., Ji, W., Baillie, G. S., Naseem, K. M., Nikitenko, L. L., & Rivero, F. (2023). MYPT1 is a non-canonical AKAP that tethers PKA to the MLCP signaling node. https://doi.org/10.1101/2023.04.27.538407

Kimura, M. (1968). Evolutionary rate at the molecular level. *Nature*, *217*(5129), 624-626. https://doi.org/10.1038/217624a0

Kimura, M. (1983). The Neutral Theory of Molecular Evolution. https://doi.org/10.1017/cbo9780511623486

Kimura, M., & Ohta, T. (1974). On Some Principles Governing Molecular Evolution. *Proceedings of the National Academy of Sciences*, *71*(7), 2848-2852. https://doi.org/doi:10.1073/pnas.71.7.2848

Kocher, C., & Dill, K. A. (2023). Origins of life: first came evolutionary dynamics. *QRB Discov*, *4*, e4. https://doi.org/10.1017/qrd.2023.2

Kocher, C. D., & Dill, K. A. (2024). Origins of life: The Protein Folding Problem all over again? *Proceedings of the National Academy of Sciences*, *121*(34), e2315000121. https://doi.org/doi:10.1073/pnas.2315000121

Kozlov, A. M., Darriba, D., Flouri, T., Morel, B., & Stamatakis, A. (2019). RAxML-NG: a fast, scalable and user-friendly tool for maximum likelihood phylogenetic inference. *Bioinformatics*, *35*(21), 4453-4455. https://doi.org/10.1093/bioinformatics/btz305

Krebs, E. G., Blumenthal, D. K., Edelman, A. M., & Hales, C. N. (1985). The functions of the cAMP-dependent protein kinase. In S. T. Crooke & G. Poste (Eds.), *Mechanisms of Receptor Regulation* (pp. 324-367). Plenum.

Kultgen, P. L., Byrd, S. K., Ostrowski, L. E., & Milgram, S. L. (2002). Characterization of an A-Kinase Anchoring Protein in Human Ciliary Axonemes. *Molecular Biology of the Cell*, *13*(12), 4156-4166. https://doi.org/https://doi.org/10.1091/mbc.e02-07-0391

Kvissel, A.-K., Ørstavik, S., Eikvar, S., Brede, G., Jahnsen, T., Collas, P., Akusjärvi, G., & Skålhegg, B. S. (2007). Involvement of the catalytic subunit of protein kinase A and of HA95 in pre-mRNA splicing. *Experimental Cell Research*, *313*(13), 2795-2809. https://doi.org/https://doi.org/10.1016/j.yexcr.2007.05.014

Langeberg, L. K., & Scott, J. D. (2015). Signalling scaffolds and local organization of cellular behaviour. *Nat Rev Mol Cell Biol*, *16*(4), 232-244. https://doi.org/https://doi.org/10.1038/nrm3966

Lee, H., Lee, T. J., Galloway, C. A., Zhi, W., Xiao, W., de Mesy Bentley, K. L., Sharma, A., Teng, Y., Sesaki, H., & Yoon, Y. (2023). The mitochondrial fusion protein OPA1 is dispensable in the liver and its absence induces mitohormesis to protect liver from drug-induced injury. *Nature Communications*, *14*(1), 6721. https://doi.org/https://doi.org/10.1038/s41467-023-42564-0

Lee, Y.-T., Ayoub, A., Park, S.-H., Sha, L., Xu, J., Mao, F., Zheng, W., Zhang, Y., Cho, U.-S., & Dou, Y. (2021). Mechanism for DPY30 and ASH2L intrinsically disordered regions to modulate the MLL/SET1 activity on chromatin. *Nature Communications*, *12*(1). https://doi.org/https://doi.org/10.1038/s41467-021-23268-9

Lemmon, M. A. (2008). Membrane recognition by phospholipid-binding domains. *Nat Rev Mol Cell Biol*, *9*(2), 99-111. https://doi.org/https://doi.org/10.1038/nrm2328

Lemmon, M. A., Ferguson, K. M., O'Brien, R., Sigler, P. B., & Schlessinger, J. (1995). Specific and high-affinity binding of inositol phosphates to an isolated pleckstrin homology domain. *Proc. Natl. Acad. Sci. USA*, *92*, 10472-10476. https://doi.org/https://doi.org/10.1073/pnas.92.23.10472

Lenaers, G., Hamel, C., Delettre, C., Amati-Bonneau, P., Procaccio, V., Bonneau, D., Reynier, P., & Milea, D. (2012). Dominant optic atrophy. *Orphanet Journal of Rare Diseases*, *7*(1), 46. https://doi.org/https://doi.org/10.1186/1750-1172-7-46

León, D. A., Herberg, F. W., Banky, P., & Taylor, S. S. (1997). A Stable α-Helical Domain at the N Terminus of the RIα Subunits of cAMP-dependent Protein Kinase Is a Novel Dimerization/Docking Motif*. *Journal of Biological Chemistry*, *272*(45), 28431-28437. https://doi.org/10.1074/jbc.272.45.28431

Levy, M., Miller, S. L., Brinton, K., & Bada, J. L. (2000). Prebiotic Synthesis of Adenine and Amino Acids Under Europa-like Conditions. *Icarus*, *145*(2), 609-613. https://doi.org/https://doi.org/10.1006/icar.2000.6365

Li, W., Hu, J., Shi, B., Palomba, F., Digman, M. A., Gratton, E., & Jiang, H. (2020). Biophysical properties of AKAP95 protein condensates regulate splicing and tumorigenesis. *Nature Cell Biology*, *22*(8), 960-972. https://doi.org/https://doi.org/10.1038/s41556-020-0550-8

Li, Y.-F., He, W., Mandal, A., Kim, Y.-H., Digilio, L., Klotz, K., Flickinger, C. J., Herr, J. C., & Herr, J. C. (2011). CABYR binds to AKAP3 and Ropporin in the human sperm fibrous sheath. *Asian Journal of Andrology*, *13*(2), 266-274. https://doi.org/10.1038/aja.2010.149

Lincoln, T. A., & Joyce, G. F. (2009). Self-sustained replication of an RNA enzyme. *Science*, *323*(5918), 1229-1232. https://doi.org/10.1126/science.1167856

Lisanza, S. L., Gershon, J. M., Tipps, S. W. K., Sims, J. N., Arnoldt, L., Hendel, S. J., Simma, M. K., Liu, G., Yase, M., Wu, H., Tharp, C. D., Li, X., Kang, A., Brackenbrough, E., Bera, A. K., Gerben, S., Wittmann, B. J., McShan, A. C., & Baker, D. (2024). Multistate and functional protein design using RoseTTAFold sequence space diffusion. *Nature Biotechnology*. https://doi.org/https://doi.org/10.1038/s41587-024-02395-w

Liu, Q., Tong, D., Liu, G., Yi, Y., Zhang, D., Zhang, J., Zhang, Y., Huang, Z., Li, Y., Chen, R., Guan, Y., Yi, X., & Jiang, J. (2017). Carney complex with PRKAR1A gene mutation: A case report and literature review. *Medicine (Baltimore)*, *96*(50), e8999. https://doi.org/10.1097/md.0000000000008999

Lohmann, S. M., DeCamilli, P., Einig, I., & Walter, U. (1984). High-affinity binding of the regulatory subunit (RII) of cAMP-dependent protein kinase to microtubule-associated and other cellular proteins. *Proceedings of the National Academy of Sciences*, *81*(21), 6723-6727. https://doi.org/10.1073/pnas.81.21.6723

Lu, T.-W., Wu, J., Aoto, P. C., Weng, J.-H., Ahuja, L. G., Sun, N., Cheng, C. Y., Zhang, P., & Taylor, S. S. (2019). Two PKA RIα holoenzyme states define ATP as an isoform-specific orthosteric inhibitor that competes with the allosteric activator, cAMP. *Proceedings of the National Academy of Sciences*, *116*(33), 16347-16356. https://doi.org/doi:10.1073/pnas.1906036116

Ma, M., Zhou, J., Ma, Z., Chen, H., Li, L., Hou, L., Yin, B., Qiang, B., Shu, P., & Peng, X. (2022). The Ash2l SDI Domain Is Required to Maintain the Stability and Binding of DPY30. *Cells*, *11*(9), 1450. https://doi.org/10.3390/cells11091450

Macleod, J., Mei, X., Erlichman, J., & Orr, G. A. (1994). Association of the regulatory subunit of a type II cAMP-dependent protein kinase and its binding proteins with the fibrous sheath of rat sperm flagellum. *Eur. J. Biochem.*, *225*, 107-114. https://doi.org/https://doi.org/10.1111/j.1432-1033.1994.00107.x

Mangel, M., & Samaniego, F. J. (1984). Abraham Wald's Work on Aircraft Survivability. *Journal of the American Statistical Association*, *79*(386), 259-267. https://doi.org/10.1080/01621459.1984.10478038

Margulis, L., Chapman, M., Guerrero, R., & Hall, J. (2006). The last eukaryotic common ancestor (LECA): Acquisition of cytoskeletal motility from aerotolerant spirochetes in the Proterozoic Eon. *Proceedings of the National Academy of Sciences*, *103*(35), 13080-13085. https://doi.org/10.1073/pnas.0604985103

McCartney, S., Little, B. M., Langeberg, L. K., & Scott, J. D. (1995). Cloning and Characterization of A-kinase Anchor Protein 100 (AKAP100): A PROTEIN THAT TARGETS A-KINASE TO THE SARCOPLASMIC RETICULUM *. *Journal of Biological Chemistry*, *270*(16), 9327-9333. https://doi.org/10.1074/jbc.270.16.9327

Means, C. K., Lygren, B., Langeberg, L. K., Jain, A., Dixon, R. E., Vega, A. L., Gold, M. G., Petrosyan, S., Taylor, S. S., Murphy, A. N., Ha, T., Santana, L. F., Tasken, K., & Scott, J. D. (2011). An entirely specific type I A-kinase anchoring protein that can sequester two molecules of protein kinase A at mitochondria. *Proceedings of the National Academy of Sciences*, *108*(48), E1227-E1235. https://doi.org/10.1073/pnas.1107182108

Mei, X., Singh, I. S., Erlichman, J., & Orr, G. A. (1997). Cloning and characterization of a testis-specific, developmentally regulated A-kinase-anchoring protein (TAKAP-80) present on the fibrous sheath of rat sperm. *Eur. J. Biochem.*, *246*, 425-432. https://doi.org/https://doi.org/10.1111/j.1432-1033.1997.t01-1-00425.x

Michie, K. A., Bermeister, A., Robertson, N. O., Goodchild, S. C., & Curmi, P. M. G. (2019). Two Sides of the Coin: Ezrin/Radixin/Moesin and Merlin Control Membrane Structure and Contact Inhibition. *Int J Mol Sci*, *20*(8). https://doi.org/ https://doi.org/10.3390/ijms20081996

Milara, J., Armengot, M., Mata, M., Morcillo, E. J., & Cortijo, J. (2010). Role of Adenylate Kinase Type 7 Expression on Cilia Motility: Possible Link in Primary Ciliary Dyskinesia. *American Journal of Rhinology & Allergy*, *24*(3), 181-185. https://doi.org/10.2500/ajra.2010.24.3468

Miller, B. R., McGee, T. D., Swails, J. M., Homeyer, N., Gohlke, H., & Roitberg, A. E. (2012). MMPBSA.py: An Efficient Program for End-State Free Energy Calculations. *Journal of Chemical Theory and Computation*, *8*(9), 3314-3321. https://doi.org/10.1021/ct300418h

Minh, B. Q., Schmidt, H. A., Chernomor, O., Schrempf, D., Woodhams, M. D., von Haeseler, A., & Lanfear, R. (2020). IQ-TREE 2: New Models and Efficient Methods for Phylogenetic Inference in the Genomic Era. *Molecular Biology and Evolution*, *37*(5), 1530-1534. https://doi.org/10.1093/molbev/msaa015

Misaka, T., Miyashita, T., & Kubo, Y. (2002). Primary Structure of a Dynamin-related Mouse Mitochondrial GTPase and Its Distribution in Brain, Subcellular Localization, and Effect on Mitochondrial Morphology. *Journal of Biological Chemistry*, *277*(18), 15834-15842. https://doi.org/https://doi.org/10.1074/jbc.m109260200

Mitchell, B. F., Pedersen, L. B., Feely, M., Rosenbaum, J. L., & Mitchell, D. R. (2005). ATP Production in Chlamydomonas reinhardtii Flagella by Glycolytic Enzymes. *Molecular Biology of the Cell*, *16*(10), 4509-4518. https://doi.org/10.1091/mbc.e05-04-0347

Moore, A. D., Björklund, Å. K., Ekman, D., Bornberg-Bauer, E., & Elofsson, A. (2008). Arrangements in the modular evolution of proteins. *Trends in Biochemical Sciences*, *33*(9), 444-451. https://doi.org/10.1016/j.tibs.2008.05.008

Morohoshi, A., Miyata, H., Shimada, K., Nozawa, K., Matsumura, T., Yanase, R., Shiba, K., Inaba, K., & Ikawa, M. (2020). Nexin-Dynein regulatory complex component DRC7 but not FBXL13 is required for sperm flagellum formation and male fertility in mice. *PLOS Genetics*, *16*(1), e1008585. https://doi.org/10.1371/journal.pgen.1008585

Morrow, K. A., & Shevde, L. A. (2012). Merlin: the wizard requires protein stability to function as a tumor suppressor. *Biochim Biophys Acta*, *1826*(2), 400-406. https://doi.org/https://doi.org/10.1016/j.bbcan.2012.06.005

Mukhopadhyay, S., Wen, X., Ratti, N., Loktev, A., Rangell, L., Suzie, & Peter. (2013). The Ciliary G-Protein-Coupled Receptor Gpr161 Negatively Regulates the Sonic Hedgehog Pathway via cAMP Signaling. *Cell*, *152*(1-2), 210-223. https://doi.org/10.1016/j.cell.2012.12.026

Nei, M., & Kumar, S. (2000). *Molecular Evolution and Phylogenetics*. Oxford University Press. https://global.oup.com/academic/product/molecular-evolution-and-phylogenetics-9780195135855?cc=us&lang=en&

Newell, A. E. H., Fiedler, S. E., Ruan, J. M., Pan, J., Wang, P. J., Deininger, J., Corless, C. L., & Carr, D. W. (2008). Protein kinase A RII-like (R2D2) proteins exhibit differential localization and AKAP interaction. *Cell Motility*, *65*(7), 539-552. https://doi.org/10.1002/cm.20279

Newlon, M. G., Roy, M., Morikis, D., Carr, D. W., Westphal, R., Scott, J. D., & Jennings, P. A. (2001). A novel mechanism of PKA anchoring revealed by solution structures of anchoring complexes. *The EMBO Journal*, *20*(7), 1651-1662. https://doi.org/10.1093/emboj/20.7.1651

Newlon, M. G., Roy, M., Morikis, D., Hausken, Z. E., Coghlan, V., Scott, J. D., & Jennings, P. A. (1999). The molecular basis for protein kinase A anchoring revealed by solution NMR. *Nat. Struct. Biol.*, *6*(3), 222-227. https://doi.org/https://doi.org/10.1038/6663

Nowick, J. S. (2008). Exploring beta-sheet structure and interactions with chemical model systems. *Acc Chem Res*, *41*(10), 1319-1330. https://doi.org/10.1021/ar800064f

Nyenhuis, S. B., Wu, X., Strub, M.-P., Yim, Y.-I., Stanton, A. E., Baena, V., Syed, Z. A., Canagarajah, B., Hammer, J. A., & Hinshaw, J. E. (2023). OPA1 helical structures give perspective to mitochondrial dysfunction. *Nature*, *620*(7976), 1109-1116. https://doi.org/https://doi.org/10.1038/s41586-023-06462-1

Nygren, P. J., Mehta, S., Schweppe, D. K., Langeberg, L. K., Whiting, J. L., Weisbrod, C. R., Bruce, J. E., Zhang, J., Veesler, D., & Scott, J. D. (2017). Intrinsic disorder within AKAP79 fine-tunes anchored phosphatase activity toward substrates and drug sensitivity. *eLife*, *6*, e30872. https://doi.org/10.7554/eLife.30872

Ohno, S. (1970). *Evolution by Gene Duplication*. Springer Berlin Heidelberg. https://doi.org/10.1007/978-3-642-86659-3

Omar, M. H., Byrne, D. P., Jones, K. N., Lakey, T. M., Collins, K. B., Lee, K.-S., Daly, L. A., Forbush, K. A., Lau, H.-T., Golkowski, M., McKnight, G. S., Breault, D. T., Lefrançois-Martinez, A.-M., Martinez,

A., Eyers, C. E., Baird, G. S., Ong, S.-E., Smith, F. D., Eyers, P. A., & Scott, J. D. (2022). Mislocalization of protein kinase A drives pathology in Cushing's syndrome. *Cell Reports*, *40*(2), 111073. https://doi.org/10.1016/j.celrep.2022.111073

Omar, M. H., Byrne, D. P., Shrestha, S., Lakey, T. M., Lee, K.-S., Lauer, S. M., Collins, K. B., Daly, L. A., Eyers, C. E., Baird, G. S., Ong, S.-E., Kannan, N., Eyers, P. A., & Scott, J. D. (2024). Discovery of a Cushing's syndrome protein kinase A mutant that biases signaling through type I AKAPs. *Science Advances*, *10*(8). https://doi.org/10.1126/sciadv.adl1258

Omar, M. H., Kihiu, M., Byrne, D. P., Lee, K. S., Lakey, T. M., Butcher, E., Eyers, P. A., & Scott, J. D. (2023). Classification of Cushing's syndrome PKAc mutants based upon their ability to bind PKI. *Biochem J*, *480*(12), 875-890. https://doi.org/10.1042/BCJ20230183

Omar, M. H., & Scott, J. D. (2020). AKAP Signaling Islands: Venues for Precision Pharmacology. *Trends in Pharmacological Sciences*, *41*(12), 933-946. https://doi.org/https://doi.org/10.1016/j.tips.2020.09.007

Ou, Y., Ruan, Y., Cheng, M., Moser, J. J., Rattner, J. B., & van der Hoorn, F. A. (2009). Adenylate cyclase regulates elongation of mammalian primary cilia. *Experimental Cell Research*, *315*(16), 2802-2817. https://doi.org/10.1016/j.yexcr.2009.06.028

Panayiotou, C., Solaroli, N., Xu, Y., Johansson, M., & Karlsson, A. (2011). The characterization of human adenylate kinases 7 and 8 demonstrates differences in kinetic parameters and structural organization among the family of adenylate kinase isoenzymes. *The Biochemical Journal*, *433*(3), 527-534. https://doi.org/10.1042/BJ20101443

Pawson, T., & Nash, P. (2000). Protein-protein interactions define specificity in signal transduction. *Genes Dev*, *14*(9), 1027-1047. https://doi.org/https://doi.org/10.1101/GAD.14.9.1027

Pawson, T., & Nash, P. (2003). Assembly of cell regulatory systems through protein interaction domains. *Science*, *300*(5618), 445-452. https://doi.org/https://doi.org/10.1126/science.1083653

Peng, M., Aye, T. T., Snel, B., van Breukelen, B., Scholten, A., & Heck, A. J. R. (2015). Spatial Organization in Protein Kinase A Signaling Emerged at the Base of Animal Evolution. *Journal of Proteome Research*, *14*(7), 2976-2987. https://doi.org/10.1021/acs.jproteome.5b00370

Perino, A., Ghigo, A., Ferrero, E., Morello, F., Santulli, G., George, Damilano, F., Allan, Pawson, C., Walser, R., Levi, R., Altruda, F., Silengo, L., Lorene, Neubauer, G., Heymans, S., Lembo, G., Matthias, Wetzker, R.,…Hirsch, E. (2011). Integrating Cardiac PIP3 and cAMP Signaling through a PKA Anchoring Function of p110γ. *Molecular Cell*, *42*(1), 84-95. https://doi.org/10.1016/j.molcel.2011.01.030

Pidoux, G., Witczak, O., Jarnæss, E., Myrvold, L., Urlaub, H., Stokka, A. J., Küntziger, T., & Taskén, K. (2011). Optic atrophy 1 is an A-kinase anchoring protein on lipid droplets that mediates adrenergic control of lipolysis. *The EMBO Journal*, *30*(21), 4371-4386. https://doi.org/10.1038/emboj.2011.365

Ponting, C. P., & Russell, R. R. (2002). The Natural History of Protein Domains. *Annual review of biophysics*, *31*(Volume 31, 2002), 45-71. https://doi.org/https://doi.org/10.1146/annurev.biophys.31.082901.134314

Porter, M. E., & Sale, W. S. (2000). The 9 + 2 Axoneme Anchors Multiple Inner Arm Dyneins and a Network of Kinases and Phosphatases That Control Motility. *The Journal of Cell Biology*, *151*(5), F37-F42. https://doi.org/10.1083/jcb.151.5.f37

Rao, V. G., Shendge, A. A., D'Gama, P. P., Martis, E. A. F., Mehta, S., Coutinho, E. C., & D'Souza, J. S. (2024). A-kinase anchoring proteins are enriched in the central pair microtubules of motile cilia in Chlamydomonas reinhardtii. *FEBS Letters*, *598*(4), 457-476. https://doi.org/https://doi.org/10.1002/1873-3468.14791

Rastogi, S., & Liberles, D. A. (2005). Subfunctionalization of duplicated genes as a transition state to neofunctionalization. *BMC Evolutionary Biology*, *5*(1), 28. https://doi.org/10.1186/1471-2148-5-28

Rawat, V. P., Humphries, R. K., & Buske, C. (2012). Beyond Hox: the role of ParaHox genes in normal and malignant hematopoiesis. *Blood*, *120*(3), 519-527. https://doi.org/https://doi.org/10.1182/blood-2012-02-385898

Reinton, N., Haugen, T. B., Ørstavik, S., Skålhegg, B. S., Hansson, V., Jahnsen, T., & Taskén, K. (1998). The Gene Encoding the Cγ Catalytic Subunit of cAMP-Dependent Protein Kinase Is a Transcribed Retroposon. *Genomics*, *49*(2), 290-297. https://doi.org/https://doi.org/10.1006/geno.1998.5240

Rogne, M., Chu, D. T., Küntziger, T. M., Mylonakou, M. N., Collas, P., & Tasken, K. (2018). OPA1-anchored PKA phosphorylates perilipin 1 on S522 and S497 in adipocytes differentiated from human adipose stem cells. *Mol Biol Cell*, *29*(12), 1487-1501. https://doi.org/10.1091/mbc.E17-09-0538

Rosenthal, K. J., Gordan, J. D., & Scott, J. D. (2024). Protein kinase A and local signaling in cancer. *Biochemical Journal*, *481*(22), 1659-1677. https://doi.org/10.1042/bcj20230352

Sarkar, D., Erlichman, J., & Rubin, C. S. (1984). Identification of a calmodulin-binding protein that co-purifies with the regulatory subunit of brain protein kinase II. *Journal of Biological Chemistry*, *259*(15), 9840-9846. https://doi.org/10.1016/S0021-9258(17)42776-1

Schindelin, J., Arganda-Carreras, I., Frise, E., Kaynig, V., Longair, M., Pietzsch, T., Preibisch, S., Rueden, C., Saalfeld, S., Schmid, B., Tinevez, J.-Y., White, D. J., Hartenstein, V., Eliceiri, K., Tomancak, P., & Cardona, A. (2012). Fiji: an open-source platform for biological-image analysis. *Nature Methods*, *9*(7), 676-682. https://doi.org/10.1038/nmeth.2019

Schrödinger, L. L. C. (2024). The PyMOL Molecular Graphics System, Version 3.0. In.

Scott, J. D., & Pawson, T. (2009). Cell signaling in space and time: where proteins come together and when they're apart. *Science*, *326*(5957), 1220-1224. https://doi.org/https://doi.org/10.1126/science.1175668

Scott, J. D., Stofko, R. E., McDonald, J. R., Comer, J. D., Vitalis, E. A., & Mangeli, J. (1990). Type II regulatory subunit dimerization determines the subcellular localization of the cAMP-dependent protein kinase. *J. Biol. Chem.*, *265*, 21561-21566. https://doi.org/https://doi.org/10.1016/S0021-9258(18)45777-8

Semenova, I., Ikeda, K., Ivanov, P., & Rodionov, V. (2009). The Protein Kinase A-Anchoring Protein Moesin is Bound to Pigment Granules in Melanophores. *Traffic*, *10*(2), 153-160. https://doi.org/https://doi.org/10.1111/j.1600-0854.2008.00852.x

Sheridan, J., Grata, A., Suva, E. E., Bresteau, E., Mitchell, L. R., Hassan, O., & Mitchell, B. (2023). *Novel centriolar defects underlie a primary ciliary dyskinesia phenotype in an adenylate kinase 7 deficient ciliated epithelium*. Cold Spring Harbor Laboratory. https://dx.doi.org/10.1101/2023.07.25.550535

Sherpa, R. T., Moshal, K. S., Agarwal, S. R., Ostrom, R. S., & Harvey, R. D. (2024). Role of protein kinase A and A kinase anchoring proteins in buffering and compartmentation of cAMP signalling in human airway smooth muscle cells. *British Journal of Pharmacology*, *n/a*(n/a). https://doi.org/10.1111/bph.16357

Shoji, S., Parmelee, D. C., Wade, R. D., Kumar, S., Ericsson, L. H., Walsh, K. A., Neurath, H., Long, G. L., Demaille, J. G., Fischer, E. H., & Titani, K. (1981). Complete amino acid sequence of the catalytic subunit of bovine cardiac muscle cyclic AMP-dependent protein kinase. *Proceedings of the National Academy of Sciences*, *78*(2), 848-851. https://doi.org/doi:10.1073/pnas.78.2.848

Skalhegg, B. S., & Tasken, K. (2000). Specificity in the cAMP/PKA signaling pathway. Differential expression,regulation, and subcellular localization of subunits of PKA. *Front Biosci*, *5*, D678-693. http://www.ncbi.nlm.nih.gov/cgi-bin/Entrez/referer?http://www.bioscience.org/2000/v5/d/skalhegg/list.htm

Smith, F. D., Esseltine, J. L., Nygren, P. J., Veesler, D., Byrne, D. P., Vonderach, M., Strashnov, I., Eyers, C. E., Eyers, P. A., Langeberg, L. K., & Scott, J. D. (2017). Local protein kinase A action proceeds through intact holoenzymes. *Science (New York, N.Y.)*, *356*(6344), 1288-1293. https://doi.org/10.1126/science.aaj1669

Smith, F. D., Reichow, S. L., Esseltine, J. L., Shi, D., Langeberg, L. K., Scott, J. D., & Gonen, T. (2013). Intrinsic disorder within an AKAP-protein kinase A complex guides local substrate phosphorylation. *eLife*, *2*, e01319. https://doi.org/10.7554/eLife.01319

Søberg, K., Moen, L. V., Skålhegg, B. S., & Laerdahl, J. K. (2017). Evolution of the cAMP-dependent protein kinase (PKA) catalytic subunit isoforms. *PLOS ONE*, *12*(7), e0181091. https://doi.org/10.1371/journal.pone.0181091

Solaroli, N., Panayiotou, C., Johansson, M., & Karlsson, A. (2009). Identification of two active functional domains of human adenylate kinase 5. *FEBS Letters*, *583*(17), 2872-2876. https://doi.org/10.1016/j.febslet.2009.07.047

Stierl, M., Stumpf, P., Udwari, D., Gueta, R., Hagedorn, R., Losi, A., Gärtner, W., Petereit, L., Efetova, M., Schwarzel, M., Oertner, T. G., Nagel, G., & Hegemann, P. (2011). Light Modulation of Cellular cAMP by a Small Bacterial Photoactivated Adenylyl Cyclase, bPAC, of the Soil Bacterium

Beggiatoa. *Journal of Biological Chemistry*, *286*(2), 1181-1188. https://doi.org/10.1074/jbc.M110.185496

Strada, S. J., Uzunov, P., & Weiss, B. (1974). Ontogenetic development of a phosphodiesterase activator and the multiple forms of cyclic AMP phosphodiesterase of rat brain. *Journal of Neurochemistry*, *23*(6), 1097-1103. https://doi.org/10.1111/j.1471-4159.1974.tb12204.x

Sun, G., Wang, C., Wang, S., Sun, H., Zeng, K., Zou, R., Lin, L., Liu, W., Sun, N., Song, H., Liu, W., Zhou, T., Jin, F., Shan, Z., & Zhao, Y. (2020). An H3K4me3 reader, BAP18 as an adaptor of COMPASS-like core subunits co-activates ERα action and associates with the sensitivity of antiestrogen in breast cancer. *Nucleic Acids Research*, *48*(19), 10768-10784. https://doi.org/10.1093/nar/gkaa787

Taylor, S. S., Ilouz, R., Zhang, P., & Kornev, A. P. (2012). Assembly of allosteric macromolecular switches: lessons from PKA. *Nat Rev Mol Cell Biol*, *13*(10), 646-658. https://doi.org/10.1038/nrm3432

Theobald, D. L., & Wuttke, D. S. (2005). Divergent Evolution Within Protein Superfolds Inferred from Profile-based Phylogenetics. *Journal of Molecular Biology*, *354*(3), 722-737. https://doi.org/10.1016/j.jmb.2005.08.071

Thornton, J. W. (2004). Resurrecting ancient genes: experimental analysis of extinct molecules. *Nat Rev Genet*, *5*(5), 366-375. https://doi.org/10.1038/nrg1324

Tingley, W. G., Pawlikowska, L., Zaroff, J. G., Kim, T., Nguyen, T., Young, S. G., Vranizan, K., Kwok, P. Y., Whooley, M. A., & Conklin, B. R. (2007). Gene-trapped mouse embryonic stem cell-derived cardiac myocytes and human genetics implicate AKAP10 in heart rhythm regulation. *Proc Natl Acad Sci U S A*, *104*(20), 8461-8466. http://www.ncbi.nlm.nih.gov/entrez/query.fcgi?cmd=Retrieve&db=PubMed&dopt=Citation&list_uids=17485678

Toda, T., Cameron, S., Sass, P., Zoller, M., Scott, J. D., McMullen, B., Hurwitz, M., Krebs, E. G., & Wigler, M. (1987). Cloning and Characterization of BCY1, a Locus Encoding a Regulatory Subunit of the Cyclic AMP-Dependent Protein Kinase in Saccharomyces cerevisiae. *Molecular and Cellular Biology*, *7*(4), 1371-1377. https://doi.org/10.1128/mcb.7.4.1371-1377.1987

Torday, J., & Miller, W. (2020). The Information Cycle and Biological Information Management. In (pp. 47-56). Springer International Publishing. https://doi.org/10.1007/978-3-030-38133-2_7

Tremblay, V., Zhang, P., Chaturvedi, C.-P., Thornton, J., Joseph, Skiniotis, G., Shilatifard, A., Brand, M., & Couture, J.-F. (2014). Molecular Basis for DPY-30 Association to COMPASS-like and NURF Complexes. *Structure*, *22*(12), 1821-1830. https://doi.org/https://doi.org/10.1016/j.str.2014.10.002

Trifonov, E. N. (2012). Definition of Life: Navigation through Uncertainties. *Journal of Biomolecular Structure and Dynamics*, *29*(4), 647-650. https://doi.org/10.1080/073911012010525017

Tsukita, S., & Yonemura, S. (1999). Cortical Actin Organization: Lessons from ERM (Ezrin/Radixin/Moesin) Proteins. *Journal of Biological Chemistry*, *274*(49), 34507-34510. https://doi.org/https://doi.org/10.1074/jbc.274.49.34507

Tunquist, B. J., Hoshi, N., Guire, E. S., Zhang, F., Mullendorff, K., Langeberg, L. K., Raber, J., & Scott, J. D. (2008). Loss of AKAP150 perturbs distinct neuronal processes in mice. *Proceedings of the National Academy of Sciences*, *105*(34), 12557-12562. https://doi.org/10.1073/pnas.0805922105

Turnham, R. E., & Scott, J. D. (2016). Protein kinase A catalytic subunit isoform PRKACA; History, function and physiology. *Gene*, *577*(2), 101-108. https://doi.org/https://doi.org/10.1016/j.gene.2015.11.052

Ueland, P. M., & Doskeland, S. O. (1976). Adenosine 3':5'-cyclic monophosphate-dependence of protein kinase isoenzymes from mouse liver. *Biochemical Journal*, *157*(1), 117-126.

Uhler, M. D., Chrivia, J. C., & McKnight, G. S. (1986). Evidence for a second isoform of the catalytic subunit of cAMP-dependent protein kinase. *Journal of Biological Chemistry*, *261*(33), 15360-15363. https://doi.org/https://doi.org/10.1016/S0021-9258(18)66717-1

Uzunov, P., & Weiss, B. (1972). Separation of multiple molecular forms of cyclic adenosine-3′,5′-monophosphate phosphodiesterase in rat cerebellum by polyacrylamide gel electrophoresis. *Biochimica et Biophysica Acta (BBA) - Enzymology*, *284*(1), 220-226. https://doi.org/10.1016/0005-2744(72)90060-5

van Hooff, J. J. E., Tromer, E., van Dam, T. J. P., Kops, G. J. P. L., & Snel, B. (2019). Inferring the Evolutionary History of Your Favorite Protein: A Guide for Molecular Biologists. *BioEssays*, *41*(5), 1900006. https://doi.org/10.1002/bies.201900006

Venkatakrishnan, A. J., Deupi, X., Lebon, G., Tate, C. G., Schertler, G. F., & Babu, M. M. (2013). Molecular signatures of G-protein-coupled receptors. *Nature*, *494*(7436), 185-194. https://doi.org/10.1038/nature11896

Vermeulen, M., Eberl, H. C., Matarese, F., Marks, H., Denissov, S., Butter, F., Lee, K. K., Olsen, J. V., Hyman, A. A., Stunnenberg, H. G., & Mann, M. (2010). Quantitative Interaction Proteomics and Genome-wide Profiling of Epigenetic Histone Marks and Their Readers. *Cell*, *142*(6), 967-980. https://doi.org/10.1016/j.cell.2010.08.020

Viswanatha, R., Wayt, J., Ohouo, P. Y., Smolka, M. B., & Bretscher, A. (2013). Interactome analysis reveals ezrin can adopt multiple conformational states [Research Support, N.I.H., Extramural]. *J Biol Chem*, *288*(49), 35437-35451. https://doi.org/https://doi.org/10.1074/jbc.M113.505669

Von Der Malsburg, A., Sapp, G. M., Zuccaro, K. E., Von Appen, A., Moss, F. R., Kalia, R., Bennett, J. A., Abriata, L. A., Dal Peraro, M., Van Der Laan, M., Frost, A., & Aydin, H. (2023). Structural mechanism of mitochondrial membrane remodelling by human OPA1. *Nature*, *620*(7976), 1101-1108. https://doi.org/https://doi.org/10.1038/s41586-023-06441-6

Walker, C., Wang, Y., Olivieri, C., Karamafrooz, A., Casby, J., Bathon, K., Calebiro, D., Gao, J., Bernlohr, D. A., Taylor, S. S., & Veglia, G. (2019). Cushing's syndrome driver mutation disrupts protein kinase A allosteric network, altering both regulation and substrate specificity. *Sci Adv*, *5*(8), eaaw9298. https://doi.org/10.1126/sciadv.aaw9298

Walsh, D. A., Perkins, J. P., & Krebs, E. G. (1968). An Adenosine 3′,5′-Monophosphate-dependant Protein Kinase from Rabbit Skeletal Muscle. *Journal of Biological Chemistry*, *243*(13), 3763-3765. https://doi.org/10.1016/S0021-9258(19)34204-8

Wang, Y., Ho, T. G., Franz, E., Hermann, J. S., Smith, F. D., Hehnly, H., Esseltine, J. L., Hanold, L. E., Murph, M. M., Bertinetti, D., Scott, J. D., Herberg, F. W., & Kennedy, E. J. (2015). PKA-type I selective constrained peptide disruptors of AKAP complexes. *ACS Chemical Biology*, *10*(6), 1502-1510. https://doi.org/10.1021/acschembio.5b00009

Weiner, J., Beaussart, F., & Bornberg-Bauer, E. (2006). Domain deletions and substitutions in the modular protein evolution. *The FEBS Journal*, *273*(9), 2037-2047. https://doi.org/10.1111/j.1742-4658.2006.05220.x

Weiss, M. C., Sousa, F. L., Mrnjavac, N., Neukirchen, S., Roettger, M., Nelson-Sathi, S., & Martin, W. F. (2016). The physiology and habitat of the last universal common ancestor. *Nature Microbiology*, *1*(9), 16116. https://doi.org/10.1038/nmicrobiol.2016.116

Whiting, J. L., Nygren, P. J., Tunquist, B. J., Langeberg, L. K., Seternes, O.-M., & Scott, J. D. (2015). Protein Kinase A Opposes the Phosphorylation-dependent Recruitment of Glycogen Synthase Kinase 3β to A-kinase Anchoring Protein 220. *The Journal of Biological Chemistry*, *290*(32), 19445-19457. https://doi.org/10.1074/jbc.M115.654822

Whiting, J. L., Ogier, L., Forbush, K. A., Bucko, P., Gopalan, J., Seternes, O. M., Langeberg, L. K., & Scott, J. D. (2016). AKAP220 manages apical actin networks that coordinate aquaporin-2 location and renal water reabsorption. *Proc Natl Acad Sci U S A*, *113*(30), E4328-4337. https://doi.org/https://doi.org/10.1073/pnas.1607745113

Wigington, C. P., Roy, J., Damle, N. P., Yadav, V. K., Blikstad, C., Resch, E., Wong, C. J., Mackay, D. R., Wang, J. T., Krystkowiak, I., Bradburn, D. A., Tsekitsidou, E., Hong, S. H., Kaderali, M. A., Xu, S.-L., Stearns, T., Gingras, A.-C., Ullman, K. S., Ivarsson, Y.,…Cyert, M. S. (2020). Systematic Discovery of Short Linear Motifs Decodes Calcineurin Phosphatase Signaling. *Molecular Cell*, *79*(2), 342-358.e312. https://doi.org/10.1016/j.molcel.2020.06.029

Woese, C. R., Kandler, O., & Wheelis, M. L. (1990). Towards a natural system of organisms: proposal for the domains Archaea, Bacteria, and Eucarya. *Proc Natl Acad Sci U S A*, *87*(12), 4576-4579. https://doi.org/10.1073/pnas.87.12.4576

Wong, W., & Scott, J. D. (2004). AKAP signalling complexes: focal points in space and time. *Nat Rev Mol Cell Biol*, *5*(12), 959-970. https://doi.org/10.1038/nrm1527

Yang, J.-P., Tang, H., Reddy, T. R., & Wong-Staal, F. (2001). Mapping the Functional Domains of HAP95, a Protein That Binds RNA Helicase A and Activates the Constitutive Transport Element of Type D Retroviruses*. *Journal of Biological Chemistry*, *276*(33), 30694-30700. https://doi.org/ https://doi.org/10.1074/jbc.M102809200

Yang, P., Diener, D. R., Yang, C., Kohno, T., Pazour, G. J., Dienes, J. M., Agrin, N. S., King, S. M., Sale, W. S., Kamiya, R., Rosenbaum, J. L., & Witman, G. B. (2006). Radial spoke proteins of

Chlamydomonas flagella. *Journal of Cell Science*, *119*(6), 1165-1174. https://doi.org/10.1242/jcs.02811

Yen, M.-Y., Wang, A.-G., Lin, Y.-C., Fann, M.-J., & Hsiao, K.-J. (2010). Novel Mutations of the OPA1 Gene in Chinese Dominant Optic Atrophy. *Ophthalmology*, *117*(2), 392-396.e391. https://doi.org/https://doi.org/10.1016/j.ophtha.2009.07.019

Zaccolo, M., & Kovanich, D. (2024). Nanodomain cAMP signalling in cardiac pathophysiology: potential for developing targeted therapeutic interventions. *Physiol Rev*. https://doi.org/10.1152/physrev.00013.2024

Zhang, J. Z., Lu, T.-W., Stolerman, L. M., Tenner, B., Yang, J. R., Zhang, J.-F., Falcke, M., Rangamani, P., Taylor, S. S., Mehta, S., & Zhang, J. (2020). Phase Separation of a PKA Regulatory Subunit Controls cAMP Compartmentation and Oncogenic Signaling. *Cell*, *182*(6), 1531-1544.e1515. https://doi.org/10.1016/j.cell.2020.07.043

Zhang, Q., Carr, D. W., Lerea, K. M., Scott, J. D., & Newman, S. A. (1996). Nuclear Localization of Type II cAMP-Dependent Protein Kinase during Limb Cartilage Differentiation Is Associated with a Novel Developmentally Regulated A-Kinase Anchoring Protein. *Developmental Biology*, *176*(1), 51-61. https://doi.org/10.1006/dbio.1996.9995

Zhao, L., Hou, Y., Picariello, T., Craige, B., & Witman, G. B. (2019). Proteome of the central apparatus of a ciliary axoneme. *Journal of Cell Biology*, *218*(6), 2051-2070. https://doi.org/https://doi.org/10.1083/jcb.201902017

Zheng, X., Fu, Z., Su, D., Zhang, Y., Li, M., Pan, Y., Li, H., Li, S., Grassucci, R. A., Ren, Z., Hu, Z., Li, X., Zhou, M., Li, G., Frank, J., & Yang, J. (2020). Mechanism of ligand activation of a eukaryotic cyclic nucleotide−gated channel. *Nature Structural & Molecular Biology*, *27*(7), 625-634. https://doi.org/10.1038/s41594-020-0433-5

Zoller, M. J., Kerlavage, A. R., & Taylor, S. S. (1979). Structural comparisons of cAMP-dependent protein kinases I and II from porcine skeletal muscle. *J Biol Chem*, *254*(7), 2408-2412.

Curriculum Vitae

Education

University of Washington, PhD 2018-2025

Pharmacology

Advisor: Dr. John D. Scott

Thesis: “The ascent of AKAPs: from architectural elements to isotype selective PKA scaffolds”

Stony Brook University, BS 2013-2017

Pharmacology

Research Experience

University of Washington, John Scott lab June 2019 – March 2025

Graduate Student Researcher – During my time in the Scott lab, I performed bioinformatic, phylogenetic, *in vitro, in silico, in situ*, and *in vivo* experiments to investigate features of AKAP amphipathic helices that make them prefer binding to either type I or type II PKA. This involved analyzing the composition of AKAP helices and identifying a leading “aromatic alanine” motif in type I preferential AKAPs. I then created mutants of AKAP79, a type II AKAP to convert it to preferring type I PKA. Using molecular dynamics simulations, purified protein binding assays, FRAP microscopy, immunoprecipitations, and a biased Cushing’s syndrome model, I demonstrated that the “aromatic alanine” motif is necessary and sufficient for type I selective AKAPs. Additionally I characterized the evolution of AKAPs and their precursors, DDIPs along with docking and dimerization (d/d) domain proteins. Through production of phylogenetic trees and analysis of protein conservation I determined that d/d proteins evolved divergently, where their helical anchors evolved convergently.

University of Washington, Chris Hague lab September 2018 – December 2018

Rotation Student – During my rotation in the Hague lab, I measured the half-life of the β_2 adrenergic receptors in Hek293T cells by performing cycloheximide chase assays.

University of Washington, Rich Gardner lab April 2019 – June 2019

Rotation Student – During my rotation in the Gardner lab, I studied the role of ubiquitination sites on RNA polymerase I degradation by producing mutants at three lysines involved in ubiquitination and measuring their stability in yeast.

Stony Brook University, Martin Kaczocha lab April 2015 – August 2017

Undergraduate researcher – During my time in the Kaczocha lab I performed behavioral and biochemical studies on the analgesic and anti-inflammatory properties of fatty acid binding protein 5 (FABP5) inhibitors. I also participated in a study trialing analogs of our lead compound SBFI26 which would be better suited for oral administration.

Publications

Falcone J, Scott J. *The ascent of AKAPs, from architectural elements to kinase anchors: A perspective.* BCJ 2025, **In review**

Falcone JI, Cleveland KH, Kang M, Odle BJ, Forbush KA, and Scott JD. *The evolution of AKAPs and emergence of PKA isotype selective anchoring determinants.* JBC 2025, **In review**

Gopalan J, Omar MH, Roy A, Cruz NM, **Falcone J**, Jones KN, Forbush KA, Himmelfarb J, Freedman BS, Scott JD. *Targeting an anchored phosphatase-deacetylase unit restores renal ciliary homeostasis*. Elife. 2021 Jul 12;10:e67828. doi: 10.7554/eLife.67828.

Yan S, Elmes MW, Tong S, Hu K, Awwa M, Teng GYH, Jing Y, Freitag M, Gan Q, Clement T, Wei L, Sweeney JM, Joseph OM, Che J, Carbonetti GS, Wang L, Bogdan DM, **Falcone J**, Smietalo N, Zhou Y, Ralph B, Hsu HC, Li H, Rizzo RC, Deutsch DG, Kaczocha M, Ojima I. *SAR studies on truxillic acid mono esters as a new class of antinociceptive agents targeting fatty acid binding proteins*. Eur J Med Chem. 2018 Jun 25;154:233-252. doi: 10.1016/j.ejmech.2018.04.050.

Bogdan D*, **Falcone J***, Kanjiya MP, Park SH, Carbonetti G, Studholme K, Gomez M, Lu Y, Elmes MW, Smietalo N, Yan S, Ojima I, Puopolo M, Kaczocha M. Fatty acid-binding protein 5 controls microsomal prostaglandin E synthase 1 (mPGES-1) induction during inflammation. J Biol Chem. 2018 Apr 6;293(14):5295-5306. doi: 10.1074/jbc.RA118.001593.

Teaching and Other Experiences

Teaching assistant Autumn 2020–Winter 2021

I led a weekly study session which entailed making and giving presentations summarizing the material covered in the past week of pharmacology lectures, writing quizzes, and grading the quizzes.